沖縄本島南部の石灰岩帯水層における地下水硝酸性窒素の挙動

農工研報 52
59 ～ 110, 2013

Dynamics of Groundwater Nitrates in Limestone Aquifer of the Southern Okinawa Island

YOSHIMOTO Shuhei*

Contents

* Renewable Resources Engineering Division

Accepted on 31st December, 2012
Keywords: groundwater resources, water quality conservation, numerical models, karst hydrology, geochemistry, hydrogeology

I Introduction

1 Groundwater Quality Problems in the Ryukyu Islands

The increasing nitrate concentration in groundwater has become a matter of worldwide concern. Nitrates are implicated in methemoglobinemia and may be causative factors in other health disorders including cancer, although at present the evidence is inconclusive (e.g., Kunikane, 1996, Townsend et al., 2003). Additionally, groundwater runoff with a high concentration of nitrate has been pointed out as a cause of eutrophication in surface waters (e.g., McClelland and Valiela, 1998).

The World Health Organization (WHO) recommends that the concentration of nitrogen as nitrate (NO_3-N) in drinking water should not exceed 11.3 mg L^{-1}, but occasional levels up to 22.6 mg L^{-1} are sometimes acceptable (WHO, 1970). In Japan, the water quality standard for NO_3-N concentration in drinking water was determined as 10 mg L^{-1} in 1978, and the environmental quality standard for NO_3-N concentration in groundwater adopted the same value in 1999 for the maximum acceptable level. These standards have accentuated concerns about NO_3-N concentration in groundwater.

It is generally considered that nitrate pollution is caused by nitrogen loading as a result of human activity such as increased use of chemical fertilizers, improper management of livestock manure, and discharge of effluent from septic tanks (e.g., Tase, 2003).

Groundwater in karst aquifers is particularly vulnerable to chemical pollution because water moves rapidly through the fractures and fissures of an aquifer (e.g., Field, 1988). Numerous studies have reported the presence of nitrates in the groundwater of chalk aquifers in England (e.g., Young et al., 1976; Wellings, 1984; Carey and Lloyd, 1985; Andrews et al., 1997) and limestone aquifers in the United States (e.g., Scanlon, 1990; Peterson et al., 2002). The nitrogen loading processes in karst aquifers are strongly influenced by the characteristics of groundwater flow, which are closely related to hydrogeological features such as caves and caverns. To achieve control of groundwater nitrates, it is essential to understand the predominant sources and transport processes of nitrates, which are related to the impact of karstic features on the nitrogen loading processes.

Japan's Ryukyu Islands, which consist of Cenozoic rocks composed mainly of reefs and uplifted reef deposits, are a chain of various-sized islands that stretch southwestward from Kyushu Island to Taiwan. The largest of the Ryukyu Islands is Okinawa Island. Ryukyu Limestone, of the Quaternary age, is extensively distributed on these islands.

Recently, the rising nitrate concentration in the groundwater has become a problem. Many studies on groundwater nitrates have been conducted on Miyako Island, one of the isolated Ryukyu Islands where agriculture is predominant and two subsurface dams were constructed. Nagata (1993) revealed that the nitrate concentration has been increasing since the 1970s, and concluded that the predominant source was chemical fertilizers applied to the sugarcane fields.

The southern part of Okinawa Island differs in social structure compared to that of Miyako Island. The area is a suburban region with many livestock farms as well as numerous agricultural farms growing mainly vegetables and sugarcane. Tokuyama et al. (1990) studied water quality at springs in this region from 1983 to 1987, and reported that nitrate concentrations in the Ryukyu Limestone area were much higher than in the marlstone area adjacent to the Ryukyu Limestone area. Agata et al. (2001) compared the results of a water quality survey in 1996 with water quality reported by Tokuyama et al. (1990), and showed that nitrate concentrations in the groundwater increased during the 1990s. Agata et al. (2001) also suggested that chemical fertilizers applied to the sugarcane farms affect groundwater quality in this region.

2 Subsurface Dams in the Ryukyu Limestone Regions

The Ryukyu Limestone is extensively distributed in the Ryukyu Islands. Because Ryukyu Limestone is very porous and permeable, there is not enough surface water for agricultural and domestic use, and so local people draw water primarily from groundwater in limestone aquifers. However, there is not enough natural groundwater in limestone aquifers to satisfy the irrigation demand in extensive upland fields, and so there is a need to develop groundwater resources by building subsurface dams. A subsurface dam is a facility that stores shallow groundwater in the pores of the stratum, which is then used in a sustainable way, by damming up the groundwater level or preventing saltwater intrusion. Until now, on some of the islands such as Miyako and Okinawa, subsurface dams were constructed to secure a stable supply of irrigation water (Ishida et al., 2011).

The southern part of Okinawa Island is a suburban region where mainly vegetables and sugarcane are cultivated and there are also many livestock farms. In this region, two subsurface dams were constructed in the Komesu and Giza groundwater basins in 2005, and farmers started to use groundwater from these dams as irrigation water in 2006. The Komesu subsurface dam is the first full-scale subsurface dam constructed to prevent saltwater intrusion in Japan (Nawa and Miyazaki, 2009), while the Giza subsurface dam is designed to dam up the groundwater level.

3 Research Aim and Objectives

Subsurface dams are beneficial for the development of water resources, but the subterranean environment is significantly changed by the construction of the cutoff walls. Hence, local residents are concerned about the impact of a subsurface dam on groundwater quality.

There are two issues of particular concern: nitrate contamination of groundwater and decrease of groundwater resources caused by climate change. Rising nitrate concentrations in groundwater is a problem in regions where large quantities of inorganic fertilizers and compost were applied to arable land in the 1990s. The nitrogen concentration in groundwater observed at many points exceeds the environmental standard of 10 mg L^{-1} as NO_3-N. Concerns about the impact of a subsurface dam on groundwater quality are based on the potential changes to the natural groundwater flow.

In addition, the global hydrological system is expected to intensify due to ongoing climate change such as increasing heavy rainfall events and rising temperature. The increased vulnerability of groundwater due to global warming is of particular concern in the Ryukyu Islands where the water supply depends mainly on groundwater. However, there have been few studies on the impact of historical and projected variations in the climate system on groundwater resources.

To predict the impact on the amount and quality of groundwater and to develop effective countermeasures, it is necessary to identify the mechanisms of water and solute transport in the aquifer and to build effective simulation models for subsurface dam groundwater.

The main objectives of this research are:

1. To determine the hydrogeological properties of the Ryukyu Limestone aquifer, by analyzing the fluctuation characteristics of groundwater levels and NO_3-N concentrations.
2. To determine the groundwater flow and the transport and potential source of groundwater nitrates in the Ryukyu Limestone aquifer.
3. To develop a regional quantitative model that can describe prolonged daily groundwater recharge and nitrogen dynamics in the catchment area of a subsurface dam.

4 Structure of the Report

This report consists of seven chapters, three of which describe the author's original work. These chapters supplement the former chapters, maintaining consistency with the purpose of the report.

The introductory chapter explains the groundwater quality problems and subsurface dam conservation in the Ryukyu Limestone regions, and the objectives of this report.

In Chapter 2, literature related to the hydrogeological characteristics of carbonate aquifers is reviewed. Furthermore, approaches adopted to identify the mechanisms of water and solute transport, and simulation models for groundwater, are reviewed to establish a strong foundation for this research.

In Chapter 3, the geological characteristics, groundwater properties and land-use situations in the southern part of Okinawa Island, which is the study area of this research, are described.

In Chapter 4, the changes in groundwater levels and NO_3-N concentrations in the Komesu basin are discussed along with the characteristics of short-term fluctuations and long-term trends. In addition, a time-series model was applied to the analysis of groundwater hydrographs and the properties of the Ryukyu Limestone aquifer are examined (Yoshimoto et al., 2007, 2011).

In Chapter 5, to clarify how the transport of groundwater nitrates is affected by the state of groundwater flow closely associated with hydrogeological features such as caves and caverns in the Ryukyu Limestone aquifer, the ratio of two stable isotopes of nitrogen in nitrate, ^{14}N and ^{15}N, and radon (^{222}Rn) were used as tracers to evaluate the transport of nitrates in groundwater (Yoshimoto et al., 2007, 2011).

Chapter 6 describes a regional quantitative model developed to represent prolonged daily groundwater recharge and nitrogen dynamics in the catchment area of a subsurface dam, and its application to the reservoir area of the Komesu subsurface dam (Yoshimoto et al., 2012).

A summary and the conclusions of this study as well as comments on future work are given in Chapter 7.

II Literature Review

1 Introduction

Domenico and Schwartz (1998) pointed out the challenge of characterizing the hydrogeology in carbonate terrains given that the rocks are soluble and susceptible to the formation of self-organized networks of solutionally enlarged fractures, with the result being a doubleporosity aquifer. Nevertheless, for appropriate groundwater conservation, it is indispensable to identify the water and solute dynamics in carbonate aquifers and then to build an effective simulation model.

In this chapter, the hydrogeological characteristics of a carbonate aquifer are firstly reviewed. Next, approaches adopted to identify the mechanisms of water and solute transport in an aquifer with these complex characteristics are described. Finally, simulation models that have been developed are summarized.

2 Karst Hydrology

a. Heterogeneity of carbonate aquifers

Generally, groundwater moves through pores in the aquifer, and thus porosity is particularly important. Two types of porosity can be distinguished according to its origin: (1) meaning interstitial porosity, and (2) meaning fracture and solution porosity (Domenico and Schwartz, 1998).

Groundwater flow usually occurs only through secondary porosity if the primary porosity in the matrix is lower than 0.005 m^3m^{-3} (e.g., Skagius and Neretnieks, 1986). However, granite has a primary porosity of more than 0.01 m^3m^{-3} (Abelin et al., 1991), where groundwater flow through primary porosity is considered to occur even in the granite matrix. Therefore, matrix diffusion may play a significant role in the process of solute transport in fractured rocks (Novakowski and Lapcevic, 1994). It is necessary to consider dual porosity (both primary and secondary porosities) in groundwater flow and solute transport in fractured rocks.

Additionally, as secondary porosity, it has been noted that large continuous openings in field soils, called "macropores", are important in the movement of water and solute (Beven and Germinn, 1982; Yasuhara et al., 1992; Yasuike, 1996). After Ishiguro (1994) reviewed solute transport influenced by macropores, extensive research has been done on infiltration and percolation through macropores. This thesis, however, focuses on cases in carbonate aquifers. Hereafter, "matrix flow" and "fracture flow" mean groundwater flow in the matrix and through fractures and macropores, respectively.

The zone between the top of the ground surface and the groundwater table is referred to as the "vadose" zone. For example, calcareous caves are normally located in this zone. In the vadose zone of a limestone aquifer, rainwater in which atmospheric CO_2 is dissolved reacts with the limestone according to the following chemical equation:

$$CaCO_3 + H_2O + CO_2 \rightleftarrows Ca^{2+} + 2HCO_3^{-}. \quad (1)$$

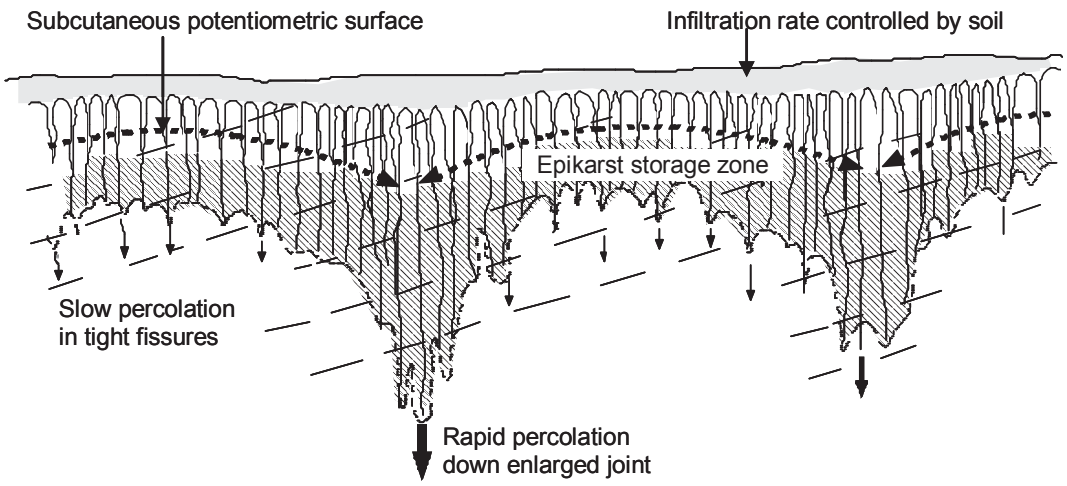

Fig. 1 Epikarst storage and percolation of rainwater (modified from Williams, 1983)

Here, the right-direction reaction means the dissolution of limestone by rainwater. Meanwhile, the left-direction reaction is the precipitation of calcite, which often forms stalactites and stalagmites. The limestone aquifer just beneath the groundwater table has suitable conditions for the right-direction reaction in Eq. (1), because the groundwater in the vicinity of the table has a high concentration of dissolved CO_2 (Okimura and Takayasu, 1976). Therefore, caves have formed and developed along groundwater tables in the past and continue to do so (Kita-Bingo Plateau Research Group, 1969; Atetsu Research Group, 1970; Kono, 1972). Such caves are also found in the Ryukyu limestone region, and Imaizumi et al. (2002a) revealed that continuous cave networks have extended to several levels in the Komesu basin.

Discontinuity between the carbonate rocks and weathered soil layer, as shown in **Fig. 1**, corresponds to the layered heterogeneity. This discontinuous boundary is called the "epikarst zone" (e.g., Peterson et al., 2002). The epikarst is the uppermost weathered zone of carbonate rocks. Beneath this zone, permeability decreases in the depth direction, because the width of a fracture becomes narrower as it goes deeper. As a result, percolation of rainwater is gradually suppressed, with the exception of that through open joints and faults. After a rainfall event, rainwater is temporarily stored in this zone, and then percolates slowly. The epikarst zone reduces the rate of percolation in the vadose zone (Williams, 1983), and impedes the entry of surface materials into the groundwater, which is called the "buffer effect".

b. Types of groundwater flow in carbonate aquifers

Where carbonate sediments containing coral and foraminifera have emerged, karst features such as sinkholes, pinnacles, uvalas and poljes have formed. These karst features continuously evolve through the dissolution of limestone. Changes in groundwater flow caused by karstification can be categorized into three phases: diffusion, mixed, and conduit (**Fig. 2**; Quinlan and Ewers, 1985). In a diffuse-type aquifer, the initial phase, groundwater flow occurs as matrix flow through primary pores (**Fig. 2(a)**). As time goes by, conduits (such as caves) begin developing from the dissolution of carbonate rocks. Then, part of the groundwater flow passing the conduit network becomes larger, and the phase changes from diffusion to mixed (**Fig. 2(b)**). Sinkholes are generally found in the initial phase of the evolution of karst topography. As the sinkholes become larger, surface water starts entering the conduit network directly, promoting further development of the conduit network. When the karst aquifer matures into the conduit type, the groundwater flow collects in the major channels of the network, and dependence on the matrix flow is significantly reduced (**Fig. 2(c)**).

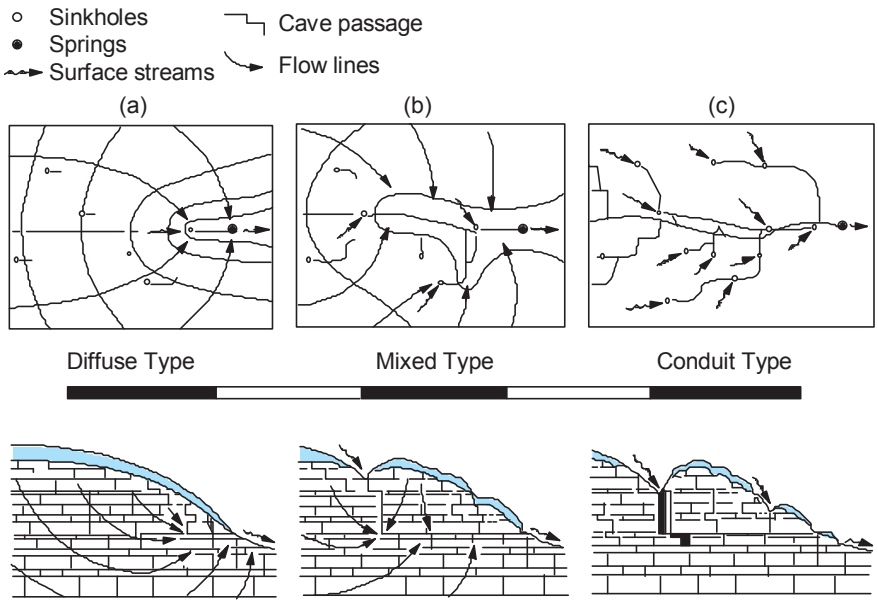

Fig. 2 Development of karst terrains and change in groundwater flow (Quinlan and Ewers, 1985)

3 Geochemical and Isotopic Approaches for Carbonate Aquifers

a. Piper diagram

A piper diagram, which illustrates equivalent relationships among major ions, is broadly used to understand groundwater chemistry. The geochemical evolution of groundwater in general carbonate aquifers is also clarified by using the piper diagram (Hanshaw and Back, 1979). The evolution is explained with using the abbreviations R, D, and M which mean the general composition of major ions in the recharge water (rainwater), downgradient groundwater, and marine water, respectively, in a carbonate aquifer. Recharge water evolves to downgradient water through the pathway R→D as a result of the dissolution of gypsum and dolomite during the flow of water in a carbonate aquifer. If mixed with marine water, the water quality will turn towards M (Hanshaw and Back, 1979).

b. Nitrogen isotopes

Until now, researchers have studied nitrogen isotopes to understand the source and transport of groundwater nitrates. However, it is difficult to sample groundwater affected by a single source, because the effects of isotopic fractionation during biochemical reactions such as ammonia volatilization and denitrification must be taken into account (e.g., Kreitler, 1979; Létolle, 1980; Hübner, 1986; Mariotti et al., 1988).

The range of $\delta^{15}N$ values in the referred literature and the values applied to this study are summarized in **Fig. 3**. Values of $\delta^{15}N$ in groundwater nitrates beneath fertilized upland fields generally range from 0 to 6‰ under the influence of isotopic fractionation during biochemical reactions (Fogg et al., 1998; Böhlke, 2002). Since the range of $\delta^{15}N$ values in livestock manure is similar to that in domestic wastewater, it is difficult to distinguish between these nitrogen sources by $\delta^{15}N$ values in groundwater nitrates (e.g., Heaton, 1986). The normal range of $\delta^{15}N$ values in groundwater nitrates derived from livestock and human manure is 8–22‰ (Kreitler and Jones, 1975; Heaton, 1986; Fogg et al., 1998). This range includes the effects of isotopic fractionation during ammonia volatilization and denitrification. The range of $\delta^{15}N$ values in groundwater nitrates derived from natural soil nitrogen is about 2–6‰ (Kreitler and Jones, 1975; Heaton, 1986; Fogg et al., 1998; Böhlke, 2002; Yoneyama et al., 1987).

Approaches with nitrogen isotopes were also applied to the Ryukyu Limestone regions. Kondo et al. (1997) measured the stable isotopes of nitrogen (^{15}N) in shallow groundwater from wells and springs under three land-use settings and reported that the typical land-use settings and corresponding ratios of ^{15}N ($\delta^{15}N$ values) were: residential areas, 8.0‰; agricultural areas, 5.2‰; and natural, undeveloped areas, 5.6‰. The values exceeding 7‰ in residential areas suggested that nitrogen from sewage existed in the groundwater. In contrast, the values of less than 7‰ in agricultural areas and part of the natural, undeveloped areas suggested that nitrogen in the groundwater was supplied by commercial inorganic fertilizers. However, the study pointed out that these values were

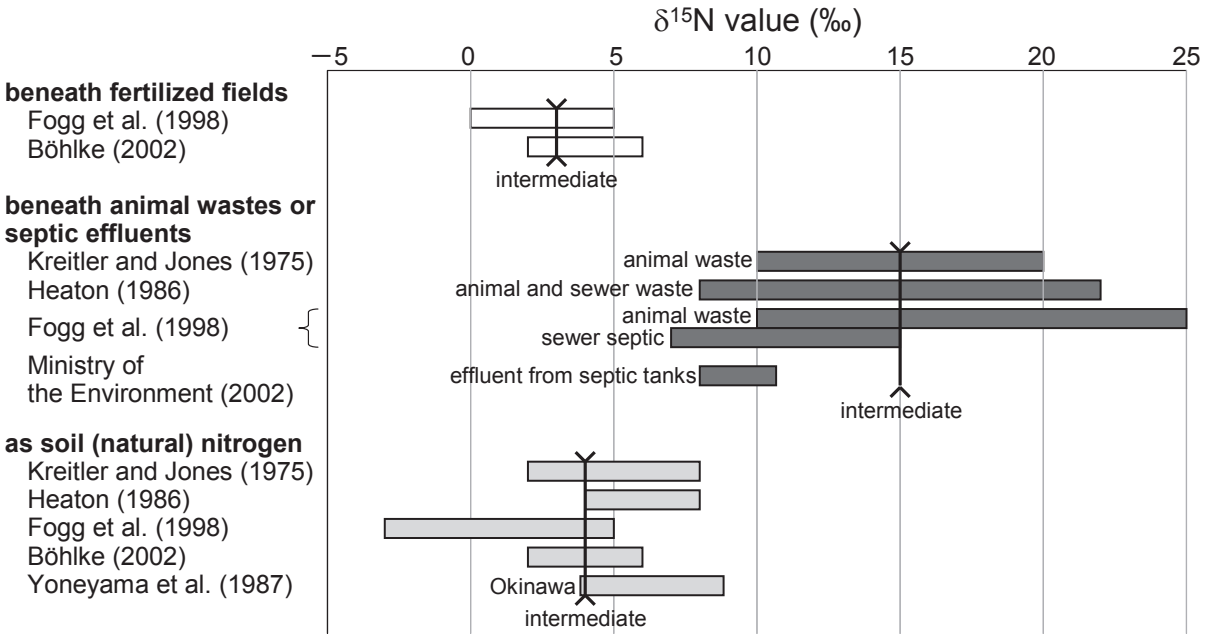

Fig. 3 Range of $\delta^{15}N$ values in the reference literature in this study

not necessarily correlated to each other due to other factors such as hydrogeological conditions. Nakanishi et al. (1995) calculated the contribution of three nitrogen sources: (1) chemical fertilizer, (2) livestock and human waste, and (3) soil nitrogen, using a linear mixing model based on mass balance equations with data obtained from nitrogen-isotope analyses at 22 sites on Miyako Island. The study compared the results with actual land-use composition such as human and livestock population and arable land area; the estimated contribution at 12 sites was poorly related to the actual land-use composition, whereas the other contributions from simple hydrogeological conditions were well matched. These studies showed the difficulty of estimating nitrogen sources using the simple relationship between isotopic composition of nitrogen in groundwater nitrates and land use, and thus it is necessary to consider the properties of groundwater flow in karstic features such as caves and caverns in the Ryukyu Limestone region.

c. Radon

Radon (^{222}Rn) is a radioactive noble gas generated in an aquifer by the alpha decay of ^{226}Ra, and dissolves easily in water and decays with a half-life of 3.8 days. The concentration of ^{222}Rn in groundwater leaches 98% of its value at secular equilibrium after three weeks underground. In general, ^{222}Rn concentration in groundwater is higher than that in surface water (Hamada and Komae, 1998). ^{222}Rn was also found in groundwater of carbonate aquifers (e.g., Dongarrà et al., 1995). ^{222}Rn is useful as an indicator to distinguish the impact of caves and caverns, because its concentration in the groundwater of caves and caverns is relatively low (e.g., Pane, 1995).

4 Numerical Models for Groundwater Nitrates

a. Simulation models for nitrate concentrations in groundwater

Numerical models for simulating nitrate concentrations in groundwater are generally composed of one-dimensional leaching models and two- or three-dimensional saturated groundwater flow models. To date, several leaching models based on physical theories have been proposed, such as the improved NITS (Birkinshaw and Ewen, 2000) and FLOCR/ANIMO (Hendriks et al., 1999) models, but these are difficult to apply in the field because many parameters must be determined. Meanwhile, Andrews et al. (1997) developed IMPACT, a simple model composed of empirical equations for simulation of nitrogen leaching, and applied it to a chalk aquifer in the U.K. Similarly, Carey and Lloyd (1985) applied a conceptual model of nitrogen leaching and a distributed model of groundwater flow to another chalk aquifer. Recently, Almasri and Kaluarachichi (2007) developed a modeling framework to estimate changes in the spatial distribution of nitrate concentrations according to protection measures, by using computer codes such as MODFLOW (Harbaugh and McDonald, 1996) and MT3D (Zheng and Wang, 1999) linked to GIS.

Some Japanese studies have also developed nitrogen leaching models. Kiho and Islam (1995) proposed a model composed of a water balance submodel and a nitrogen balance submodel, to estimate nitrogen leaching (hereafter called the Kiho-Islam model). Takeuchi and Kawachi (2007) proposed a numerical optimization technique incorporating the Kiho-Islam model to control nitrate leaching while maintaining crop yields. Inoue et al. (2003) developed a one-dimensional finite element model that provides simple functions for nitrification, denitrification, and plant uptake, and demonstrated that the model can trace changes in the forms of nitrogen and predict nitrate dynamics over a short term.

Somura et al. (2003) also modeled nitrogen dynamics, ranging from loading on farmlands to flows in groundwater in Japan. Although this model considered differences in land use and the effects of nitrogen reactions, it could not clarify spatial nitrogen dynamics in groundwater because it modeled unconfined aquifers in a single tank.

b. Models for simulating the impacts of global warming on groundwater

Climate change is expected to affect groundwater resources. However, there have been only a few studies on the relation between climate change and groundwater resources; many previous researches focused on the potential impacts of global warming on surface water hydrology. Generally, the future impacts of global warming on groundwater systems have been simulated by large-scale and coarse-resolution models (e.g., York et al., 2002), with few exceptions of small-scale investigations (e.g., Malcolm and Soulsby, 2000).

Scibek et al. (2007) estimated future impacts of climate change on groundwater-surface water interactions and groundwater levels within an unconfined aquifer in south-central British Columbia using a three-dimensional transient groundwater flow model and climate data calculated from a GCM, but long-term changes in climate were not explicitly modeled due to computing constraints. Although the model grid should be smaller than the basin areas to appropriately investigate the impacts of climate change on groundwater resources, downscaled GCM-projected precipitation involves considerable uncertainty.

III Study Area

1 Introduction

In this study, the Komesu and Giza groundwater basins in the southern part of Okinawa Island were selected as a study area, where two subsurface dams were constructed by a national irrigation project. Here, geological settings, groundwater properties, and land-use situations are described.

2 Geology

The study area is located at the southern tip of Okinawa Island (**Fig. 4**). A large proportion of the study area is in Itoman City (46.63 km^2), and the rest is in Yaese Town (26.90 km^2). Topographically, the area is comprised of a series of coastal marine terraces.

The climate is humid subtropical according to the Köppen climate classification. Rainfall averages 1,944 mm annually, and the annual mean air temperature was 21.0℃ from 1971 to 2000 as measured at the Itokazu weather radar station in Nanjo City. Despite high rain, most of the annual rainfall is concentrated in the rainy season (May–June) and the typhoon season (July–September) and the annual range is relatively large, so frequent droughts have ravaged agricultural productions.

A columnar section and a geological map of the study area are shown in **Table 1** and **Fig. 5**. The Ryukyu Limestone of the Quaternary age is distributed broadly in the southern Okinawa Island. This limestone is sedimentary rock composed of uplifted coral reefs and foraminifer tests. It is very porous and has very high permeability with an effective porosity of 9% and a hydraulic conductivity of approximately 1.0×10^{-4} m s^{-1} (Okinawa General Bureau, 2006). The Shimajiri Group of the Neogene age, which underlies the Ryukyu Limestone, consists mainly of alternating layers of sandstone and mudstone. The Shimajiri Group is relatively impermeable with a hydraulic conductivity of less than 2.0×10^{-7} m s^{-1} (Okinawa General Bureau, 2006).

The terraces are complexly blocked by a conjugate fault system running northeast-southwest and northwest-southeast (**Fig. 5**). Long thin ridges composed of resistant limestone formed by hardening with repeated solubilization and recrystallization of soft calcareous sediments are distributed along the fault scarps.

3 Groundwater

Groundwater in this region occurs mainly in the pores of the Ryukyu Limestone, above the Shimajiri Group rocks. Groundwater basins are formed by one or two tectonic blocks where the groundwater flows through buried valleys of the upper surface of the Shimajiri Group. Furukawa et al. (1976) found eight groundwater basins in this region; this study covers the following three basins: Komesu, Giza, and Nashiro (**Fig. 5**). These basins have an area of 9.04, 5.20, and 1.65 km^2, respectively.

The study area is typical karst terrain with many sinkholes, springs and caves (**Fig. 5**), and continuously evolves with the

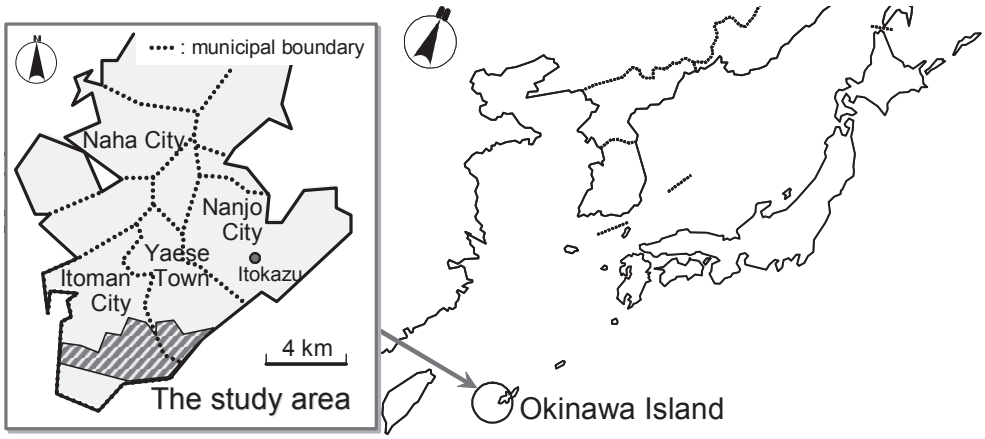

Fig. 4 Location of the study area

Table 1 Columnar section (Kaneko and Ujiié, 2006)

Geologic age			Formation or sediments	
Cenozonic	Quaternary	Holocene	Coral reef Beach rock Dune deposits Beach sand deposits Alluvium	
		?	block	Cave or fissure deposits
		Pleostocene	Ryukyu Group (**Ryukyu Limestone**)	MInatogawa Formation
				Naha Formation
				Itoman Formation / Chinen Formation
	Neogene	Pliocene	**Shimajiri Group**	Shinzato Formation
				Yonabaru Formation
				Tomigusuku Formation: Nakagusuku Sand Member
		Miocene		Tomigusuku Formation: Oroku Sand Member

Regend — Conformity; Unconformity; Unknown or no contact; Contemporaneous heterotopic faces or interfingering

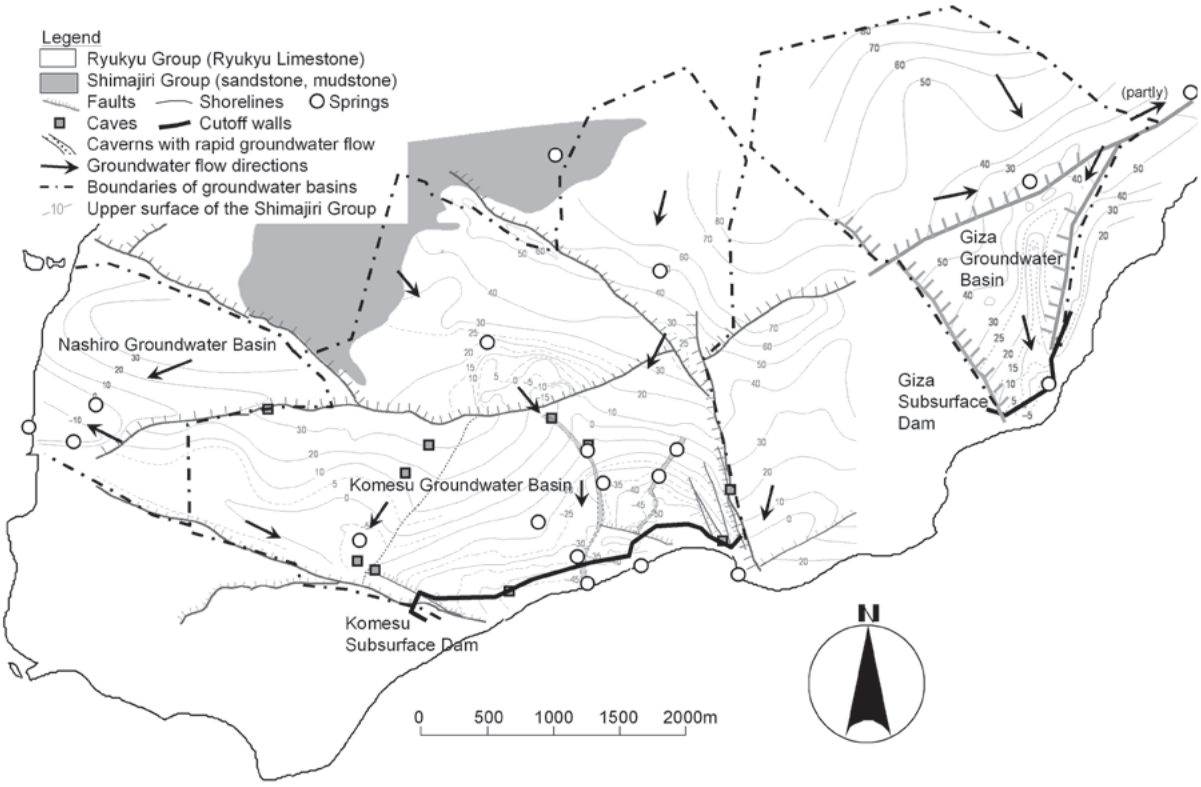

Fig. 5 Hydrogeological settings of the study area (modified from Okinawa General Bureau, 2006)

dissolution of calcite and dolomite in groundwater. Springs exist in the following situations: (1) flowing in caves as underground rivers, (2) appearing as water tables in sinkholes and (3) gushing from cracks in rocks (**Fig. 6**).

Caves in the study area are distributed along horizontal planes at several underground levels. The lowest cave is at about –45 m and

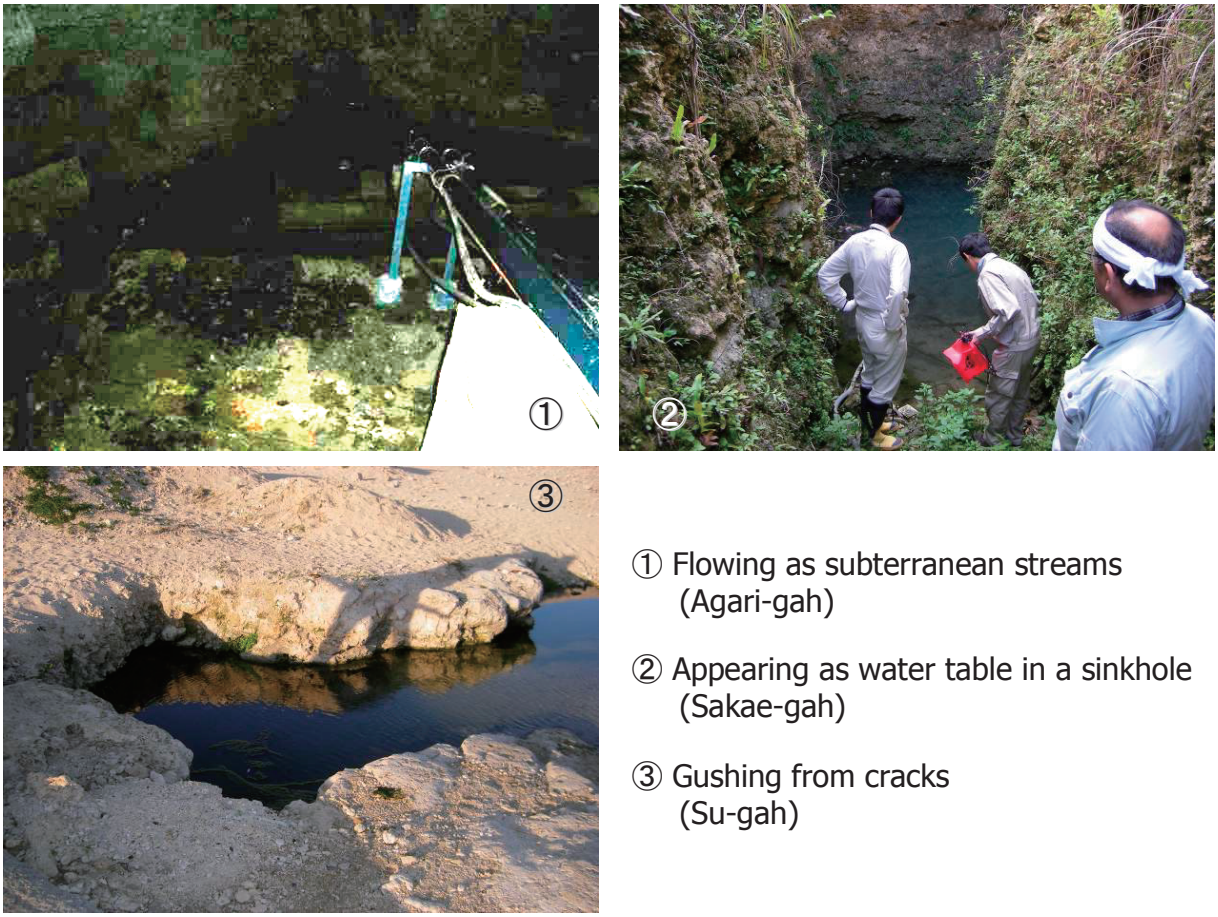

Fig. 6 Types of springs in the study area

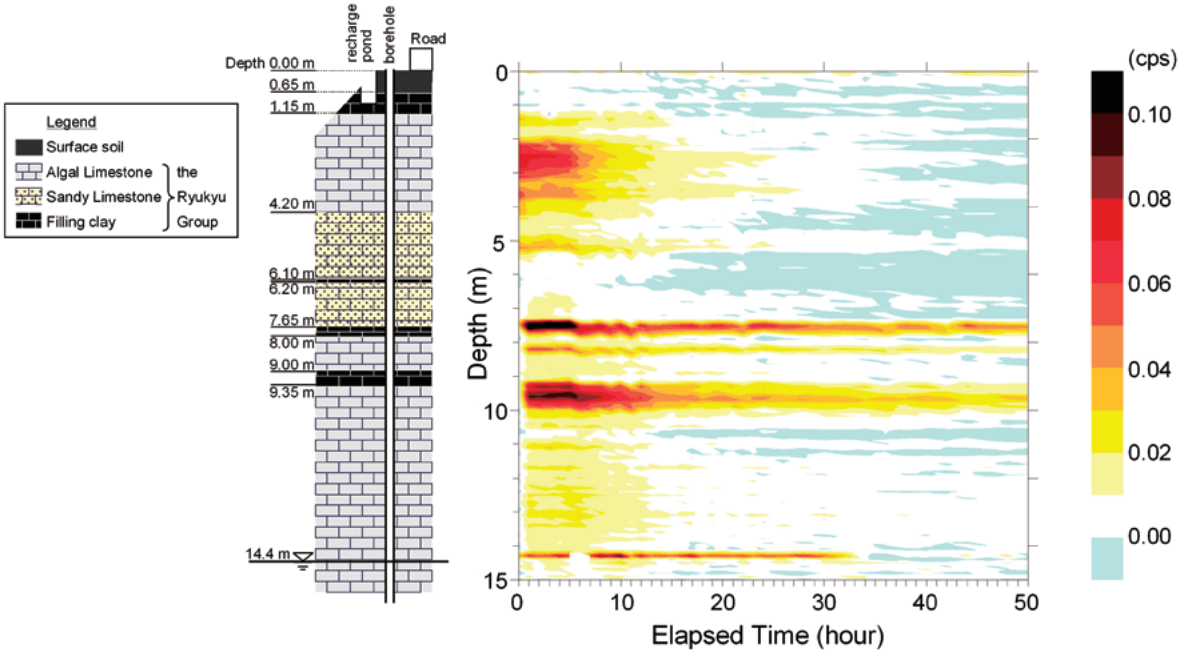

Fig. 7 Result of neutron moisture logging in Miyako Island (Yoshimoto et al., 2008)

corresponds to a groundwater level of 9800–8200 B.C. (Imaizumi et al., 2002a). It was also reported that two great caverns connect some of the caves with the seashore and some springs are located in these caverns. The groundwater flow in the caves and caverns is preferential (Imaizumi et al., 2002b).

Caves formed in the Ryukyu Limestone are sometimes filled by clay. This clay, called “filling clay”, is soft and displays a medium to dark brown color, and contains calcite, quartz, vermiculite and illite as major minerals, which implies that it is originated from the surface soils (Okinawa General Bureau, 1983). In the Komesu basin, a red-tinged clay layer is distributed at 20–24 m depth from the ground, which is important as a key bed in this region (Imaizumi et al., 2002a). Similarly, continuous and planar layers of filling clay are also found at other depths.

Yoshimoto et al. (2008) analyzed results of an artificial recharge test in Miyako Island. Methodologies of the artificial recharge test are explained in detail in Ishida et al. (2005). The result of neutron moisture logging is shown in **Fig. 7**, where high rates of counts of thermal neutron are interpreted to be compatible with increased rates of soil moisture. A belt zone of high count rate just after the beginning of recharge might be because discharge of water from a capillary zone directly above the groundwater table (see Sakura, 1989). A high-rate zones were also found at the depths around 7.5 and 9.5 m, which were corresponding to the layers of filling clay. It would be noteworthy that this high-rate counts lasted over 50 hours while that the capillary-zone discharge finished nearly 33 hours after the beginning of recharge. From this, the filling clay may have the buffer effect against the preferential flow. But, this buffer effect did not completely block the downward flow, because the count rate below these layers rose immediately after the recharge.

4 Land Use

The study area is a suburban agricultural area near Naha City, land use in which is typical in Itoman City. It consists mainly of upland fields of sugarcane and vegetables, but several residential areas are situated among the upland fields (**Fig. 8**). Forests are distributed along the fault scarps (**Fig. 8**). Other areas in **Fig. 8** include uncultivated land and public property. Statistical data in Itoman City are shown in **Figs. 9** and **10**.

Urbanization in the area has advanced recently, and the proportion of residential land use and population is gradually increasing

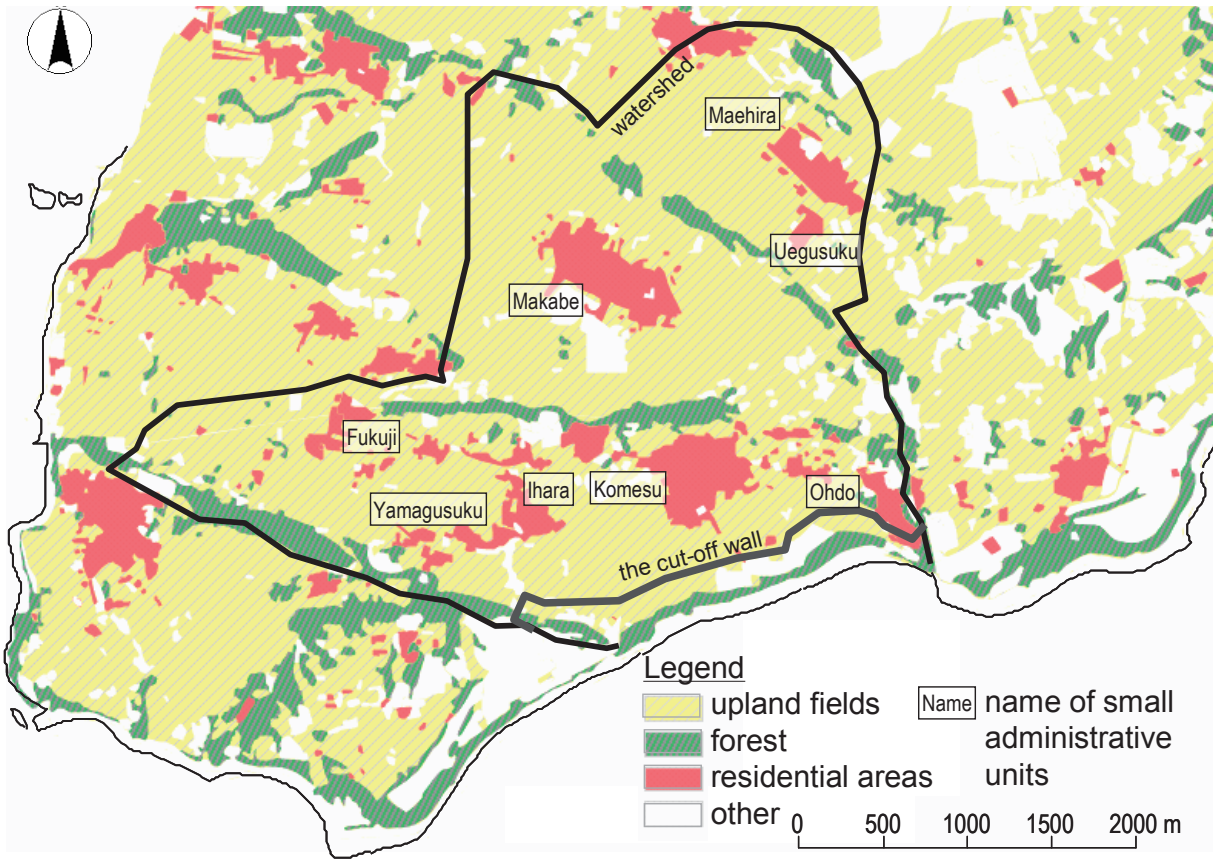

Fig. 8 Land use in the study area (Okinawa Prefecture, 2001)

(**Fig. 9**). In contrast, the total cultivated acreage is gradually declining (**Fig. 9**). In the past, fields were mainly used for sugarcane farming, because sugarcane is drought tolerant. Nowadays, some farmers grow vegetables and flowers of commercial value instead of sugarcane, so the sugarcane yield is decreasing. However, sugarcane is still dominant, and the acreage of sugarcane harvested in Itoman City was 5.30 km^2 in 2006, whereas the acreage of vegetables was 3.16 km^2 in 2006 and that of flowers was 1.01 km^2 in 2007 (Okinawa Prefecture, 2009). A large proportion of the sugarcane cultivation in the study area is done by ratooning. Guidelines for sugarcane cultivation (Okinawa Prefecture, 2006a) recommend that 0.22 kg m^{-2} per year of nitrogen fertilizer be applied and organic materials such as compost be continuously added. Croplands for vegetables and flowers are also similarly fertilized (Okinawa Prefecture, 2003a, 2006b).

Moreover, livestock operations such as hog farms have been established in the residential areas, and the livestock population is increasing (**Fig. 10**). Most of the livestock farms are located in residential areas. In 2005, the number of beef cattle, cows, hogs and chickens in Itoman City was 1,620, 310, 20,300, and 104,000, respectively (Okinawa Prefecture, 2009).

Treatment of livestock manure has gradually improved with the enforcement of the "Law on Promoting Proper Management and Use of Livestock Excreta" established in 1999 (Okinawa Prefecture, 2008). On the other hand, "Law for Promoting the Introduction of Sustainable Agricultural Production Practices", which went into effect in 1999, recommends framers to apply composts for improving soil quality. In addition, transition to environmentally friendly farming including effective use of composts is encouraged in accordance with the principles of the environmental policy in agriculture, forestry and fisheries (MAFF, 2003).

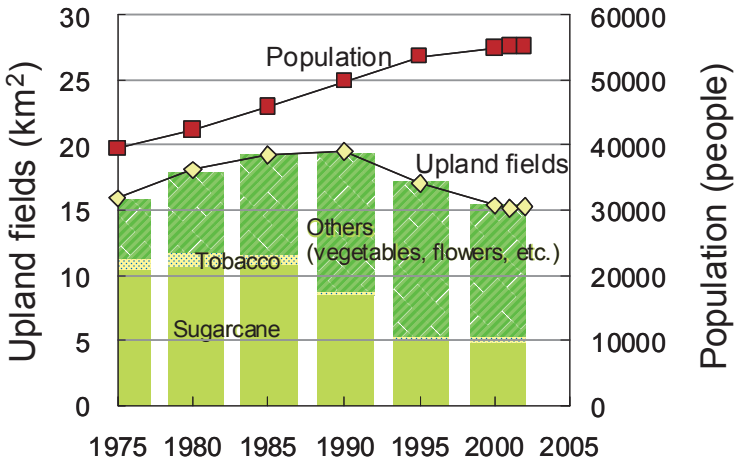

Fig. 9 Acreage of upland fields and population in Itoman City (Okinawa Prefecture, 2003a)

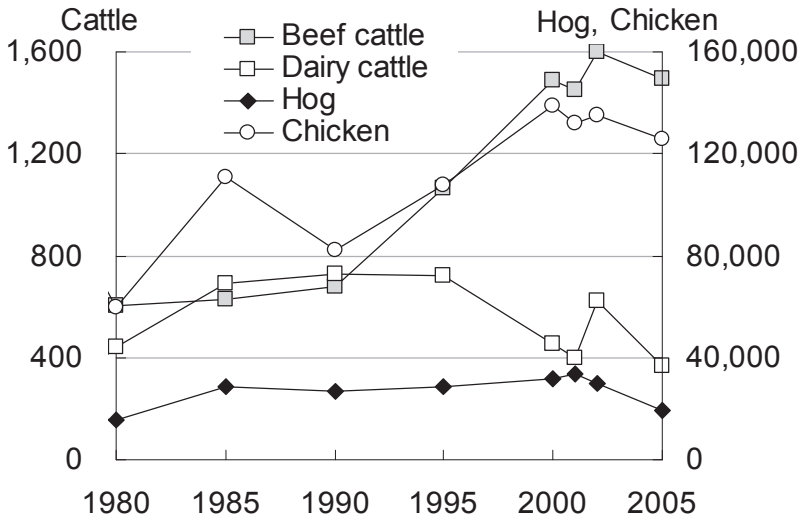

Fig. 10 Numbers of livestock (Okinawa Prefecture, 2003b; 2009)

Domestic wastewater, which is composed of human waste and miscellaneous drainage, in the residential areas is gathered and disposed of mainly by means of septic tanks. In 2006, about 35% of the septic tanks in Itoman City were for the combined treatment of all domestic wastewater, and the rest were old-fashioned tanks for individual treatment of human waste (Ministry of the Environment, 2009). Nitrogen in domestic wastewater generated in the residential areas may leach into the groundwater without sufficient removal, because the old-fashioned tanks have limited capacities for nitrogen removal (Urata et al., 2007) and do not treat wastewater other than human waste.

IV Characteristics of Groundwater Flow and Nitrate Fluctuation in the Ryukyu Limestone Aquifer

1 Introduction

Many researchers have investigated water and solute transport in double-porosity carbonate aquifers, as discussed in Chapter 2. The Quaternary Ryukyu Limestone is also one of carbonate rocks, but much younger than the other rock such as the Chalk which the earlier researches have long dealt with, so groundwater flow conditions might differ between them. The Ryukyu Limestone regions have a lot of caves and caverns with rapid groundwater flow, hence it could be said that conduit-type groundwater flow (fracture flow) exists the aquifer. On the other hand, Shoji et al. (1999) and Momii et al. (2003) applied numerical models based on the Darcy's Law to analyses on groundwater flow in the Ryukyu Limestone aquifer, which implies diffuse-type flow (matrix flow) is also possible. These suggest that groundwater flow in the Ryukyu Limestone aquifer would be “mixed-type”. However, its properties have not been conclusively revealed yet.

In this chapter, changes in groundwater levels and nitrate (NO_3-N) concentrations in the Komesu basin were surveyed, and their characteristics of short-term fluctuations and long-term trends are investigated. In addition, a time-series model was applied to analyses of groundwater hydrographs. The double-porosity condition of the Ryukyu Limestone aquifer was examined from their results.

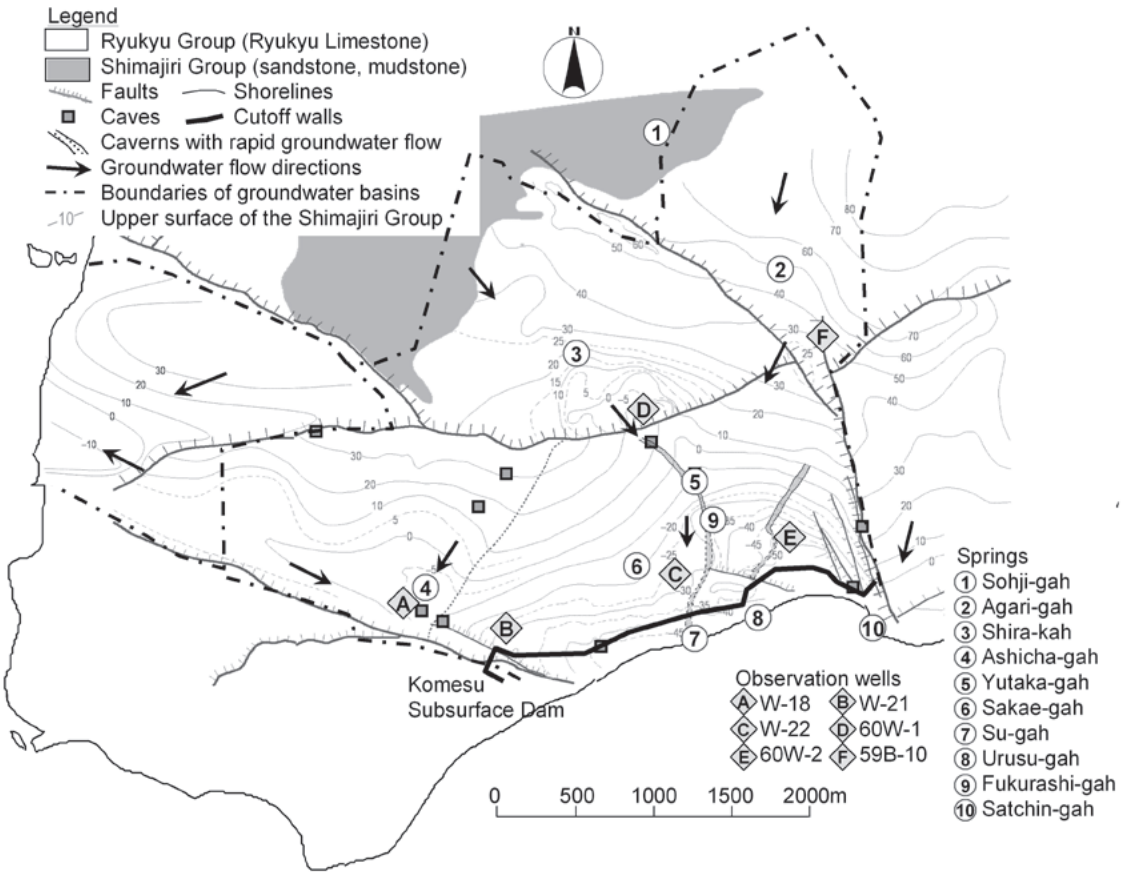

Fig. 11 Observation sites (modified from Okinawa General Bureau, 2006)

2 Methods

a. Research on groundwater levels and NO_3-N concentrations

In preparation for the subsurface dams project, groundwater levels were monitored by the Okinawa General Bureau during 1982–2003 at six wells in the Komesu basin (W-18, W-21, W-22, 60W-1, 60W-2, and 59B-10; **Fig. 11**). Rainfall was also recorded in the downstream area of the basin over this period. For our study, we used the data for the period 1990–1992, which predates the effects of dam construction.

The groundwater quality, including NO_3-N concentration, at springs in and near the study area from 1990 to 2003 and observed groundwater levels in boreholes continuously during the same period had been monitored by Okinawa General Bureau for the subsurface dam project. In this paper, data covering a period from 1990 to 2003 were used for the discussion. The data is not affected by subsurface dam because the subsurface dam was under preparation from 1990 to 2003.

The Nadaraya-Watson estimator (see Simonoff, 1996), a nonparametric regression analysis technique, is applied to the NO_3-N concentration data to smooth the data and clarify their long-term trends

b. Analysis of groundwater hydrographs

Karstification is terrain evolution in which the dissolution of carbonate rocks over time generates karst features, such as caves and sinkholes, and results in the gradual development of an integrated conduit system (Quinlan and Ewers, 1985). Initially, diffuse flow passes through the matrices of younger carbonate aquifers. Conduit systems subsequently develop with time, and the flow in the conduit systems increases. In mature karst aquifers, there is essentially no diffuse flow. The stage between diffuse and conduit flow is referred to as “mixed flow” where diffuse flow coexists with conduit flow in a “mixed aquifer”.

The Quaternary Ryukyu Limestone aquifer is regarded as a mixed aquifer and, as such, would not be suitable for applying a deterministic approach such as a numerical model since it is impossible to determine in detail the spatial distribution of hydrologic properties such as hydraulic conductivity in a mixed aquifer. In hydrology, time-series models are often preferred to mathematical models if no other data except the hydrological time series is available (e.g., Chen et al., 2002, 2004; Yi and Lee, 2004). Here, we applied a statistical model to rainfall and groundwater level data to clarify the differences between diffuse and conduit flow.

Assuming that the groundwater level H at time t at a particular site is proportional to the effective rainfall P (approximately equal to recharge) with a delay (until recharge) of Δt (Chen et al., 2002), then

$$H(t) = \chi + \alpha P(t - \Delta t), \tag{2}$$

where C and α are constants. We defined P as rainfall events exceeding a certain threshold that has an impact on observed recharge events. However, the threshold is influenced not only by antecedent soil-moisture conditions but also by soil-infiltration capacity and evapotranspiration. Since the threshold value in the study area was unclear, we used daily rainfall events as a first-order approximation.

The response of groundwater level to rainfall varies with permeability of the sediments overlying the aquifer (Chen et al., 2002). In accordance with Chen et al. (2002), we considered that rainfall (as observed in the form of aquifer recharge) comprises three components: long-term component P_L, short-term fluctuation P_S, and seasonal variation P_{SV}, and can be written as

$$P = P_L + P_S + P_{SV}, \tag{3}$$

where P_L on the groundwater hydrographs appears as a low-frequency component that slowly responds to rainfall and may reflect lateral flow through the pores in the aquifer. P_S is a high-frequency component that represents rapid vertical groundwater flow via sinkholes and horizontal flow through caves and caverns. P_{SV} represents anthropogenic activity such as groundwater extraction or artificial recharge. Here, we eliminated P_{SV} because there was no large-scale pumping of groundwater for irrigation in the Komesu basin during 1990–1992.

Considering that fluctuations in groundwater levels were driven by two rainfall components, P_L and P_S, Eq. (2) can be rewritten as

$$H(t) = C + \alpha_1\beta\, P_L\,(t - \Delta t_L) + \alpha_2(1 - \beta)\, P_S\,(t - \Delta t_S), \tag{4}$$

where C, α_1 and α_2 are constants, Δt_L and Δt_S are time delays until long- and short-term recharges, and β is the ratio of components

P_L and P_S. Although the time delay Δt was defined by Chen et al. (2002) as the interval between the recharge peak and the groundwater level peak, we used the moving average of rainfall (described below) instead of P_L and P_S and assumed that the time delay (Δt_L and Δt_S) was included in the moving average. The number of sample points (days) included in the moving average (T_{MA}) for the low-frequency component of the response to rainfall was determined at well W-18 from the best correlation between rainfall and groundwater level. For the high-frequency component, the best correlation between rainfall and groundwater level at well 60W-1 was used. The correlation calculation was performed for T_{MA} = 3, 6, 10, 20, 30, 40, 50, 60, 70, 80, 90, 100, and 110 days. T_{MA} = 70 (P_{70} hereafter) and T_{MA} = 6 (P_6) gave the best correlation between rainfall and groundwater level at W-18 and 60W-1, respectively. We therefore equated $P_{70}(t)$ and $P_6(t)$ to $P_L(t - \Delta t_L)$ and $P_S(t - \Delta t_S)$, respectively. For the other wells in the study area, we used the following equation to model the mixture of two rainfall components:

$$H(t) = C + \alpha_1 \beta P_{70} + \alpha_2 (1 - \beta) P_6. \quad (5)$$

The values of C, α_1, α_2 and β was estimated by trial and error so that the correlation between two time series of observed and calculated groundwater levels for each well was the maximum.

3 Results and Discussion

a. Fluctuations in groundwater levels and NO_3-N concentrations

Observed groundwater levels are shown in **Fig. 12**. Groundwater level fluctuations in the boreholes are roughly classified into two types: at type 1 sites, the water level rose rapidly, and at type 2 sites slowly, following a rainfall (**Fig. 13**).

Observed NO_3-N concentrations are shown in **Fig. 14**. Fluctuations of NO_3-N concentration observed at different observation sites are also classified by short-term variation property into two types (**Fig. 15**): type A sites are characterized by large short-term fluctuations, whereas type B sites show much less short-term variation. At all sites, however, values declined over the long term from the mid-1990s.

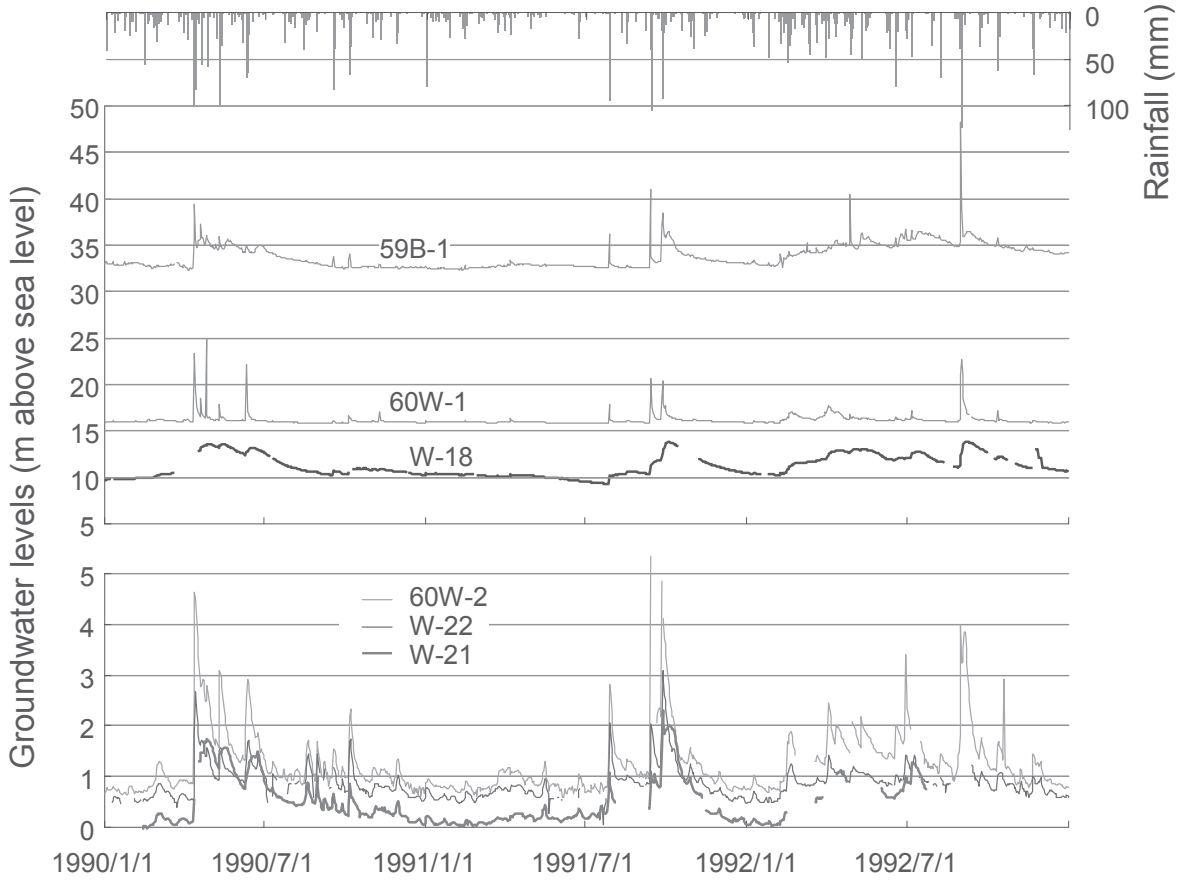

Fig. 12 Fluctuation in rainfall and groundwater levels observed in the Komesu Basin

Type A springs and type 1 boreholes are located near great caverns or caves (**Fig. 11**), which suggests a relationship between type A and type 1 characteristics and caves.

Groundwater behavior in the mix flow aquifer is explained with a schematic model by Drogue (1980) (**Fig. 16**). Type A NO_3-N fluctuations occur near caves, along with type 1 water level fluctuations, because rapid rises in the groundwater following a rainfall result in high concentrations of NO_3-N being quickly diluted by rainwater. In contrast, groundwater flow in a homogeneous aquifer without caves is slow, in accordance with Darcy's law, and therefore type B and type 2 fluctuations are observed.

Meanwhile, sharp NO_3-N declines of type a fluctuations are due to temporal effect of dilution by rainwater, and the long-term trends in NO_3-N for both type A and type B would be same.

b. Existence of two components of groundwater flow

As referring to Eq. (3), fluctuation in rainfall and groundwater levels observed in the Komesu basin (**Fig. 12**) falls into three categories: (1) groundwater levels that peaked about 10 days after a rainfall event ($P = P_L$ in Eq. 2); groundwater fluctuation at W-18

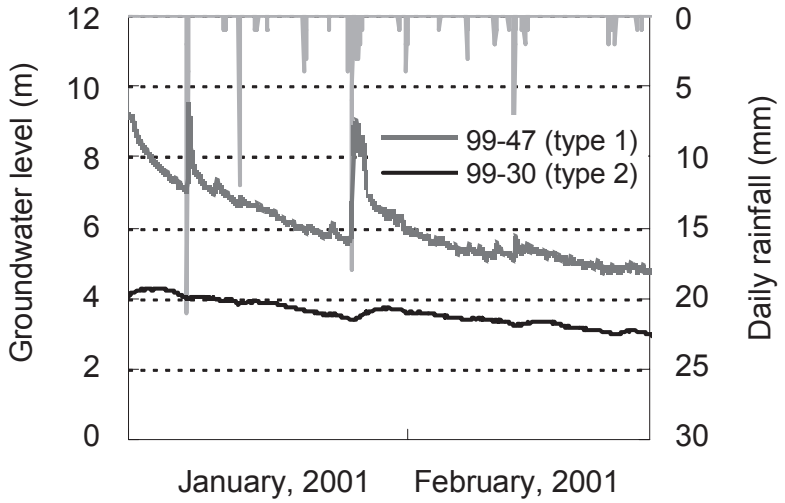

Fig. 13 Categorization of fluctuations of groundwater levels

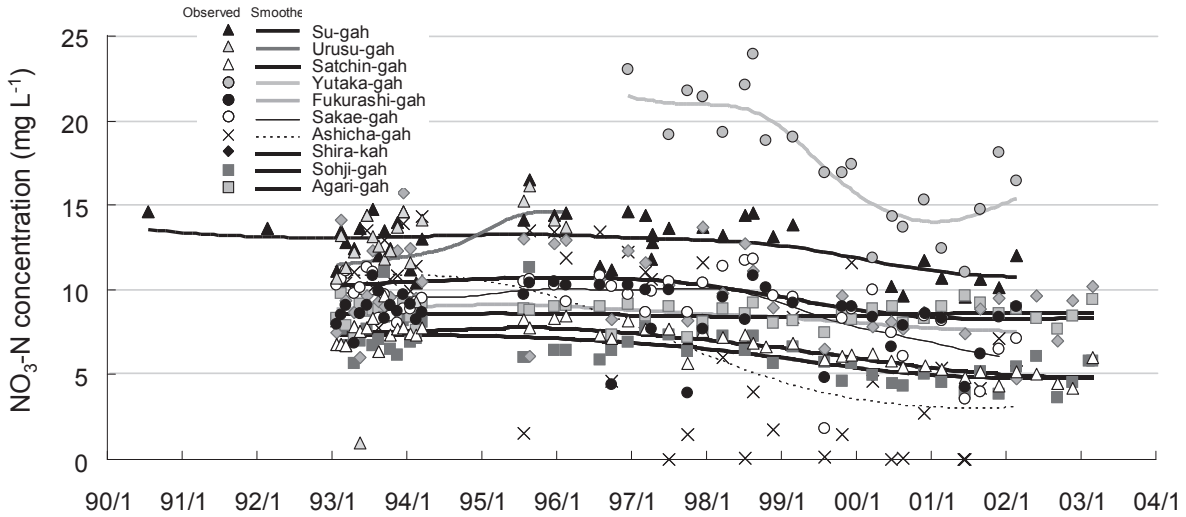

Fig. 14 Observed NO_3-N concentrations in spring waters

was of this type. (2) Groundwater levels that peaked sharply around one day after a rainfall event ($P = P_S$); fluctuations of this type were observed at 60W-1, which is at the entrance to large caverns (**Fig. 11**). (3) Fluctuations observed at W-21, W-22, 60W-2, and 59B-1 represent a mixture of P_L and P_S ($P = P_L + P_S$).

The relationship between T_{MA} and the correlation coefficients between moving-average rainfall and groundwater level is shown in **Fig. 17**. The relationship between the moving-average rainfall for T_{MA} = 6 and 70 days and the groundwater level at wells W-18 and 60W-1 is also shown. The value of T_{MA} that showed the strongest correlation at W-18 was 70 days (R = 0.84). The strongest correlation at well 60W-1 was for T_{MA} = 6 (R = 0.56). Therefore, 70 and 6 days were used as the values of T_{MA} for the low- and high-frequency components, respectively, of the groundwater response to rainfall. At W-21, the strongest correlation was for T_{MA} = 50 (R = 0.81; **Fig. 17**). At W-22, 60W-2, and 59B-1, the correlation coefficients were lower than 0.45 for all values of T_{MA} up to 110 days (**Fig. 17**).

The estimated values of C, α_1, α_2 and β are shown in **Table 2**. The observed groundwater levels at 60W-2 and those calculated from Eq. (5) are shown in **Fig. 18**. The correlation became stronger (R = 0.81; **Fig. 18**) than that between the observed groundwater

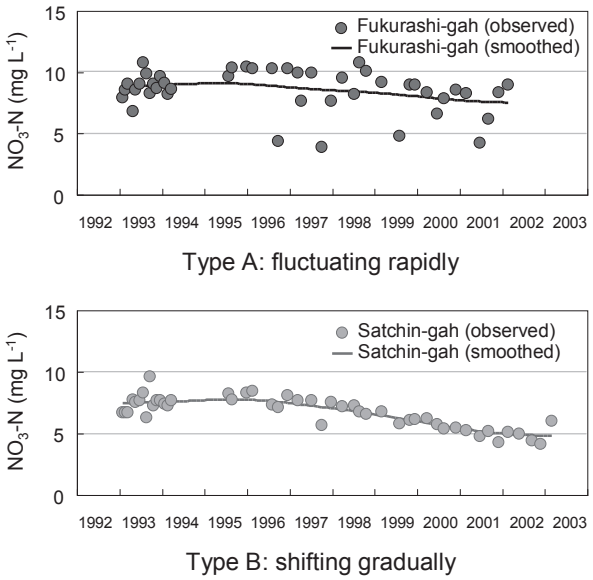

Fig. 15 Categorization of fluctuations of NO_3-N concentrations

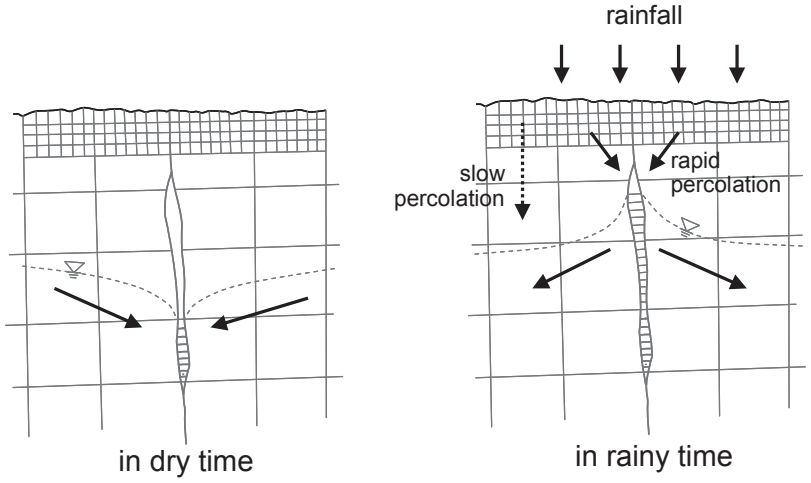

Fig. 16 Percolation and infiltration mechanism in the karst aquifer of caves (Drouge, 1980)

level and the effective rainfall (R = 0.45), which showed that the model in Eq. (5) adequately represented the mixture of the two rainfall components denoted by $P = P_L + P_S$.

The properties of groundwater flow in the Ryukyu Limestone aquifer were investigated from groundwater hydrographs. The fluctuations in groundwater level observed at W-18 and 60W-1 (**Fig. 12**) were regarded as representative low- and high-frequency responses to rainfall, and their period of the moving average (T_{MA}) was calculated as 70 and 6 days from the correlation analyses (**Fig. 17**), respectively. The low-frequency response was interpreted to reflect slow diffuse groundwater flow in the rock matrix, and the high-frequency response to reflect rapid conduit flow in the caves and caverns. The calculated T_{MA} value of 70 days was considered to represent the travel time from rainfall input to groundwater for diffuse flow, and T_{MA} of 6 days for conduit flow. 60W-1 which is located at the entrance to one of the large caverns (**Fig. 11**) supported the existence of conduit flow at that location.

The groundwater response to rainfall was likely to be mixed at the other well sites. W-21 and 59B-1 are located far away from any known caves and caverns (**Fig. 11**), and the mixture ratio (β) at these wells was calculated to be higher than that at 60W-2 and W-22 (**Table 2**), suggesting that W-21 and 59B-1 were in areas where diffuse flow is predominant. In contrast, 60W-2 and W-22 are located within 200 m of large caverns (**Fig. 11**), where the effect of conduit flow might be stronger.

4 Conclusions

Fluctuation characteristics of groundwater levels and NO_3-N concentrations in the Ryukyu Limestone aquifer were studied, and the hydrogeological properties of the Ryukyu Limestone aquifer was discussed.

The short-term fluctuations of NO_3-N concentrations in groundwater are classified into two types: large short-term fluctuations

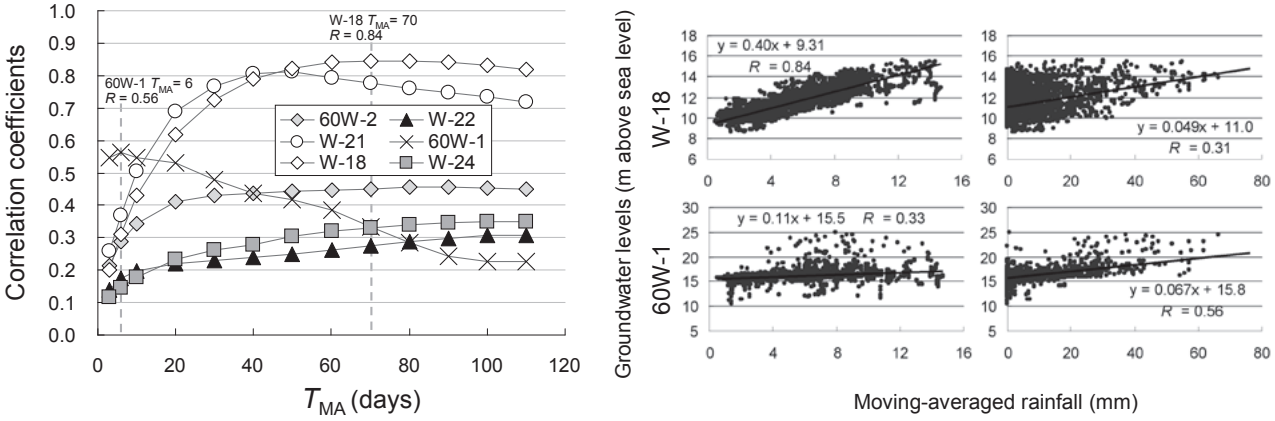

Fig. 17 Relationship between the period of moving average (T_{MA}) and correlation coefficients (R) between the moving-average rainfall and the groundwater levels, and the relationship between the moving-average rainfall for T_{MA} = 6, 70 days and the groundwater level at W-18 and 60W-1

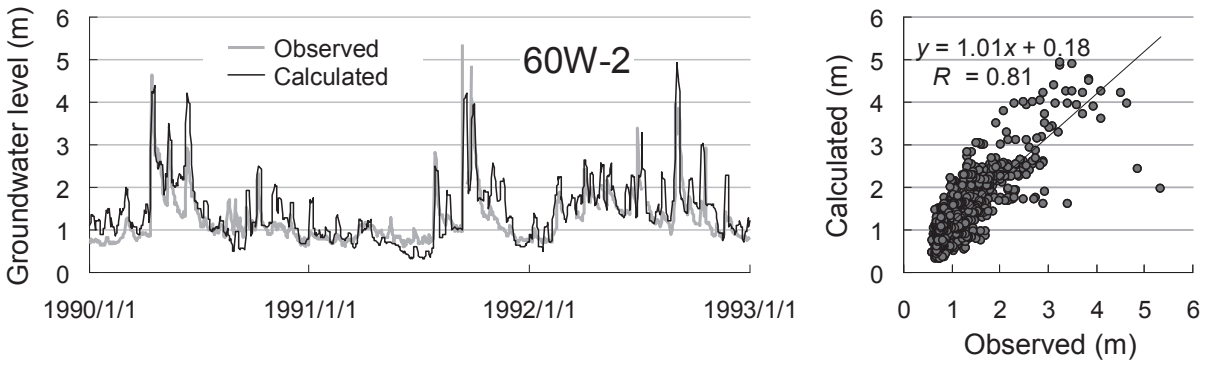

Fig. 18 Change in the groundwater level at 60W-2 and calculated groundwater level from R_{70} and R_6 using the model of Eq. (5), and relationship between the observed and calculated groundwater levels at 60W-2

Table 2 Estimated values of α 1, α 2, β and C in Eq. (5)

	α_1	α_2	β	C
W-18	0.40	0	1	9.31
60W-1	0	0.067	0	15.8
60W-2	0.59	0.11	0.32	0.20
W-22	0.10	0.050	0.60	0.41
W-21	0.13	0.30	0.98	0.00
59B-1	0.60	0.60	0.96	31.0

(type a) and small short-term fluctuations (type b). The springs showing type a fluctuation were near caves, where rainwater rapidly enters the groundwater and dilutes the NO_3-N concentration. Similarly, boreholes in which groundwater level rose rapidly after rainfall events are also located near caves. These imply that the aquifer has both diffuse- and conduit-type groundwater flow. On the other hand, the long-term trend in NO_3-N concentration observed at springs of both types was generally decreasing from the mid-1990s.

In addition, groundwater hydrographs were analyzed with application of a time-series model. The hydrographs can be decomposed into low- and high-frequency components. The low-frequency response was interpreted to reflect slow diffuse groundwater flow in the rock matrix, and the high-frequency response to reflect rapid conduit flow in the caves and caverns. Simultaneous appearance of these components also suggested that the Ryukyu Limestone is a "mixed flow" aquifer with the coexistence of slow diffuse flow in the matrices and rapid conduit flow in the caves and caverns.

V Transport and Potential Sources of Groundwater Nitrates in the Ryukyu Limestone as a Mixed Flow Aquifer

1 Introduction

The southern part of Okinawa Island is a suburban region with many livestock farms as well as numerous agricultural farms growing mainly vegetables and sugarcane. Nitrate concentration in the groundwater had increased until the mid-1990s, and was believed to be caused by chemical fertilizer applied to upland fields (e.g., Agata et al., 2001).

In this area, two subsurface dams were completed in 2005 (Nawa and Miyazaki, 2009). Imaizumi et al. (2002a) demonstrated that caves and caverns in the Ryukyu Limestone aquifer had a significant effect on groundwater flow in the Komesu subsurface dam basin. The rapid groundwater flow may increase short-term fluctuations in nitrate concentration in the groundwater near caves and caverns. Therefore, it is necessary to identify the predominant nitrogen sources in order to understand the impact of rapid groundwater flow on the nitrogen loading process. However, there has currently been no investigation on groundwater nitrates under the condition of such groundwater flow characteristics.

The objective of this chapter is to clarify how the transport of groundwater nitrates are affected by the state of groundwater flow closely associated with hydrogeological features such as caves and caverns in the Ryukyu Limestone aquifer. Here, the ratio of two stable isotopes of nitrogen in nitrate, ^{14}N and ^{15}N, and radon (^{222}Rn) were used as tracers to evaluate the transport of nitrates in groundwater.

2 Methods

a. Estimation of nitrogen emission

An emission factor model is used to estimate nitrogen loads in Itoman City from statistical data, where an emission factor is defined as nitrogen emission in relation to the area under cultivation, number of livestock, or number of people, and the load factor is defined as ratio of leached nitrogen to emitted nitrogen. Chemical fertilizer applied to sugarcane fields, livestock manure, and domestic wastewater are considered as anthropogenic nitrogen sources and calculated the total nitrogen load as the sum of the loads from these three sources. Emission factor values are set following Tashiro and Takahira (2001; see **Table 3**), except the basic unit of chemical fertilizer is doubled because of differences in the sugarcane planting system between our study area and Miyako Island, where Tashiro and Takahira (2001) conducted their study. In addition, the amount of nitrogen absorbed by sugarcane is accounted for

following Tokuyama et al. (1990), who calculated the plant uptake as 0.081% of the sugarcane yield. All statistical data are obtained from the Statistics Department, Ministry of Agriculture, Forestry and Fisheries, Japan (1972–1991) and the Okinawa General Bureau (1993–2002).

The estimated amounts of nitrogen emission were compared to the long-term changes in NO_3-N concentrations in groundwater (**Fig. 14**), to discuss the predominant nitrogen source affecting the groundwater quality.

b. Analysis of water quality

Sampling

Shallow groundwater samples were collected in February 2007, March 2008 and January 2009 from 17 springs and from the observation facilities (OF) of the two subsurface dams in the study area (**Figs. 19** and **20**).

The sampling sites were categorized, based on rate of land use (upland fields, residential areas, and others plus forests; **Fig. 20**) in a fan-shaped area with a 600-m influential zone on the upstream side, into three types: upland field (UF), residential area (RA), and cave and cavern (CC). The influential radius was set to 600-m as a product of T_{MA} in the matrices of the aquifer (70 days; see details below) and hydraulic conductivity (1.0×10^{-4} m s^{-1}). Rates of land use in the fan-shaped area are shown in **Fig. 21**. The RA type is

Table 3 Values of the emission factor and the load factor

		Emission factor	Load factor
Chemical fertilizer		22,880 kg km^{-2} year^{-1} *	
Livestock manure	cattle	140 g animal^{-1} day^{-2} **	
	hogs	47 g animal^{-1} day^{-2} **	0.39‡
	chickens	2 g animal^{-1} day^{-2} **	
Domestic wastewater		17 g person^{-1} day^{-2} ***	

*See text, ** Tsuiki and Harada (1994), ***Nishiguchi (1986), ‡ Tashiro and Takahira (2001)

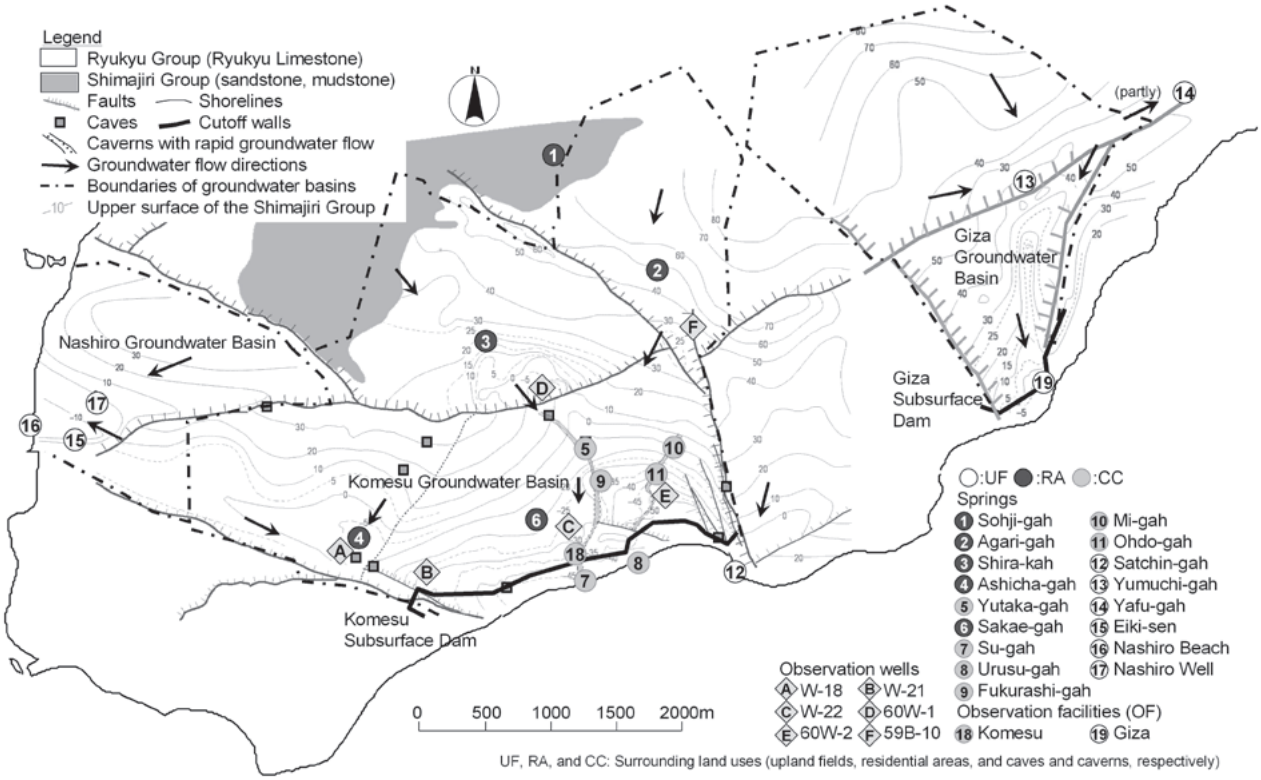

Fig. 19 Geological settings and the sampling sites (Okinawa General Bureau, 2006)

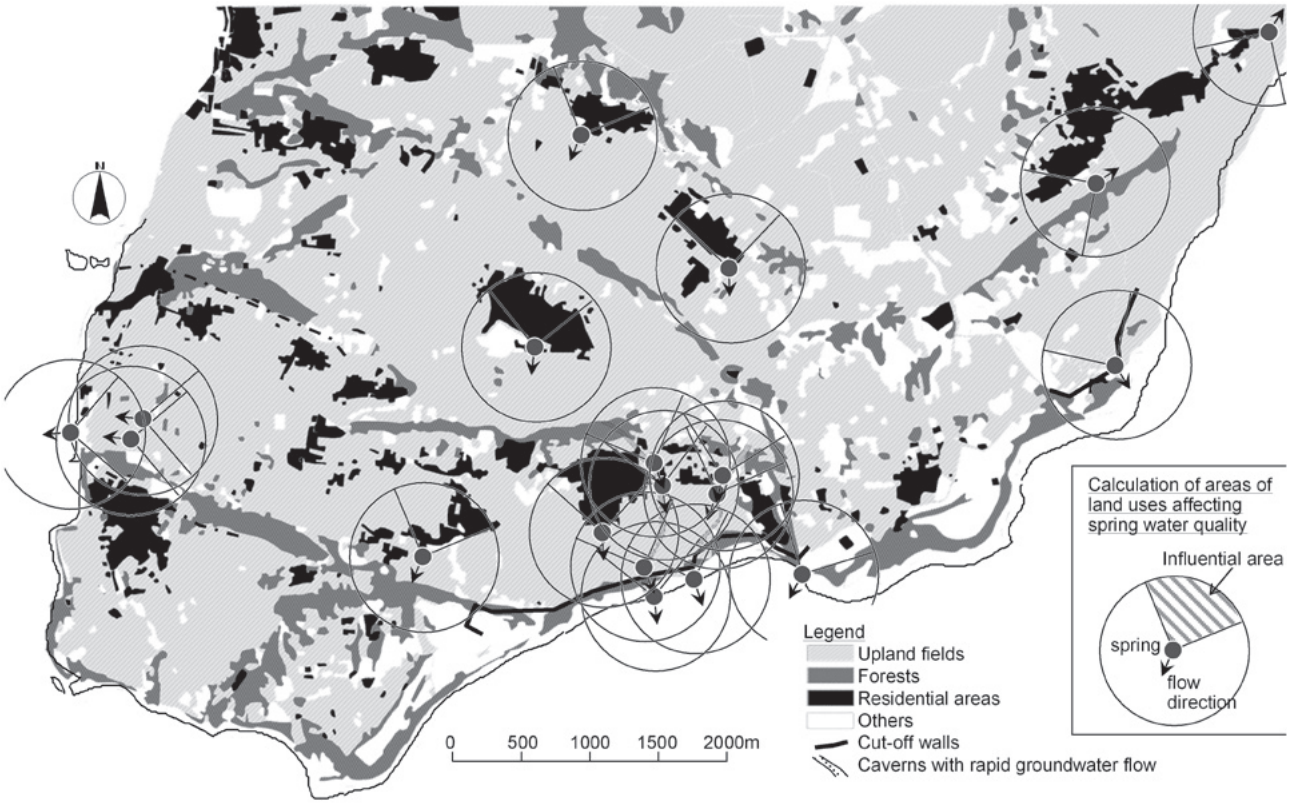

Fig. 20 Land use in the study area (modified from Okinawa Prefecture, 2001)

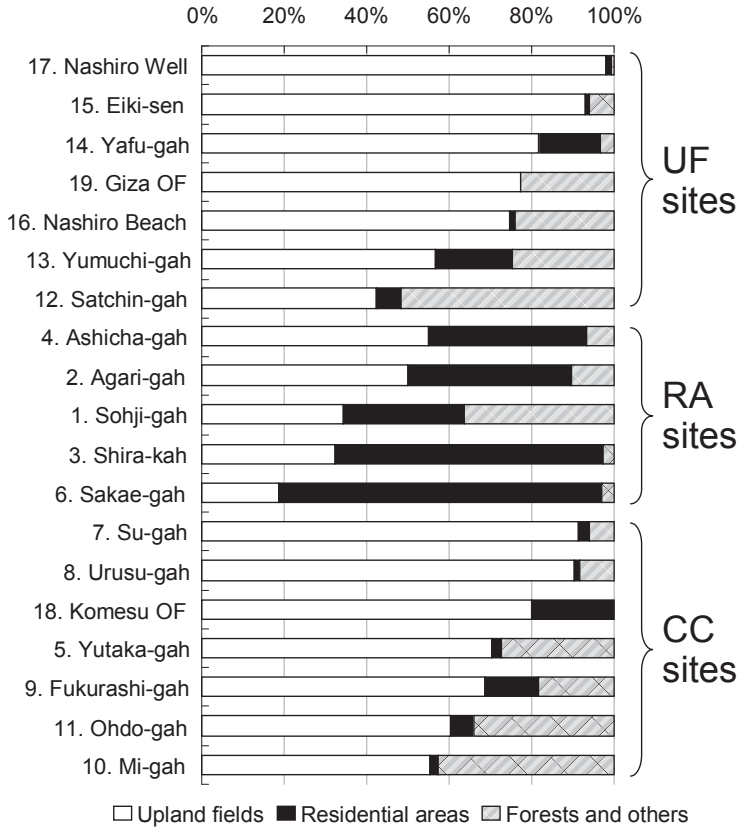

Fig. 21 Rate of land use in the 600-m influential zone of the sampling sites in this study

defined as residential areas covering over 20% of the fan-shaped area. The UF type is defined as residential areas covering 0–20%, and upland fields covering at least 40%. Those near the two caverns in the Komesu Groundwater Basin were separately categorized as the CC type, even though they should be categorized as UF in terms of land use (residential areas: 1–20%, upland fields: 55–91%).

Analyses

Concentration of major ions including NO_3-N in the collected samples was analyzed by ion chromatography (ICA-2000, DKK-TOA, Japan). HCO_3^- concentration was determined as pH 4.8 alkalinity by titration. All chemical analyses showed a balance within ±10%. For isotopic analyses, nitrate samples were enriched by the freeze-drying method (Böhlke and Denver, 1995) and then converted to N_2 gas by quartz tube combustion for mass spectrometry (FlashEA 1112, Thermo Fisher Scientific, USA). The N_2 gas was analyzed for $\delta^{15}N$ by isotope ratio mass spectrometry (Delta V Advantage, Thermo Fisher Scientific, USA) with a reproducibility of 0.15‰. Here, the value of $\delta^{15}N$ is defined by the following equation:

$$\delta^{15}N = ({}^{15}N_{sample}/{}^{14}N_{sample} - {}^{15}N_{air}/{}^{14}N_{air}) / {}^{15}N_{air}/{}^{14}N_{air} \times 1000\ [‰], \quad (6)$$

where ${}^{15}N_{sample}/{}^{14}N_{sample}$ is the ratio in samples, and ${}^{15}N_{air}/{}^{14}N_{air}$ is the ratio in air.

Radon (^{222}Rn) concentration in water samples collected in 2007 and 2009 was measured using a liquid scintillation counter (Tri-Carb 2250CA, Packard BioScience, USA) after in situ extraction with toluene following the methods of Hamada and Komae (1998). The total error was less than 0.05 Bq L^{-1}.

Estimation of contribution rates of nitrogen sources

Oelmanna et al. (2007) assumed that nitrates in the soil originate from three sources: (1) rainfall, (2) mineralization of leguminous soil organic matter (SOM), and (3) mineralization of non-leguminous SOM. They calculated the contribution of each source to $\delta^{15}N$ and $\delta^{18}O$ values in NO_3^- of soil solution using a standard linear mixing model based on these three sources. We assumed that nitrates in the groundwater originated from (1) chemical fertilizer application (CF), (2) livestock and human waste (LH), and (3) soil nitrogen (SN). We calculated the contribution ratios from these nitrogen sources: R_{CF}, R_{LH}, and R_{SN} using the linear mixing model (Oelmanna et al., 2007).

When representative $\delta^{15}N$ values are given for the groundwater nitrates derived solely from CF, LH, and SN, denoted as X_{CF}, X_{LH}, and X_{SN}, respectively, the values of R_{CF}, R_{LH}, and R_{SN} can be associated with the observed NO_3-N concentration, C_{obs}, and $\delta^{15}N$ values, X_{obs}, by means of the following simultaneous mass balance equations (Nakanishi et al., 1995):

$$1 = R_{CF} + R_{LH} + R_{SN}, \quad (7)$$

$$X_{obs} \approx X_{CF}R_{CF} + X_{LH}R_{LH} + X_{SN}R_{SN}. \quad (8)$$

Eq. (7) can be rewritten to the equation of NO_3-N concentration, as follows:

$$C_{obs} = C_{CF} + C_{LH} + C_{SN}, \quad (9)$$

where C_{CF}, C_{LH}, and C_{SN} are components of NO_3-N concentration from CF, LH, and SN, equal to $C_{obs}R_{CF}$, $C_{obs}R_{LH}$, and $C_{obs}R_{SN}$, respectively.

R_{SN} is a natural component free from anthropogenic influences such as cultivation and livestock farming. Here, nitrates in groundwater from SN were assumed to always be loaded as a constant concentration, C_{SN}, the value of which was determined from literature, as described below. Therefore, R_{SN} is given from C_{SN} and C_{obs}. On Miyako Island, Nakanishi et al. (1995) set the value of C_{SN} to 1.4 mg L^{-1}, from the observed NO_3-N concentration at wells that were free from anthropogenic impact, and Kondo et al. (1997) reported that the NO_3-N concentration beneath forest and wasteland ranged from 1.8–2.1 mg L^{-1}. In this study, 1.4 mg L^{-1} was employed as the value of C_{SN}. This was considered an appropriate assumption in view of the values obtained in past research, e.g., 0.9–2.3 mg L^{-1} at unpolluted wells in a sandstone aquifer in Israel (Oren et al., 2004).

To obtain the values of R_{CF} and R_{LH} from Eqs. (7) and (8), the values of X_{CF}, X_{LH}, and X_{SN} were needed, as well as the value of C_{SN}. We could not directly use the $\delta^{15}N$ values of the water from a sewage treatment site as X_{LH} and the incubation water from commercial

inorganic fertilizers as X_{CF} because these samples had not undergone any nitrogen processes in the actual field, such as ammonia volatilization and denitrification, although the values of X_{CF}, X_{LH}, and X_{SN} should have been determined from the results of $\delta^{15}N$ analyses of groundwater affected only by CF, LH, or SN, respectively. However, it was impossible to sample groundwater affected by a single source, and the effects of isotopic fractionation during ammonia volatilization and denitrification were not yet quantified. For these reasons, in this study, the values of X_{CF}, X_{LH}, and X_{SN} were tentatively determined from literature. The range of $\delta^{15}N$ values in the referred literature and the values applied to this study are shown in **Fig. 3**. The values of X_{CF}, X_{LH}, and X_{SN} were set to 3‰, 15‰, and 4‰, which are the intermediate value in groundwater nitrates derived from CF, LH, and SN, respectively. In this study, we lumped together the contribution rates from LH as R_{LH}, and estimated its value, because it is difficult to distinguish between these nitrogen sources by $\delta^{15}N$ values in groundwater nitrates (e.g., Heaton, 1986).

3 Results

a. Trend of nitrogen emissions

Estimated nitrogen loads from livestock manure and domestic wastewater increased overall from 1975 (**Fig. 22**), and, accordingly, the total load shows an increasing trend, even though the load from chemical fertilizer gradually decreased after peaking around 1990.

Comparing **Fig. 22** to **Fig. 14**, the trend in NO_3-N concentration at the springs matched only to that in nitrogen emission from chemical fertilizer. From this, it was thought that the changes in NO_3-N concentration could be explained by the inference that the groundwater was affected predominantly by chemical fertilizer.

The emitted nitrogen in domestic wastewater was smaller than the others, and generally, sewer systems were installed in residential areas. In addition, treatment of livestock manure has gradually improved with the enforcement of the "Law on Promoting Proper Management and Use of Livestock Excreta" established in 1999 (Okinawa Prefecture, 2008). Moreover, because most of the livestock farms are located in the residential areas, the farmers have disposed of livestock manure to prevent foul smell in consideration of the neighborhood. Therefore, the effect of livestock manure on groundwater quality seems to be relatively small.

On the other hand, chemical fertilizer is applied on the field directly. Redundant chemical fertilizer can easily be dissolved in rainwater and leach to the groundwater, because the soil in the study area, called "Shimajiri Maji", is made from weathered limestone and of less water receptivity. This fact is also consistent the inference that chemical fertilizer would affect the groundwater quality significantly.

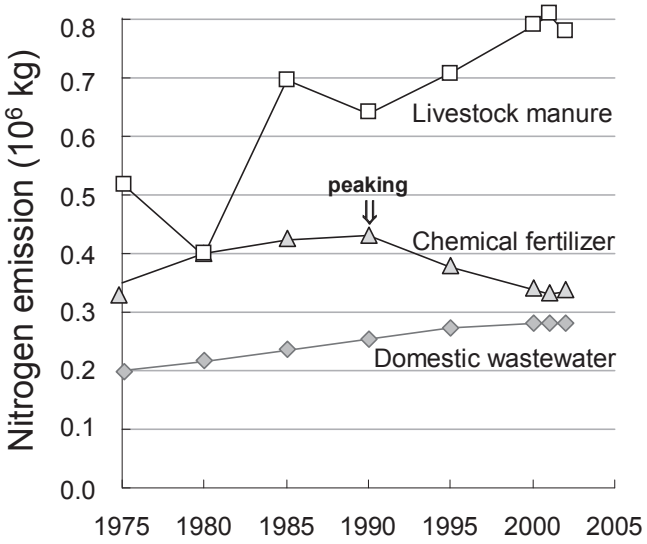

Fig. 22 Estimated nitrogen emission from chemical fertilizer, livestock manure, and domestic wastewater in Itoman City

Table 4 Nitrate concentration, nitrogen isotopic composition in nitrates, and radon concentration in the groundwater in the study area

	Type	Sampling date	Na^+ [mg L^{-1}]	K^+ [mg L^{-1}]	Mg^{2+} [mg L^{-1}]	Ca^{2+} [mg L^{-1}]	HCO_3^- [mg L^{-1}]	Cl^- [mg L^{-1}]	SO_4^{2-} [mg L^{-1}]	NO_3-N [mg L^{-1}]	$\delta^{15}N$ [‰]	^{222}Rn [Bq L^{-1}]	C/A ratio
In 2007													
Springs													
1. Sohji-gah	RA	2007/2/28 15:05	34.0	7.8	7.3	93.0	201.2	51.6	51.0	9.2	9.6	13.5	1.07
2. Agari-gah	RA	2007/2/28 15:40	29.9	5.4	10.4	115.6	274.4	42.9	98.8	11.3	10.0	2.3	0.94
3. Shira-kah	RA	2007/2/28 14:42	39.6	8.2	11.3	100.2	262.2	48.4	71.0	8.9	11.0	5.5	1.01
4. Ashicha-gah	RA	2007/2/27 16:00	41.1	7.9	13.8	135.5	347.5	59.1	98.1	9.4	10.3	7.9	0.98
5. Yutaka-gah	CC	2007/2/28 14:14	43.4	13.8	15.6	151.5	414.6	60.9	134.5	10.7	13.1	0.6	0.96
6. Sakae-gah	RA	2007/2/28 9:45	37.2	5.7	7.7	85.7	256.1	50.4	61.9	7.5	10.0	4.3	0.90
7. Su-gah	CC	2007/2/27 17:49	39.7	9.1	14.0	123.8	274.4	57.1	121.0	11.5	12.3	1.1	0.98
8. Urusu-gah	CC	2007/2/27 18:10	41.8	8.8	14.1	131.7	371.9	55.1	115.0	9.4	10.6	8.4	0.92
9. Fukurashi-gah	CC	2007/2/28 10:00	43.1	6.2	14.0	126.6	250.0	60.0	122.0	11.0	8.9	1.2	1.04
10. Mi-gah	CC	2007/2/28 10:35	34.7	5.8	11.6	107.7	286.6	48.3	96.5	8.5	12.0	1.3	0.92
11. Ohdo-gah	CC	2007/2/28 10:17	41.8	7.9	13.2	116.3	250.0	57.4	105.5	10.1	9.2	1.3	1.03
12. Satchin-gah	UF	2007/2/28 11:35	64.7	6.0	13.2	154.7	286.6	98.4	127.7	8.5	6.1	1.7	1.10
13. Yumuchi-gah	UF	2007/2/28 16:20	37.6	4.5	7.6	109.3	298.8	54.2	56.7	7.1	9.9	2.2	0.97
14. Yafu-gah	UF	2007/2/28 17:30	34.9	3.8	8.9	120.2	335.3	50.0	63.6	11.3	8.6	9.5	0.92
15. Eiki-sen	UF	2007/2/28 13:50	40.9	8.1	13.2	128.5	256.1	61.2	110.6	18.3	9.2	5.6	1.00
16. Nashiro Beach	UF	2007/2/28 12:15	507.0	23.3	67.7	139.4	317.0	887.9	206.0	15.7	7.9	5.7	0.99
17. Nashiro Well	UF	2007/3/1 9:38	45.6	6.9	15.5	151.8	286.6	64.3	117.9	18.9	8.6	6.0	0.97
Observation facilities of the subsurface dams													
18. Komesu	CC	2007/2/27 17:10	40.4	6.4	10.8	105.0	262.2	59.1	94.2	8.1	11.0	7.2	0.95
19. Giza	UF	2007/2/28 16:35	38.3	2.8	8.6	113.8	274.4	55.4	62.9	8.0	9.5	3.6	1.02
In 2008													
Springs													
1. Sohji-gah	RA	2008/3/4 9:48	31.9	6.9	5.7	76.8	176.8	46.4	41.5	5.5	8.4	—	1.07
2. Agari-gah	RA	2008/3/4 10:00	29.1	3.9	10.3	108.4	189.0	40.7	96.5	10.6	9.1	—	1.09
3. Shira-kah	RA	2008/3/4 9:35	48.5	9.6	10.9	94.1	231.7	58.1	66.8	9.1	11.6	—	1.06
4. Ashicha-gah	RA	2008/3/4 13:55	36.2	7.1	11.5	114.7	231.7	51.5	86.1	8.9	9.4	—	1.10
5. Yutaka-gah	CC	2008/3/4 15:20	50.2	11.0	16.1	149.9	304.8	69.1	135.0	14.6	10.9	—	1.04
6. Sakae-gah	RA	2008/3/4 14:13	43.8	9.3	8.9	98.6	195.1	60.8	75.2	8.9	9.4	—	1.10
7. Su-gah	CC	2008/3/4 14:31	38.5	7.1	11.9	122.6	237.8	52.4	110.2	10.7	10.0	—	1.06
8. Urusu-gah	CC	2008/3/4 14:44	47.3	4.4	12.7	122.3	286.6	66.9	105.1	9.0	10.5	—	0.99
9. Fukurashi-gah	CC	2008/3/4 15:10	35.5	4.7	11.6	111.5	225.6	50.1	103.0	9.6	8.9	—	1.03
10. Mi-gah	CC	2008/3/4 11:13	35.3	5.5	11.5	113.7	243.9	50.6	100.5	9.7	9.2	—	1.01
11. Ohdo-gah	CC	2008/3/4 14:55	32.4	4.4	11.3	90.3	207.3	44.9	93.0	8.9	7.9	—	0.96
12. Satchin-gah	UF	2008/3/4 11:28	71.8	4.9	13.9	116.4	262.2	110.6	91.0	6.0	7.1	—	1.05
13. Yumuchi-gah	UF	2008/3/4 10:37	35.2	3.8	7.6	105.6	256.1	50.7	53.7	7.0	9.1	—	1.04
14. Yafu-gah	UF	2008/3/4 10:26	37.0	5.2	9.5	131.2	262.2	55.8	76.0	11.1	9.3	—	1.10
15. Eiki-sen	UF	2008/3/4 13:24	36.7	6.2	12.8	127.0	292.7	54.9	97.4	14.7	8.4	—	0.97
16. Nashiro Beach	UF	2008/3/4 11:56	471.1	21.1	67.2	133.3	268.3	837.2	188.5	12.4	7.4	—	1.01
17. Nashiro Well	UF	2008/3/4 13:36	38.6	7.1	14.1	128.6	268.3	56.8	102.6	14.8	8.6	—	1.03
Observation facilities of the subsurface dams													
18. Komesu	CC	2008/3/4 14:24	40.9	5.7	11.1	119.3	250.0	62.4	88.5	9.8	10.0	—	1.05
19. Giza	UF	2008/3/4 10:46	33.4	3.0	6.5	108.3	256.1	51.0	61.1	7.3	9.0	—	1.01

Table 4 Nitrate concentration, nitrogen isotopic composition in nitrates, and radon concentration in the groundwater in the study area (cont.)

	Type	Sampling date	Na^+ [mg L^{-1}]	K^+ [mg L^{-1}]	Mg^{2+} [mg L^{-1}]	Ca^{2+} [mg L^{-1}]	HCO_3^- [mg L^{-1}]	Cl^- [mg L^{-1}]	SO_4^{2-} [mg L^{-1}]	NO_3-N [mg L^{-1}]	$\delta^{15}N$ [‰]	^{222}Rn [Bq L^{-1}]	C/A ratio
In 2009													
Springs													
1. Sohji-gah	RA	2009/1/29 10:00	35.2	4.9	4.7	72.0	164.6	41.3	38.9	6.5	9.9	5.6	1.10
2. Agari-gah	RA	2009/1/29 10:30	38.3	5.4	9.8	106.0	225.6	43.2	91.6	12.7	9.5	2.6	1.07
3. Shira-kah	RA	2009/1/30 9:10	54.8	7.6	5.6	71.7	189.0	52.9	39.8	11.0	11.8	2.1	1.10
4. Ashicha-gah	RA	2009/1/30 10:35	48.6	4.6	10.2	102.6	250.0	43.6	70.8	9.0	9.5	9.2	0.99
5. Yutaka-gah	CC	2009/1/30 10:18	50.4	6.4	12.9	129.5	256.1	53.7	117.3	12.4	10.7	0.8	1.09
6. Sakae-gah	RA	2009/1/29 16:50	47.9	5.9	7.0	78.6	225.6	49.8	53.5	8.6	10.7	3.9	0.96
7. Su-gah	CC	2009/1/29 17:26	46.8	4.6	10.0	107.7	219.5	48.7	92.3	10.4	10.7	1.3	1.09
8. Urusu-gah	CC	2009/1/29 17:40	63.8	3.5	11.3	110.8	243.9	69.5	99.6	9.4	10.5	6.9	1.07
9. Fukurashi-gah	CC	2009/1/29 16:33	45.1	4.6	9.6	93.2	219.5	49.3	88.7	10.8	10.5	1.3	0.99
10. Mi-gah	CC	2009/1/29 14:10	48.4	6.0	11.0	101.7	256.1	51.9	98.2	10.6	10.5	2.4	0.97
11. Ohdo-gah	CC	2009/1/29 14:25	45.8	6.4	10.9	104.5	298.8	50.9	101.2	10.5	10.7	1.6	1.04
12. Satchin-gah	UF	2009/1/29 15:05	646.1	15.9	63.7	109.6	243.9	970.4	207.9	6.7	7.6	1.5	1.08
13. Yumuchi-gah	UF	2009/1/29 12:02	41.5	2.9	6.8	100.7	250.0	49.3	56.8	8.2	9.1	2.4	1.03
14. Yafu-gah	UF	2009/1/29 11:12	47.4	3.5	8.4	110.4	268.3	54.2	67.6	10.9	8.9	9.2	1.03
15. Eiki-sen	UF	2009/1/29 18:35	45.5	5.3	11.7	114.7	280.5	49.7	88.4	16.8	8.4	6.8	0.97
16. Nashiro Beach	UF	2009/1/30 12:22	—	—	—	—	—	—	—	—	—	1.5	—
17. Nashiro Well	UF	2009/1/29 18:15	45.6	4.5	11.5	114.0	195.1	52.0	93.6	18.6	8.2	6.4	1.10
Observation facilities of the subsurface dams													
18. Komesu	CC	2009/1/29 17:15	44.9	5.6	9.6	102.5	219.5	49.6	95.6	10.4	11.7	7.4	0.90
19. Giza	UF	2009/1/29 12:12	44.0	3.1	8.0	101.7	274.4	52.8	62.9	8.1	9.4	3.8	0.98

* NO_3-N concentration and $\delta^{15}N$ value in the sample collected at Nashiro Beach in 2009 could not be analyzed due to high salinity.

b. Water quality

Concentration of major ions and NO_3-N

The Piper diagram of groundwater chemistry in the study area is shown in **Fig. 23**. The major ion compositions of all of the samples in this study were categorized as $Ca(HCO_3)_2$ type, with several exceptions for UF. Since some of the UF-type sites (Satchin-gah and Nashiro Beach) are located near the shoreline, water quality at these sites was strongly influenced by marine water. We excluded the water quality data from sites influenced by marine water (Satchin-gah and Nashiro Beach; see **Fig. 23**) in the following discussions.

Nitrate was found in all groundwater samples from the study area (**Table 4**). The average NO_3-N concentration at all sites was 10.5 mg L^{-1}, and the range was 5.5–18.9 mg L^{-1}. Although the average and range of NO_3-N concentration of each type were the same, the excess rate of 10 mg L^{-1} NO_3-N of the environmental standard was 55% for UF, 13% for RA, and 60% for CC.

The relationship between the concentration of NO_3-N and that of SO_4^{2-} is shown in **Fig. 24**. The form of nitrogen in chemical fertilizer used in the study area was $(NH_4)_2SO_4$. The nitrogen in $(NH_4)_2SO_4$ fertilizer was converted to nitrate by dissolution and nitrification, as follows (e.g. Kondo et al., 1997; Ii et al., 2003):

$$(NH_4)_2SO_4 + 4O_2 \rightarrow 2HNO_3 + H_2SO_4 + 2H_2O. \quad (10)$$

The line with a slope of 3.43 in **Fig. 24** is the theoretical line for Eq. (9). Plots for the water quality in the study area were not distributed around the theoretical line. However, UF plots were arranged along a line parallel to the theoretical line, with a high correlation (R^2 = 0.93). On the other hand, RA and CC plots were distributed linearly with steeper slopes than the theoretical line, with less high correlations (R^2 = 0.48 and 0.56).

Value of $\delta^{15}N$

The $\delta^{15}N$ values averaged 9.9‰, and ranged from 7.9‰ to 13.1‰ (**Table 4**). The $\delta^{15}N$ values for three samplings at each site were nearly identical (±1‰). The range of $\delta^{15}N$ values in our study is similar to the range of 5.6–14.6‰ reported by Nakanishi et al. (2005) who analyzed 77 groundwater samples in the southern area of Okinawa Island. The average values for UF, RA, and CC were 8.9‰, 10.0‰, and 10.5‰, respectively. The relationship between the logarithmic concentration of NO_3-N and the $\delta^{15}N$ values shows that the distribution of $\delta^{15}N$ values was similar between CC and RA and the $\delta^{15}N$ values for RA and CC were higher than those for UF at the same NO_3-N concentration (**Fig. 25**).

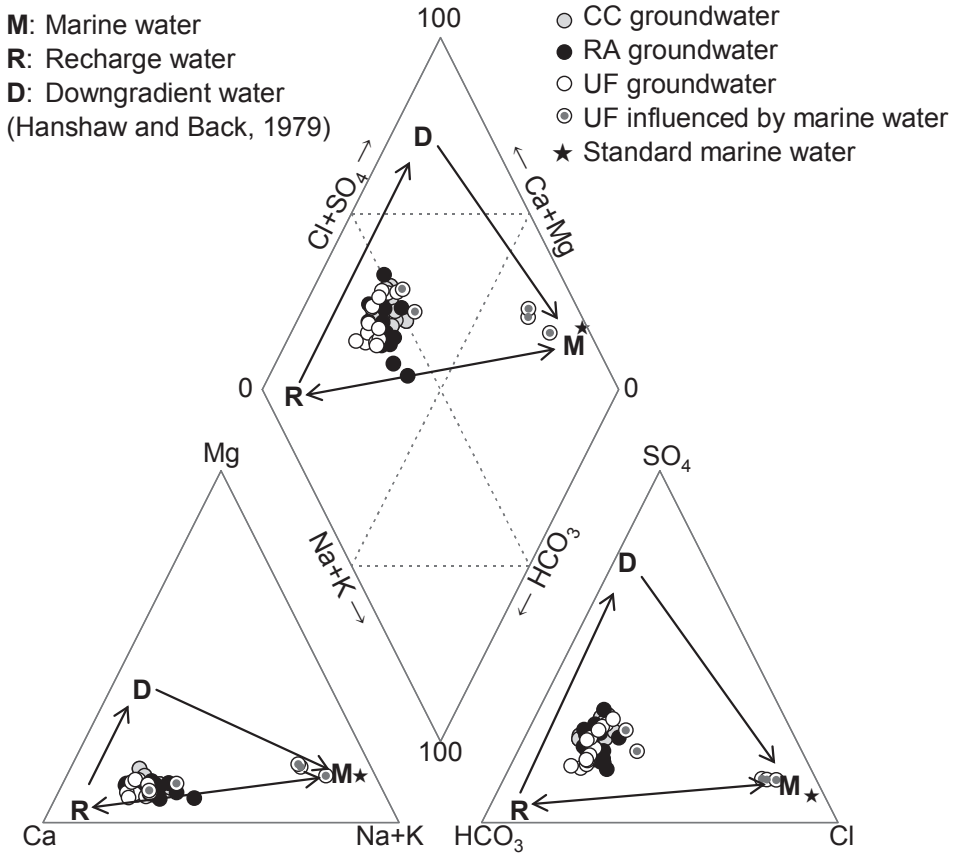

Fig. 23 Piper diagram of groundwater chemistry in the study area

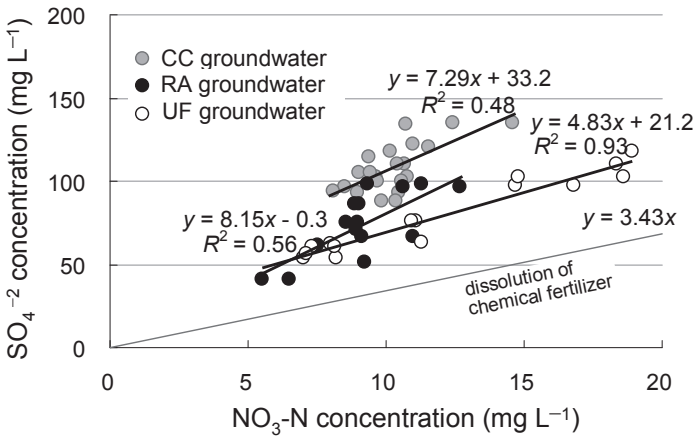

Fig. 24 Relationship between the concentrations of NO_3-N and SO_4^{2-} in the study area

Concentration of ^{222}Rn

The average ^{222}Rn concentration was 4.6 Bq L^{-1}, and the range was 0.6–13.5 Bq L^{-1} (**Table 4**). The range of ^{222}Rn concentration in the study area is the same as that in the groundwater of a carbonate aquifer in Western Sicily where the average was 5.0 Bq L^{-1} and the range was 0.1–50.7 Bq L^{-1} where a high concentration such as 50.7 Bq L^{-1} was related to an active earthquake fault zone (Dongarrà et al., 1995). The average for CC was 1.4 Bq L^{-1}, excluding Urusu-gah (8.4 Bq L^{-1}) and Komesu OF (7.2 Bq L^{-1}) where the exceptionally high concentration might be due to the existence of a cut-off wall. In contrast, the average for UF (5.5 Bq L^{-1}) and RA (5.7 Bq L^{-1}) was obviously higher than that for CC.

Table 5 Estimated contribution rates from chemical fertilizer (CF) and livestock and human waste (LH)

	Type	R_{CF} in 2007	R_{LH} in 2007	R_{CF} in 2008	R_{LH} in 2008	R_{CF} in 2009	R_{LH} in 2009
Springs							
1. Sohji-gah	RA	31%	53%	32%	43%	23%	56%
2. Agari-gah	RA	30%	57%	37%	50%	36%	53%
3. Shira-kah	RA	19%	66%	14%	71%	15%	72%
4. Ashicha-gah	RA	26%	59%	32%	52%	32%	52%
5. Yutaka-gah	CC	4%	83%	26%	65%	26%	63%
6. Sakae-gah	RA	25%	57%	32%	52%	21%	63%
7. Su-gah	CC	11%	77%	29%	58%	24%	63%
8. Urusu-gah	CC	23%	62%	24%	61%	24%	61%
9. Fukurashi-gah	CC	39%	48%	37%	48%	26%	61%
10. Mi-gah	CC	10%	74%	35%	51%	25%	62%
11. Ohdo-gah	CC	36%	50%	45%	40%	23%	63%
13. Yumuchi-gah	UF	24%	56%	31%	49%	33%	50%
14. Yafu-gah	UF	42%	46%	36%	52%	39%	48%
15. Eiki-sen	UF	41%	51%	46%	44%	47%	44%
17. Nashiro Well	UF	46%	46%	45%	46%	50%	43%
Observation facilities of the subsurface dams							
18. Komesu	CC	18%	65%	28%	57%	15%	71%
19. Giza	UF	30%	52%	33%	48%	31%	52%

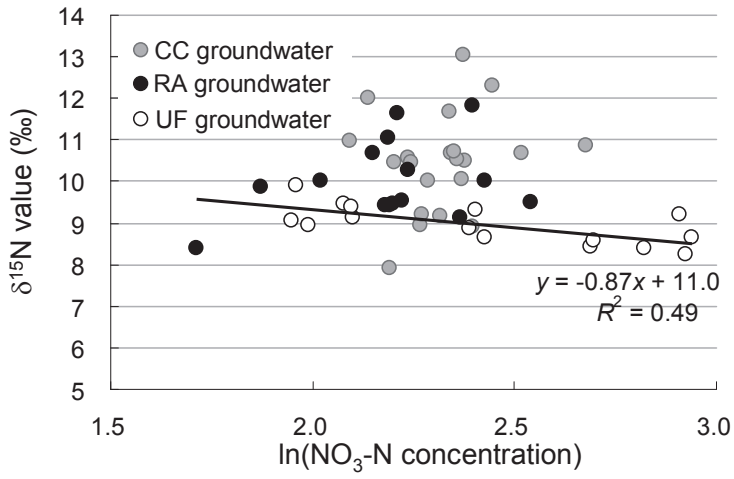

Fig. 25 Relationship between the NO_3-N concentration and the $\delta^{15}N$ values in the study area

Contribution rate of nitrogen sources

The average R_{CF} for UF, RA, and CC was 38%, 27%, and 25%, and that of R_{LH} was 48%, 57%, and 61%, respectively (**Table 5**). **Fig. 26** shows the relationship between R_{CF} and the rate of upland areas and residential areas. There was a relatively high correlation between R_{CF} for UF and RA and the rate of upland areas and of residential areas, with R^2 = 0.65 and 0.52, respectively. These results suggested that UF and RA groundwater was strongly influenced by land use. On the other hand, there was no correlation between land use and R_{CF} for CC.

4 Discussion

a. Characteristics of groundwater flow in the caverns

The ^{222}Rn data was also used to examine the existence of rapid groundwater flow in the conduit flow system. Since ^{222}Rn is generated by the decay of ^{226}Ra in strata, ^{222}Rn concentration in the water increases along with infiltrating matrices of an aquifer. After 2 or 3 weeks, equilibrium is reached between the supply, from the decay of ^{226}Ra with a half-life of about 1,600 years (O→A→B in **Fig. 27**), and loss, through the decay of ^{222}Rn, which has a half-life of 3.8 days. Thus, the concentration levels off. When water leaves the matrices of the aquifer as seepage into caves and caverns, the ^{222}Rn concentration begins to decrease, since the supply of ^{222}Rn has ceased (A→C in **Fig. 27**). Thus, the concentration in the groundwater flowing through the matrices of the aquifer is much higher than that in the groundwater flowing through the caves and caverns. It is possible to determine a travel time after its seepage into caves and caverns based on the distribution of ^{222}Rn in the groundwater.

^{222}Rn concentration in the groundwater in caves and caverns decreases through the radioactive decay of ^{222}Rn. The decrease is expressed as follows:

$$C_2 = C_1 \exp(-\lambda t_T), \tag{11}$$

where C_1 is the ^{222}Rn concentration (Bq L^{-1}) at the equilibrium of radon in the matrices of the Ryukyu Limestone aquifer at an upstream site and C_2 is the ^{222}Rn concentration (Bq L^{-1}) at a downstream site, λ is the decay constant of ^{222}Rn (0.26 day^{-1}), and t_T is the travel time between the sites (day).

The average concentration for types UF and RA, 5.6 Bq L^{-1}, may be regarded as C_1 of the equilibrium concentration of radon. On the other hand, the average ^{222}Rn concentration for type CC, 1.4 Bq L^{-1}, may be regarded as C_2. The time taken for groundwater to travel in caves and caverns from matrices with the continuous ^{222}Rn supply was calculated as about 8 days (**Fig. 27**). This travel time may be the same as the estimated residence time of the groundwater in the conduit flow system (6 days at 60W-1, see Chapter 4).

b. Transport of groundwater nitrates and the land-use categories

The application of chemical fertilizer has been considered the major cause of increasing nitrate concentration in the groundwater in the study area (Agata et al., 2001). A comparison between the long-term change in NO_3-N concentration in the groundwater and

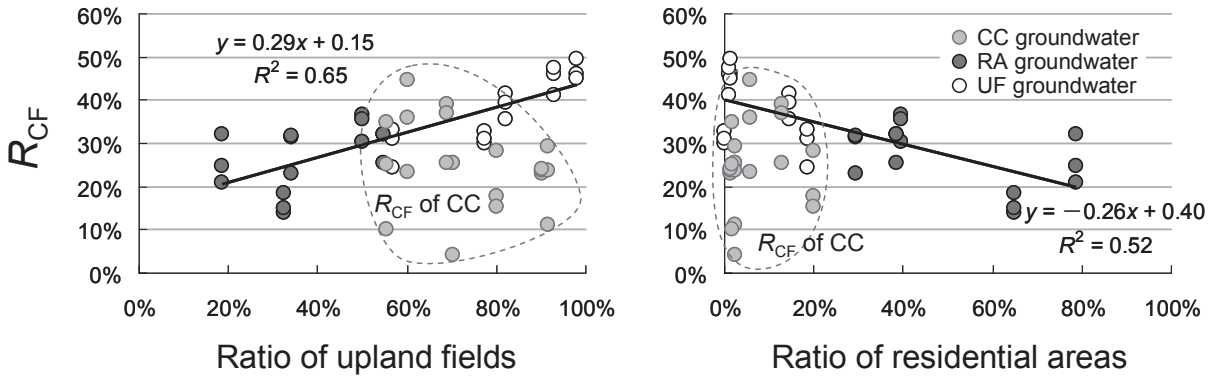

Fig. 26 Relationship between the estimated contribution rates (R_{CF}; **Table 5**) and the rates of land use (upland fields and residential areas) in the fan-shaped areas with a 600-m influential zone upstream (**Figs. 20** and **21**). The lines represent the correlation between R_{CF} and land-use rate excluding the CC type

the estimated nitrogen emission (**Figs. 14** and **22**) also implied that the predominant sources affecting the groundwater was chemical fertilizer. The inference that the significant source of groundwater nitrates for UF was chemical fertilizer was also explained by the UF plots in the diagram of NO_3-N versus SO_4^{2-} with a linear relationships arranged along a line parallel to the theoretical line of dissolved $(NH_4)_2SO_4$ fertilizer ($R^2 = 0.93$; **Fig. 24**). The difference of intercept was likely caused by the dissolution of gypsum in the groundwater evolution, plant uptake or denitrification. The existence of the pathway R→D in **Fig. 23** confirmed that dissolution of gypsum and enrichment of SO_4^{2-} in a carbonate aquifer. On the other hand, the RA and CC plots are distributed linearly with steeper slopes than the theoretical line. This indicated that the sources for RA and CC included components besides chemical fertilizer.

Previous studies on sources of groundwater nitrate using ^{15}N have focused on the relationship between the land use around the sampling points and the $\delta^{15}N$ values in groundwater nitrates because land use is the predominant factor controlling nitrate pollution, that is, most groundwater nitrates originate from sources on the land surface via vertical transport in the soil profile. However, $\delta^{15}N$ values were often contradictory to land use, so there is a common understanding among researchers that it is difficult to identify the sources of groundwater nitrates by a single application of $\delta^{15}N$ measurement.

To interpret the dissociation between $\delta^{15}N$ values and land use, researchers have considered the complexities in the nitrogen cycle where enrichment of $\delta^{15}N$ values occurs as a result of decomposition of livestock and domestic waste, oxidation of soil organic matter, as well as oxidation and volatilization of ammonia fertilizers and denitrification (e.g., Kreitler, 1979; Létolle, 1980). Moreover, two other factors should be considered for a karst aquifer: lateral groundwater flow and multiple nitrogen sources.

The shallow groundwater in the Ryukyu Limestone aquifer was influenced mainly by the lateral transport of nitrogen in groundwater flow consisting of the 70-day diffuse flow through the matrices and the 6-day rapid flow through the conduits. This indicated that the area of land use that controls groundwater nitrates has a certain extent of area as well as an area around the sampling point. Therefore, we categorized the sampling sites into UF and RA types from land-use ratios in a fan-shaped area with a 600-m influential radius. In addition, we categorized the CC type from the viewpoint of hydrogeological settings, even though it should be categorized as the UF type in terms of land use.

The average of $\delta^{15}N$ values for CC (10.5‰) is closer to that for RA (10.0‰) than UF (8.9‰). Likewise, there was a difference in the average values of the contribution ratio of chemical fertilizer (R_{CF}) between UF (38%) and RA (27%), but the R_{CF} values for CC (average: 25%) was similar to those for RA. These indicate that CC nitrates were not related to the surrounding land use. Although

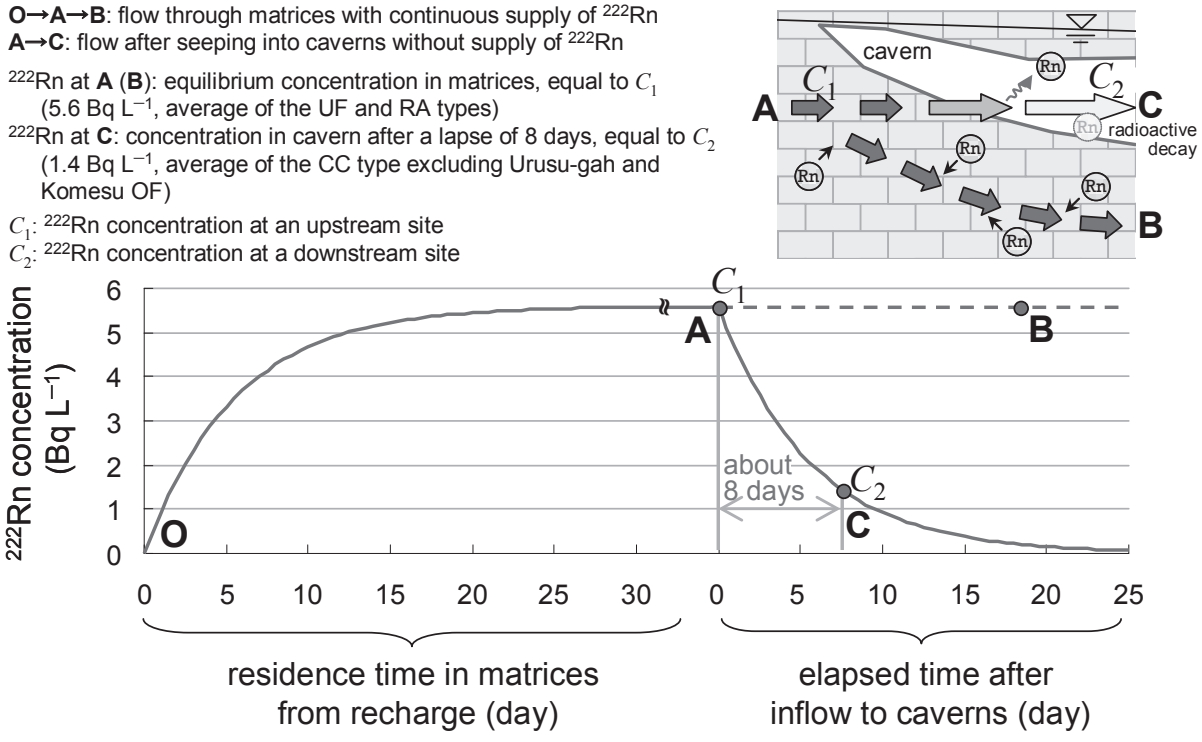

Fig. 27 Schematic diagram of change in ^{222}Rn concentration in the groundwater of karst aquifers

there was a relatively high correlation between R_{CF} for UF and RA and the rate of upland areas and of residential areas, there was no correlation between land use and R_{CF} for CC (**Fig. 26**). These phenomena were considered as evidence that CC groundwater nitrates were carried by rapid groundwater flow through caves and caverns from residential areas located higher upstream than the influential areas.

According to previous studies (**Fig. 3**), $\delta^{15}N$ values derived from animal waste sources generally range from 8 to 22‰. Human waste in the study area is collected and disposed of mainly through the use of septic tanks. The Ministry of the Environment (2002) reported $\delta^{15}N$ values ranging from 8‰ to 11‰ for human waste in septic tanks. Since the $\delta^{15}N$ values for RA and CC were consistent with the range expected for groundwater nitrates impacted by animal and human waste, this was considered to be the predominant source of nitrogen for RA and CC where the groundwater quality around residential areas may be effected by effluent percolation from septic tanks and in part by improper treatment of livestock manure.

On the other hand, the $\delta^{15}N$ values for UF (average: 8.9‰) were higher than those reported in literature for groundwater nitrates beneath fertilized upland fields (0–6‰; **Fig. 3**). This likely reflects the complexity of identifying the denitrification process and subsurface chemical mixing processes from multiple sources of nitrogen in a carbonate aquifer environment.

Soils in the Ryukyu Limestone region are typically alkaline. In alkaline soil, the volatilization of ammonia may be important (Spalding et al., 1982) as it results in the enrichment of ^{15}N in residual nitrate up to 4‰ (Kirshenbaum et al., 1947). Thus, part of the nitrogen in the chemical fertilizer applied in the study area might be volatilized just after application. Since isotopic fractionation during ammonia volatilization and denitrification enriches ^{15}N in the residual nitrate, the logarithmic concentrations of NO_3-N and the $\delta^{15}N$ values, denoted as δY and C, have a relationship written by the Rayleigh equation (e.g., Mariotti et al., 1988):

$$\delta Y = Y_0 + \varepsilon \ln C / C_0. \tag{12}$$

The slope ε is referred to the isotopic enrichment factor, and C_0 and Y_0 are the initial concentration and isotopic composition of loaded nitrogen. Here, Eq. (12) can be rewritten as a simple linear relationship between δY and ln C, as follows;

$$\delta Y = d + \varepsilon \ln C, \tag{13}$$

where the intercept d is a constant dependent on ε, C_0, and Y_0. As shown in **Fig. 25**, the relationship between ln (NO_3-N) and $\delta^{15}N$ for UF is arranged close to the line for Eq. (13), and the value of ε was estimated as −0.87‰. Hübner (1986) reported the value of ε for ammonia volatilization as −30.1‰. Hence, in this study, it was impossible to evaluate the effect of ammonia volatilization because the estimated ε value was too large. On the other hand, Mariotti et al. (1988) showed the ε value for denitrification ranging from −5.0 to 4.7‰. In the study area, there was the possibility of denitrification in spite of the larger value of ε (−0.87‰), since denitrification is a microbial activity susceptible to temperature and carbon content. However, in view of the small value of ε, denitrification is unlikely to be the sole cause of the high $\delta^{15}N$ value for UF.

Along with the increasing livestock population in residential areas, farmers have shown a tendency to apply livestock manure as organic fertilizer to upland fields for environmentally friendly farming. Thus it is reasonable to consider that the origin of UF groundwater nitrates is composed of complex sources of chemical fertilizer and livestock manure in varying rates of contribution.

Chemical fertilizer had a greater effect on UF groundwater compared to RA and CC groundwater. However, it is quite unreasonable that the contribution of livestock manure and domestic wastewater was estimated to be much larger than chemical fertilizer and the maximum R_{CF} under 98% of the rate for UF (Nashiro Well) was 50% (**Table 4**). One reason for this may be that farmers are applying a greater amount of livestock manure than that was expected from the comparison between the long-term change in NO_3-N concentration in the groundwater (**Fig. 14**) and the estimated nitrogen emission (**Fig. 22**), because the government provides additional support such as concessionary loans or farmers as incentives. Secondly, because the mass balance equations were solved under assumptions, the contribution rates depended on the assumptions. Yoneyama (1987) reported that $\delta^{15}N$ values of soil nitrogen in Okinawa ranged from 3.9 to 8.7‰ (**Fig. 3**). Nitrates in the soil originated from the following three sources: (1) rainfall, (2) mineralization of leguminous SOM, and (3) mineralization of non-leguminous SOM (Olmann et al., 2007). NO_3-N concentration and $\delta^{15}N$ values in groundwater leaching from natural soil should vary with the change in balance of the three sources. We assumed that the value of C_{SN} and X_{SN} was fixed at 1.4 mg L^{-1} and 4‰, respectively. This may partially account for the low R_{CF}. A more accurate estimate of source contributions requires the development of a more flexible model with variable parameters.

5 Conclusions

The groundwater flow and the transport and potential source of groundwater nitrates in the Ryukyu Limestone aquifer in the southern part of Okinawa Island were investigated.

The conduit flow system was also confirmed by the distribution of relatively low concentrations of ^{222}Rn near caverns, which also suggested that the Ryukyu Limestone aquifer is a "mixed flow" aquifer.

The average $\delta^{15}N$ value for CC was similar to that for RA. This was considered as evidence that CC groundwater nitrates were carried by rapid groundwater flow through caves and caverns from the residential areas located higher upstream than the influential areas. According to previous studies related to ^{15}N, animal and human waste was considered the predominant sources of nitrogen for RA and CC, although the correspondence of the long-term changes in the NO_3-N concentration in groundwater and the emitted load from chemical fertilizer seemed to suggest application of chemical fertilizer predominantly affects groundwater quality.

On the other hand, the $\delta^{15}N$ values for UF were higher than those reported in literature for groundwater nitrates beneath fertilized upland fields. Denitrification and multiple sources were considered as explanations of this dissociation, but denitrification was unlikely to be the sole cause because the enrichment factor value was small. Consequently, it was reasonable to consider that the origin of UF groundwater nitrates was complex multiple sources. This was also confirmed from the relatively high correlation between the calculated contribution ratio of chemical fertilizer and the rate of upland areas and residential areas upstream of the sites.

VI Development of a Numerical Model for Nitrates in Groundwater for the Komesu Subsurface Dam

1 Introduction

Subsurface dams have been constructed in the Ryukyu Limestone regions until now. Local residents are concerned about the impact of the subsurface dam on groundwater quality because the dam changes the natural groundwater flow. There are two issues of particular concern: nitrate contamination and climate change impacts. In the future, it will be important to monitor and control groundwater quality as well as the reservoir storage behind dams. For managing groundwater quality, it is necessary to develop simulation methods for long-term groundwater recharge and nitrate concentrations. To this end, models which properly represent characteristics of water and solute transport have to be built.

This chapter describes a regional quantitative model which was developed to represent prolonged daily groundwater recharge and nitrogen dynamics in the catchment area of a subsurface dam. The calculations of physical and chemical movements of water and nitrogen from soil to aquifer are explained, and the model application to forecast long-term changes in groundwater levels and nitrate concentrations in the reservoir area of a subsurface dam under a precipitation-decrease condition is also indicated. The procedure was developed for a specific area of the catchment of the Komesu subsurface dam, but can clearly be applied elsewhere.

2 Methods

a. Research on groundwater levels, irrigation and pumped discharges

Groundwater levels in observation wells before the dam construction had been continuously monitored by the Okinawa General Bureau for the subsurface dam project. In this paper, data observed at W-21, W-18, W-22, and W-24 (**Fig. 28**) in 1982 were used for calibration.

Groundwater levels, irrigation and pumping-up of discharges after the dam construction were observed and logged daily by the Okinawa Hontoh Nanbu Land Improvement District. Irrigation volumes were calculated from the discharge data logged at outlets of farm ponds (facilities for regulating irrigation water). Discharges pumped at four pumping sites, Komesu-West, Yamagusuku, Komesu-East, and Makabe (**Fig. 28**), were also used to calculate the model described below. Furthermore, the groundwater levels at the four wells, KR-6, YR-1, KR-3, and MR-1 (**Fig. 28**), in 2007 were used for verification of the model.

b. Observations of NO_3-N concentrations in groundwater

Nitrate concentration at springs in the study area had been observed from 1990 to 2002 by the Okinawa General Bureau. Here, data obtained from five springs, Sakae-gah, Ashicha-gah, Fukurashi-gah, Shira-kah, and Agari-gah (**Fig. 28**), were used for calibration. These data were not affected by the subsurface dam because the subsurface dam was still being constructed between 1990 and 2002.

After the dam construction, we collected water samples for analyzing NO_3-N concentrations ten times in 2007–2010 from the five springs (**Fig. 28**). Concentrations of NO_3-N in the collected samples were analyzed by ion chromatography (ICA-2000, TOA-DKK, Japan).

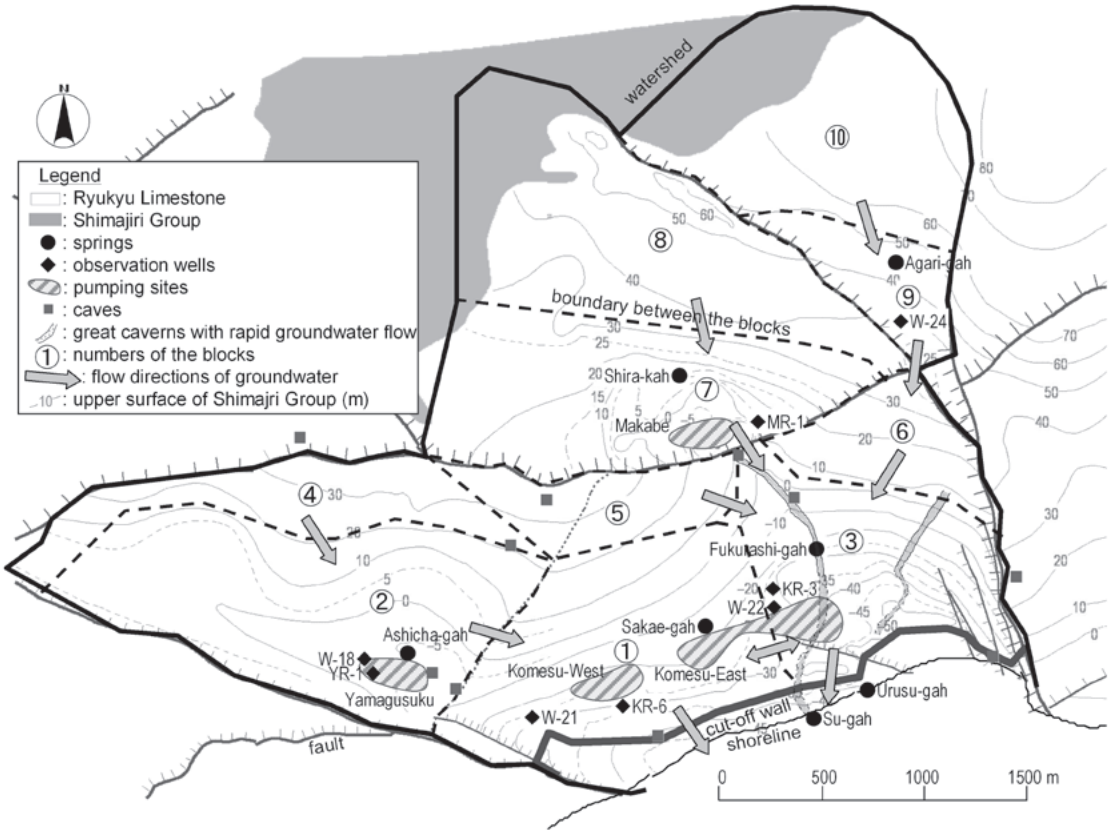

Fig. 28 Outline of the Komesu basin (modified from Okinawa General Bureau, 2006)

c. Development of the model

The model proposed here assumes that all solutes in groundwater in a sub-basin are perfectly mixed and of homogeneous concentration. This assumption is consistent with the actual situation reported by Nawa and Miyazaki (2009) that the residual saltwater in the bottom of the reservoir was pushed toward the wall and the saltwater-freshwater mixing zone rose up even when overflow beyond the cutoff wall occurred, which was confirmed by model experiments and field observations. Assuming that groundwater in the reservoir can be deemed to be mixed, the model can be used to represent water transport in the reservoir.

The model was verified to reflect the effect of the dam construction, and then the parameters of the model were optimized. Modeling was performed for each tank using a 1-day time step to determine the groundwater level and nitrate concentration in groundwater in the Komesu subsurface dam for calibration to optimize the parameters, and the model was verified for the period 2007–2010.

Water balance submodel

Generally, chemical fertilizers applied to farmland dissolve in rainwater runoff or soil water and are transported into aquifers. Compost and crop residues also contain organic nitrogen, and when they decompose the nitrogen becomes mineralized in the soil and the mineralized nitrogen leaches into the groundwater. Therefore, to estimate the dynamics of nitrogen, it is indispensable to understand the water dynamics.

We adopted a conventional computational framework for planning subsurface dams in Japan, so-called “tank models”, to calculate the water balance in the Komesu basin (Agricultural Structure Improvement Bureau, 1993). The Komesu basin was divided into ten sub-basins (0.26–1.4 km^2) on the basis of the hydrogeological structure of the basin (**Fig. 28**). Water transportation in each of the sub-basins was described by a tank model which is a simple, conceptual model comprising a series of three tanks. The framework was therefore composed of ten tank models. This framework was referred to as the water balance submodel in this study.

Model structure The general structure of the water balance submodel is shown in **Fig. 29(a)**. The uppermost and middle tanks in each sub-basin tank model represent vertical infiltration in the unsaturated aquifer. Especially, the uppermost tank is regarded as a soil layer. The lowermost tank represents the saturated groundwater, and the water level in the lowermost tank

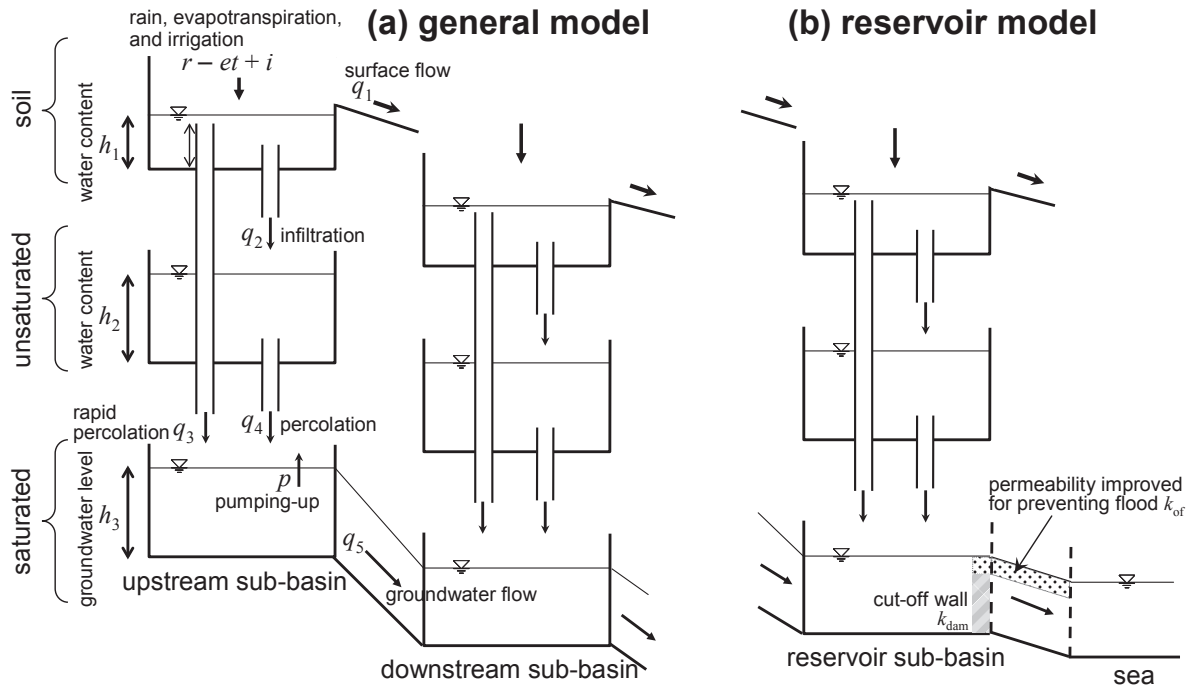

Fig. 29 Schematic structure of the water balance submodel; (a) a description of the general model for sub-basins other than 1 and 3, (b) a description of the model for sub-basins 1 and 3 which are corresponding to the reservoir areas of the Komesu subsurface dam

Rainwater reaches the groundwater table immediately from ground through many caves and caverns in limestone areas. For this reason, the tank model express the flow through fractures and macropores such as caves and caverns by a pipe connecting the uppermost tank directly to the lowermost tank (**Fig. 29(a)**).

Water transportation in the uppermost and middle tanks is expressed by the following equations:

$$q_j = \beta_j (h_1 - z_j) \quad \text{if } h_1 > z_j, \quad q_j = 0 \quad \text{if } h_1 \le z_j, \quad \text{for } j = 1, 2, \text{ and } 3, \tag{14}$$

$$q_j = \beta_j (h_2 - z_j) \quad \text{if } h_2 > z_j, \quad q_j = 0 \quad \text{if } h_2 \le z_j, \quad \text{for } j = 4, \tag{15}$$

where h_1 and h_2 are water contents in the uppermost and middle tanks (m), q_j for j = 1–4 are flow discharges for each pipe (m^3 day^{-1}), and β_j and z_j for $_j$ = 1–4 are parameters of the tank model (day^{-1} and m). q_1 represents the surface flow, and q_3 indicates the rapid percolations through fractures and macropores such as caves and caverns. The values for β_j and z_j were optimized as shown in **Table 6**. The optimization procedure is described below.

The sub-basin tank models are connected with the upstream and downstream tank models through the lowermost tanks, and these connections represent lateral groundwater flows in the Komesu basin. There are three dominant routes of groundwater flow in the Komesu basin (**Fig. 28**): (1) sub-basin 4 → 2 → 1 → sea, (2) sub-basin 8 → 7 → 3 → sea, and (3) sub-basin 10 → 9 → 6 → 3 → sea. Additionally, there is a flow from sub-basin 5 to 3, and water is exchanged between sub-basins 1 and 3, depending on water-level differences (**Fig. 28**). The volume discharge of the lateral groundwater flow from upstream to downstream tanks, denoted as q_5 (m^3 day^{-1}), is calculated using Darcy's law, as follows:

$$q_5 = k\, e\, S\, (h_3 - h_{ds}) / L \times 86{,}400, \tag{16}$$

where k, e, L, S, and h_{ds} are hydraulic conductivity (m s^{-1}), effective porosity (m^3 m^{-3}), distance between the central points of the upstream and downstream sub-basins (m), cross-sectional area between the upstream and downstream sub-basins (m^2), and

groundwater level in downstream sub-basin (m), respectively. The values for e and d, are shown in **Table 6**. In some of the sub-basins, permeability depends on depth because of the existence of highly-permeable zones consisting of caves and caverns. Consequently, in sub-basins 1, 2, 3, 7, and 9, two or three hydraulic conductivities whose values vary by range of depth were set, and the calculation of q_5 was altered as follows:

$$q_5 = e\ \{k\ S_{\mathrm{I}} + k_{\mathrm{I}}\ S_{\mathrm{II}} + k_{\mathrm{II}}\ (S - S_{\mathrm{I}} - S_{\mathrm{II}})\}\ (h_3 - h_{\mathrm{ds}})/L \times 86{,}400, \quad \text{if } h_3 > h_{\mathrm{II}}, \tag{17}$$

$$q_5 = e\ \{k\ S_{\mathrm{I}} + k_{\mathrm{I}}\ (S - S_{\mathrm{I}})\}\ (h_3 - h_{\mathrm{ds}})/L \times 86{,}400, \quad \text{if } h_{\mathrm{I}} < h_3 \le h_{\mathrm{II}}, \tag{18}$$

$$q_5 = k\ e\ S\ (h_3 - h_{\mathrm{ds}})/L \times 86{,}400, \quad \text{otherwise}, \tag{19}$$

where k_{I} and k_{II} are hydraulic conductivity (m s^{-1}) above boundary groundwater levels h_{I} and h_{II} (m), respectively. Similarly, S_{I} and S_{II} are the cross-sectional areas below h_{I} and between h_{I} and h_{II}. The values of k, k_{I}, k_{II}, h_{I}, and h_{II} were optimized by the trial-and-error method (**Table 6**), as described below.

The cross-sectional area S (m^2) and the capacity of the lowermost tank W (m^3) were calculated from the groundwater level h_3 (m) by using the h_3-S curves and the h_3-W curves, typically described as $S = a_S\ h_3^2 + b_S\ h_3 + c_S$ and $W = a_W\ h_3^2 + b_W\ h_3 + c_W$, respectively. The values of the parameters of these curves are shown in **Table 6**.

The calculation step of the model is one day. The changes in h_1, h_2, and W are calculated as follows:

Table 6 Values for parameters of the water balance submodel

sub-basin	β_1	z_1	β_2	z_2	β_3	z_3	β_4	z_4	a_S	b_S	c_S	a_W	b_W	c_W
1	1	0.5	0.014	0.0001	0.30	0.20	0.01	0.0001	18.71	1952.77	49012.00	7420	827740	19210000
2	0	1.0	0.015	0.0001	0.50	0.08	0.01	0.0001	14.79	339.58	1912.75	26990	315120	668970
3	1	0.3	0.080	0.0001	0.90	0.02	0.01	0.0001	6.88	974.99	33152.40	6790	637570	15750000
4	1	0.5	0.020	0.0001	0.50	0.05	0.01	0.0001	0.00	1609.96	−32199.50	16300	−651900	6518000
5	1	0.3	0.100	0.0001	0.10	0.03	0.01	0.0001	0.00	480.00	0.00	6360	−48720	20250
6	1	1.0	0.100	0.0001	0.10	0.08	0.01	0.0001	0.00	1100.00	0.00	6060	−40230	17750
7	0	1.0	0.010	0.0001	0.90	0.08	0.01	0.0001	32.14	−427.92	1372.24	12990	44120	1396000
8	1	1.0	0.050	0.0001	0.50	0.15	0.01	0.0001	0.00	1700.00	−34000.00	31380	−1320000	13870000
9	0	1.0	0.010	0.0001	0.20	0.12	0.01	0.0001	13.75	−832.25	12570.00	5060	−247330	3022000
10	1	1.0	0.002	0.0001	0.40	0.02	0.01	0.0001	0.00	1000.00	−50000.00	20500	−1990000	48250000
						(1↔3 exchange)			9.32	825.93	16122.90			

sub-basin	d	e	k	k_{I}	k_{II}	h_{I}	h_{II}	G
1	500	0.09	($k_{\mathrm{dam}} = 1.0 \times 10^{-8}$, $d_{\mathrm{dam}} = 0.55$, $k_{\mathrm{dr}} = 1.4 \times 10^{-2}$)					933000
2	800	0.11	5.8×10^{-5}	5.8×10^{-3}	3.5×10^{-3}	10.3	11.8	1434000
3	400	0.09	($k_{\mathrm{dam}} = 1.0 \times 10^{-8}$, $d_{\mathrm{dam}} = 0.55$, $k_{\mathrm{dr}} = 1.4 \times 10^{-2}$)					689000
4	650	0.09	3.5×10^{-5}					326000
5	1000	0.09	2.3×10^{-4}					341000
6	600	0.09	2.3×10^{-4}					333000
7	900	0.09	5.8×10^{-5}	1.1×10^{-2}		15.0		1035000
8	500	0.09	2.3×10^{-5}					1830000
9	700	0.09	6.9×10^{-5}	1.0×10^{-2}		35.7		261000
10	600	0.09	1.2×10^{-4}					1312000
	1200		2.0×10^{-3}					

$$h_1(t+1) = h_1(t) + \{ r(t) - \mathrm{et}(t) + i(t) - q_1(t) - q_2(t) - q_3(t) + q_{1\mathrm{ups}}(t)\} / G, \quad (20)$$

$$h_2(t+1) = h_2(t) + \{q_2(t) - q_4(t)\} / G, \quad (21)$$

$$W(t+1) = W(t) + q_3(t) + q_4(t) - q_5(t) + q_{5\mathrm{ups}}(t) - p(t), \quad (22)$$

where t is the time step (day), G is the area of each sub-basin (m^2), and r, et, i, and p are rainfall, evapotranspiration, irrigation and pumping-up (m^3 day^{-1}). The inputs i and p were considered only after the dam construction, because irrigation and pumping-up in the study area were not massive before the dam was built. In addition, $q_{1\mathrm{ups}}$ and $q_{5\mathrm{ups}}$ are summations of inflows of surface water and groundwater from the upstream tanks, including the groundwater interaction between sub-basins 1 and 3.

Effect of the subsurface dam construction The cutoff wall of the subsurface dam was constructed along the shoreline which is the outlet of the Komesu basin. Sub-basins 1 and 3 correspond to the reservoir area (**Fig. 28**). Consequently, we added some modifications to the tanks for sub-basins 1 and 3.

Because the permeability of the aquifer at the outlet of the Komesu basin significantly changed at the time of construction of the subsurface dam, the values for permeability after the dam construction were determined as follows: Hydraulic conductivity and thickness of the cut-off wall of the Komesu subsurface dam, denoted as k_{dam} and L_{dam}, were 1.0×10^{-8} m s^{-1} and 0.55 m, respectively (**Fig. 29(b)**; Okinawa General Bureau, 2006). Assuming elimination of the permeability of the Ryukyu Limestone aquifer between the sea and the sub-basins, the value of the transmissibility coefficient below the top of the cut-off wall between the sea and sub-basins 1 and 3 was calculated as $k_{\mathrm{dam}} / L_{\mathrm{dam}}$. In addition, from the point of view of flood prevention, permeability of the aquifer above the top of the cut-off wall, denoted as k_{of}, had been improved, and furthermore, a drainage system had been installed on the reservoir to remove groundwater near the ground surface. The calculation of q_5 in sub-basins 1 and 3 is as follows:

$$q_5 = e\ \{k_{\mathrm{dam}} S_{\mathrm{dam}} / L_{\mathrm{dam}} + k_{\mathrm{of}} (S - S_{\mathrm{dam}}) / L\}(h_3 - h_{\mathrm{sea}}) \times 86{,}400 + q_{\mathrm{su}}, \quad \text{if } h_3 > h_{\mathrm{dam}}, \quad (23)$$

$$q_5 = k_{\mathrm{dam}}\, e\, S\, (h_3 - h_{\mathrm{sea}}) / L_{\mathrm{dam}} \times 86{,}400 + q_{\mathrm{su}}, \quad \text{otherwise}, \quad (24)$$

where h_{sea} is sea level equal to 0 m, h_{dam} is the height of the cut-off wall above sea level set to 4 m, S_{dam} is the cross-sectional area below the top of the cut-off wall, and q_{su} is discharge for maintaining spring water of Su-gah (**Fig. 28**) and is set to 2086.4 m^3 day^{-1} (Okinawa General Bureau, 2006) which is applied only to sub-basin 3. The value of k_{of} was set to 2.0×10^{-2} m s^{-1}.

Nitrogen balance submodel

The nitrogen balance submodel was based on the Kiho-Islam model, which describes nitrogen movements and chemical reactions in an aquifer by simple equations (Kiho and Islam, 1995). The tank models (**Fig. 29**) were used as the water-balance submodel, which is required by the Kiho-Islam model, to describe the water dynamics in the aquifer.

In general, distributed models such as finite element models are ideal for precise calculations of nitrogen dynamics in groundwater. However, it is difficult to calculate long-term fluctuations by using distributed models with short time steps, because the computational load is huge. The model proposed here has the advantage that long-term simulations of nitrogen dynamics in groundwater can be performed with a time step of just one day.

Interactions between nitrogen forms and chemical and biochemical reactions were considered by the model (**Fig. 30**). In the uppermost tank of each sub-basin tank model, which represents the soil layer, all of the reactions shown in **Fig. 30** were taken into account. In the middle tank, nitrification, denitrification and leaching were considered. In the lowermost tank, only lateral flow was considered.

In addition to the general assumptions about the limestone aquifer mentioned above, the following were also made: (1) The physical properties of both the fluid and the aquifer are uniform in each sub-basin, (2) The mass transfer rate parameters are constant in each sub-basin, and (3) Isothermal conditions apply.

General formula for chemical and biochemical reactions The chemical and biochemical reactions of nitrogen considered here are greatly influenced by ground temperature and soil moisture. The general formula used to estimate nitrogen movements by such reactions is as follows:

$$Y = X \times a \times \tau \times \mu, \tag{25}$$

where X, Y, a, τ, and μ are amount of nitrogen in the form before reaction, generated amount of nitrogen in the form after reaction, a reaction rate parameter, a ground temperature function, and a soil moisture function, respectively. The formulas and parameters for each reaction are fully described in the Appendix.

General formula for changes in amounts of nitrogen in various forms The amounts of nitrogen in various forms, such as nitrate, ammonium, humus and so on, were increased and decreased by the chemical and biochemical reactions described above. The general formula to express the change of nitrogen in a certain form is as follows:

$$X(t + 1) = X(t) - Y(t) + Z(t), \tag{26}$$

where X is an amount of nitrogen in the form, Y is a decrease in amount of nitrogen by a reaction, Z is an increase in amount by another reaction, and t is a time step. The formula for each form of nitrogen is described in the Appendix.

Farming calendar The dominant crop in upland fields in the study area is sugarcane, and the most common sugarcane cropping method in the study area is ratooning. For simplicity of calculation, we assumed that all fields are under sugarcane cultivation by ratooning, and that fertilizing and other farming activities are performed on the same days. The fertilization calendar determined on the basis of the cultivation guidelines (Okinawa Prefecture, 2006a) is shown in **Table 7**. We also assumed that the cultivation period was 500 days, and the day ratooning is performed (February 1st) was the 136th day in the cultivation cycle of sugarcane.

Model calibration, verification and prediction

Calibration The model was calibrated by data observed before the dam construction, because much data had been gathered for the subsurface dam project. It seems valid to use the model calibrated with the data before the dam construction for the prediction after the dam construction, because the only modification to the model before and after the dam construction is the permeability at the outlet of sub-basins 1 and 3.

For calibration, the groundwater level in an observation well and the NO_3-N concentration at a spring in the center of the sub-basin before the dam construction were considered as representative of the groundwater levels and NO_3-N concentrations in the sub-basin

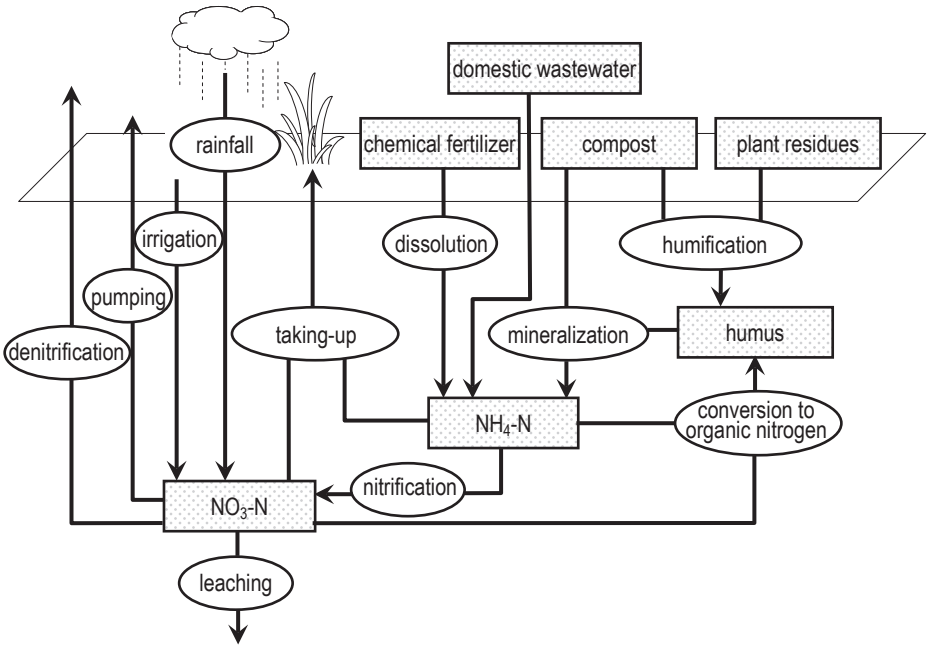

Fig. 30 Schematic diagram of the nitrogen balance submodel

(**Fig. 28**). Parameter values in the water balance submodel (and some parameters of the nitrogen balance submodel) were optimized as shown in **Table 6** by trial and error, so the normalized root mean square error (NRMSE) of groundwater levels during the calibration period (1982) became less than 10%, and the coefficient of variation of the root mean relative error (CV(RMSE)) of 4-year moving averages of NO_3-N concentrations corresponding to observed data at each spring (1992–2002) smoothed by the Nadaraya-Watson estimator (see Simonoff, 1996) were reduced to less than 20%. NRMSE and CV(RMSE) were calculated as follows:

$$\mathrm{NRMSE} = \frac{\sqrt{\sum_n (h_3 - h_{obs})^2 \Big/ n}}{h_{\max} - h_{\min}}, \tag{27}$$

$$\mathrm{CV(RMSE)} = \frac{\sqrt{\sum_m (C_N - C_{obs})^2 \Big/ m}}{C_{ave}}, \tag{28}$$

where h_{obs} is the observed time-series data value of groundwater levels, C_{obs} is the observed data value of NO_3-N concentrations at the five springs, n is the number of available data points for h_{obs}, m is the number of available data points for C_{obs}, h_{max}, and h_{min} are the maximum and minimum of h_{obs}, and C_{ave} is the average of C_{obs}. The model calculation was executed for January 1, 1980 to December 31, 2002. In addition, to pre-condition the variables of the model, the model calculation for the first year was repeated five times before the calculation for the intended period.

In the calculation before the dam construction, i and p were not considered, because large-scale irrigation and pumping-up had not been started. The values of et shown in **Table 8** were constant during each month, which were estimated by the Thornthwaite equation from monthly temperatures in 1982 at Itokazu.

Verification Groundwater levels and NO_3-N concentrations were simulated for January 1, 2006 to December 31, 2010, for

Table 7 Calendar of cultivation operations and amounts of fertilizer input into the model

Date	t_C†	Operation	Nitrogen applied [kg m^{-2}]
February 1st	136	ratooning, basal compost F_C	0.0195
February 24th	159	basal fertilizer F_F	0.0066
April 1st	195*	additional fertilizer F_F	0.0066
May 15th	239*	additional fertilizer F_F	0.0066
January 31st	500*	harvest (plant residues F_P)	0.0074

† t_C is the day in the cultivation cycle. * The values need to be plus 1 in leap years.

Table 8 Evapotranspitation values (et [mm day^{-1}])

Month	et	Month	et
January	0.98	July	6.26
February	1.27	August	5.66
March	2.08	September	4.39
April	2.33	October	3.41
May	4.20	November	2.63
June	4.66	December	1.44

verification. As in the case for the calibration, the calculation for 2006 was repeated five times before the intended calculation for pre-conditioning.

Data observed and logged by the Okinawa Hontoh Nanbu Land Improvement District were applied as the daily values for *r*, *i*, and *p*. However, data for *r*, *i*, and *p* in 2009–2010 were not available so *r* at Itokazu and *i* and *p* from 2008 were tentatively applied as alternatives. The et values used are shown in **Table 8**. The values for *i* in each sub-basin were allocated in proportion to *G*. The values of *p* in sub-basins 1, 2, 3, and 7 were given as the corresponding pumping sites, Komesu-West, Yamagusuku, Komesu-East and Makabe (**Fig. 28**), respectively. Here, the discharges pumped up at Komesu-East were allocated to sub-basin 3 for simplicity, even though the Komesu-East site lies astride sub-basins 1 and 3.

Prediction The calibrated and verified model was run for 100 years to provide a forecast of characteristics of variation trends in groundwater levels and nitrate concentrations in the reservoir area of the Komesu subsurface dam associated with future changes in climate.

Daily rainfall data (*r*) in the 100 years were generated from previously observed data while taking into account the long-term trend in precipitation. Specifically, the rainfall data were made up of repeated patterns of rainfall in 1961–1980 in a 20-year cycle with a decay rate of 5.5% per 100 years, according to a report by Kamahori and Fujibe (2009) that the trend in annual rainfall in Naha was decreasing with −5.5% per 100 years in 1901–2008. Incidentally, 1971 is the design reference year of the Komesu subsurface dam, and the annual rainfall in 1971 was 1,442 mm and its return period was estimated to be 10 years. If the rainfall pattern is the same as that in 1971, the minimum groundwater level of the reservoir area was estimated to be −11.6 m (Nawa and Miyazaki, 2009). In addition, 1963 was even drier than 1971: the annual rainfall was 1,084 mm and the return period was 90 years. On the other hand, the maximum for the 20 years was 2,953 mm in 1966. The averaged annual rainfall in 1961–1980 was 1,984 mm, which was almost equal to that in 1981–2010 (1,972 mm). Temperature data (*T*) were produced as a repetition of those in 1961–1980 without considering the long-term trend in temperature.

Irrigation amount (*i*) was calculated from the rainfall data described above, according to the Rural Development Bureau (1997), where the level of the total readily available moisture (TRAM) was set to 35 mm, and daily rainfall of more than 5 mm was judged to be effective. The daily amount of pumping-up (*p*) for each pumping site was obtained by allocating the calculated amount of irrigation, according to the irrigation system in this area. Here, time lags of *p* behind *i* caused by utilizing farm ponds and so on were not considered, because the objective of the model is long-term prediction.

3 Results and Discussion

a. Observed groundwater levels and pumping-up discharges

Observed groundwater levels before and after the dam construction are shown in **Figs. 31** and **32**. Groundwater levels at W-21 and W-22, corresponding to sub-basins 1 and 3, usually ranged from 0–4 m before the dam construction. On the other hand, most of the observed levels at KR-6 and KR-3 after the dam construction were in the over-flow condition (> 4 m) beyond the top of the cut-off wall of the subsurface dam. In addition, discharges from pumping-up in the whole study area after the dam construction are also shown in **Fig. 32**.

b. Observed NO_3-N concentrations

Regardless of whether before or after construction of the dam, nitrate was found in all groundwater samples from the study area (**Figs. 33** and **34**). Before the dam construction, the NO_3-N concentrations were more than 10 mg L^{-1} in 1992–1998, and then declined below 10 mg L^{-1} after 1998. This seemed due to a decrease in upland fields and change to environment-friendly agriculture. After the dam construction, the averaged concentrations of NO_3-N were about 10 mg L^{-1}.

c. Simulation results

Calibration

The calculated groundwater levels in the four sub-basins during the calibration period are shown in **Fig. 32**, along with the observed groundwater levels. NRMSEs of the calculated groundwater levels in sub-basins 1, 2, 3 and 9 with respect to the observed values at W-21, ships between the observed and calculated groundwater levels are shown in **Fig. 35**. Although W-18, W-22 and W-24 were 9.8%, 6.7%, 9.0%, and 6.9%, respectively. In addition, relation some peaks in the groundwater levels did not fit the observations, the results indicate that the model calculation duplicated the observed groundwater levels.

The NO_3-N concentrations calculated for the five sub-basins in 1992–2002 are shown in **Fig. 34**, along with the NO_3-N

concentrations observed at the springs. CV(RMSE)s of the calculated NO_3-N concentrations in sub-basins 1, 2, 3, 7, and 9 observed at Sakae-gah, Ashicha-gah, Fukurashi-gah, Shira-kah, and Agari-gah were 22.4%, 50.1%, 27.6%, 29.7%, and 29.3%, respectively. In this way, the short-term fluctuations in NO_3-N concentration can not necessarily be duplicated by the model. However, CV(RMSE)s of the moving average of calculated NO_3-N concentrations, which were compared with the smoothed observed concentrations, were 8.2%, 19.4%, 11.6%, 9.0%, and 12.0% for sub-basins 1, 2, 3, 7, and 9, respectively. This result suggests that the model has an advantage in simulating long-term trends in NO_3-N in the catchment area of the subsurface dam.

Verification

Fluctuations of groundwater levels and NO_3-N concentrations were computed using the calibrated model and the data observed before the dam construction. The simulated groundwater levels and NO_3-N concentrations are shown in **Figs. 32** and **34**, along with

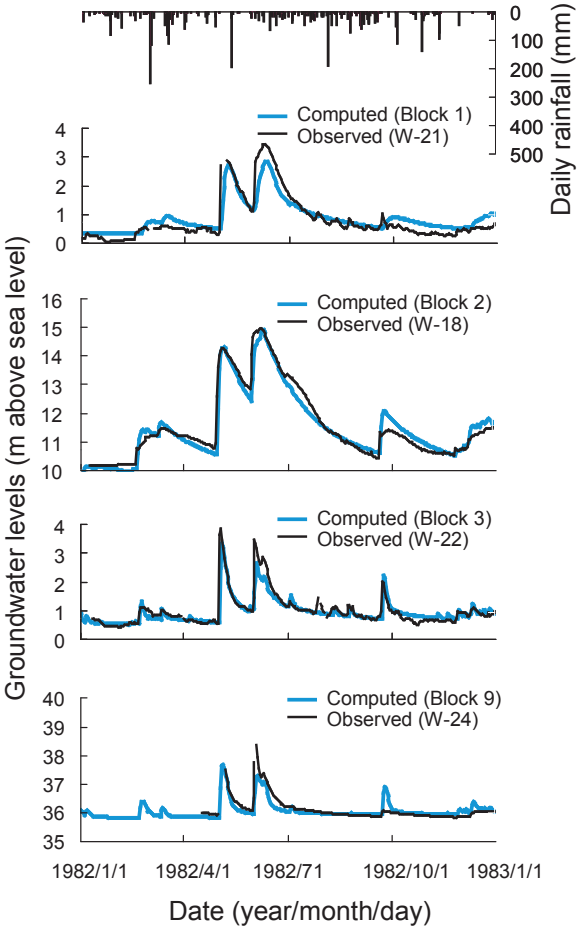

Fig. 31 Observed rainfall and observed and computed groundwater levels before the dam construction

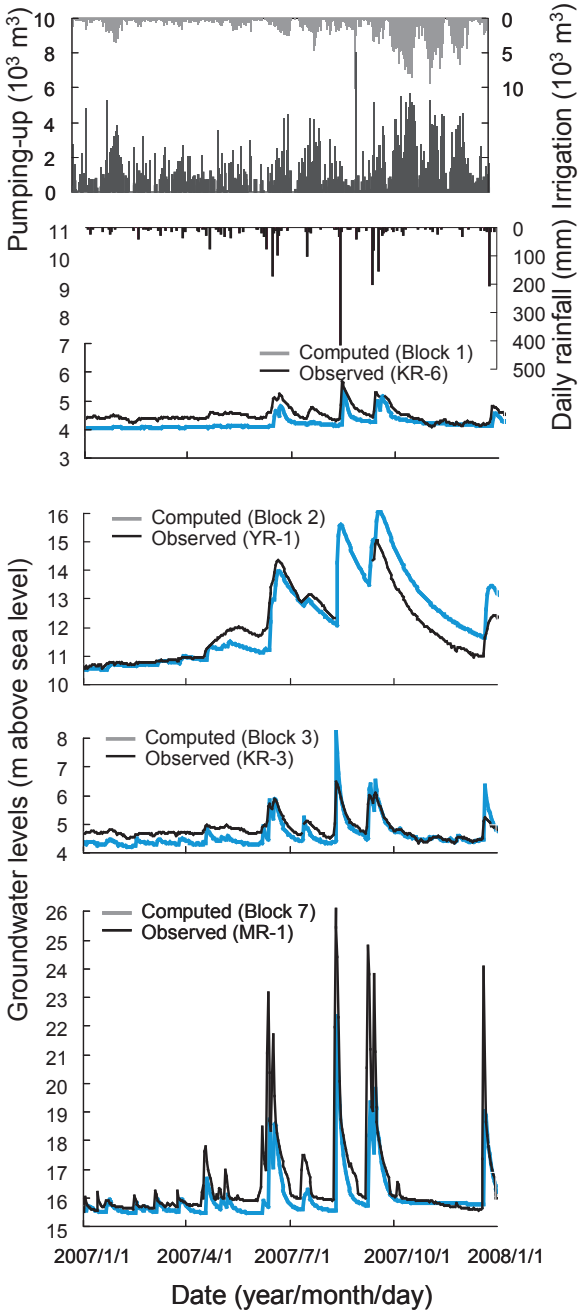

Fig. 32 Observed rainfall, amounts of irrigation and pumping-up in the study area, and observed and computed groundwater levels

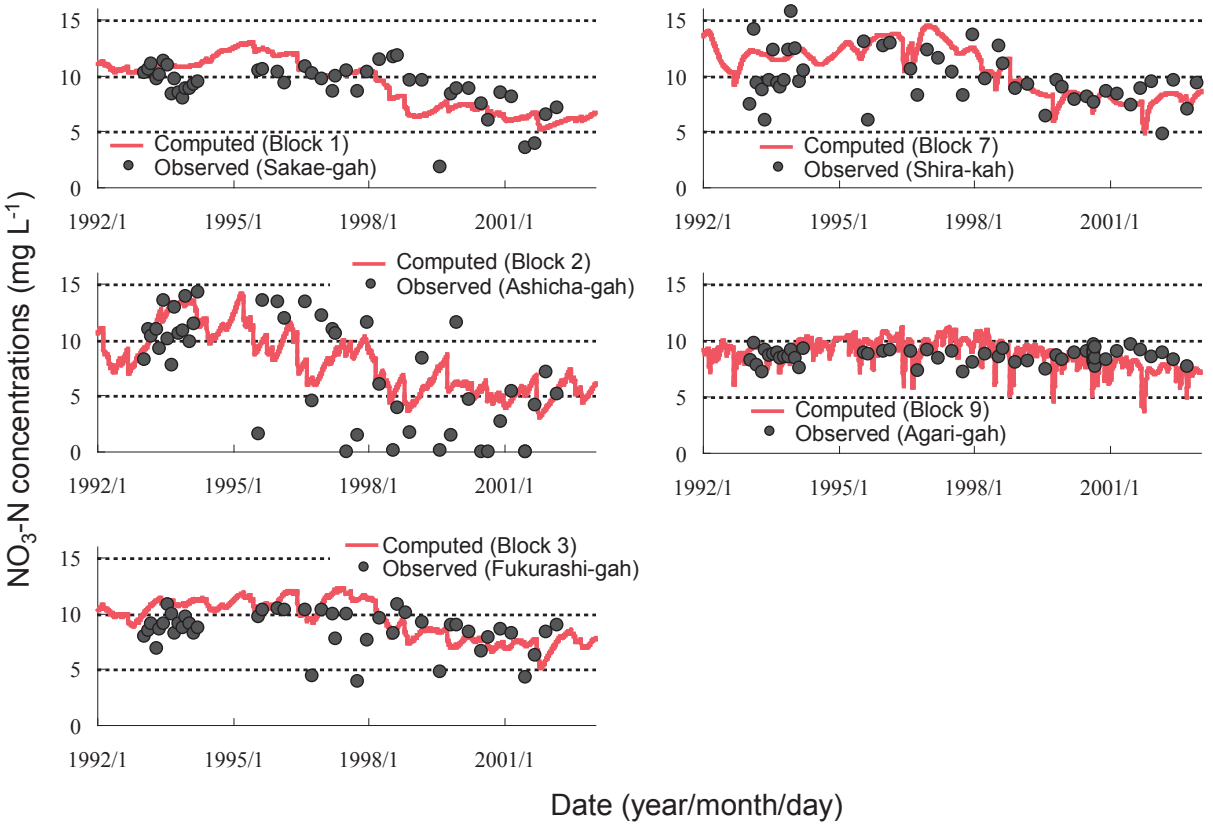

Fig. 33 Observed and computed NO_3-N concentrations in groundwater before the dam construction

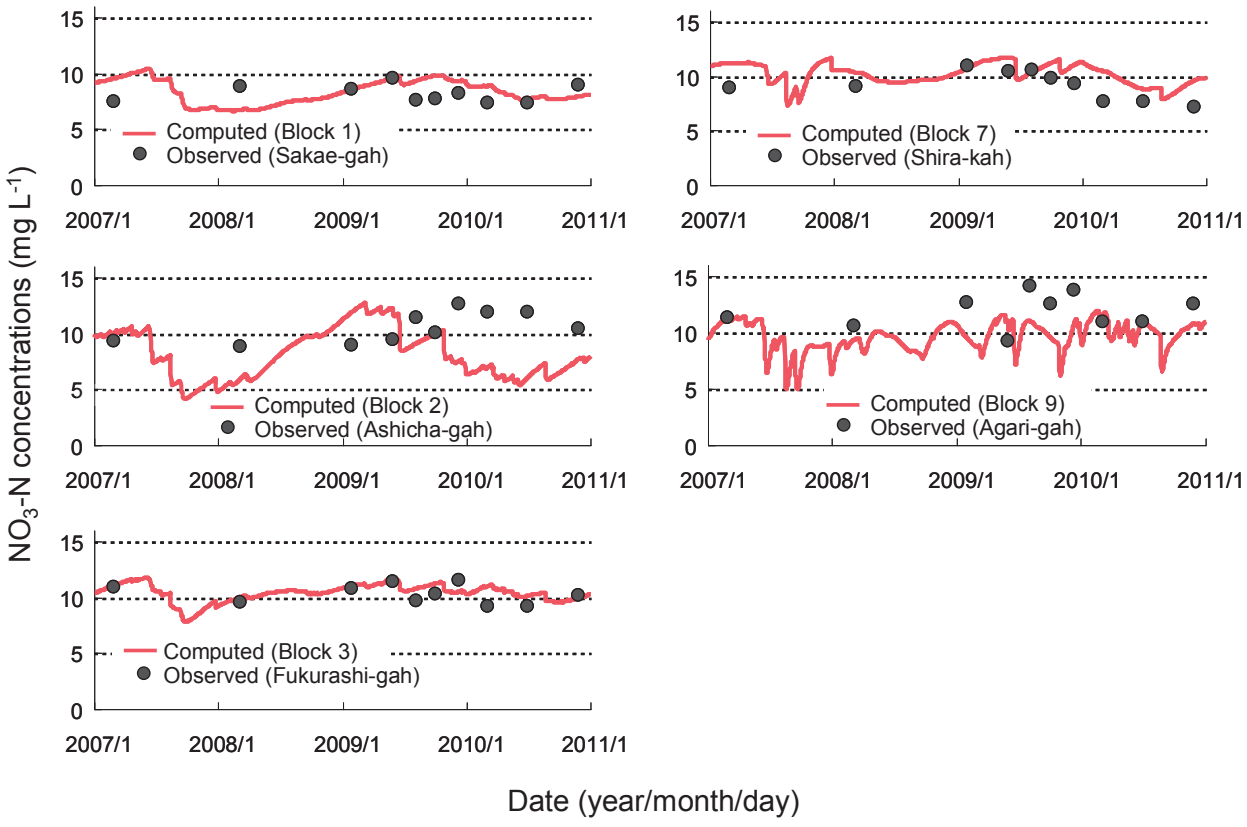

Fig. 34 Observed and computed NO_3-N concentrations in groundwater after the dam construction

the observed data.

Groundwater levels in sub-basins 1 and 3, corresponding to the reservoir area, were calculated to roughly match the observed patterns (**Fig. 32**). The calculated NO_3-N concentrations in sub-basins 1 and 3 closely agreed with those observed, with an uncertainty of 18.7% and 9.8% CV(RMSE), while the fluctuations in NO_3-N in sub-basins 2, 7, and 9 which are located upstream of the basin were not adequately duplicated (**Fig. 34**).

Thus, the model calculation for NO_3-N fluctuations in the reservoir area was verified. It would appear that the model structure regarding concentrations in a homogeneous sub-basin agreed with the situation of groundwater mixing in the reservoir area, so it is reasonable to use tank models to predict groundwater quality in reservoir areas of subsurface dams. The calculation results for short-term variations of NO_3-N in the upstream sub-basins did not closely coincide with the observed concentrations, which may have been because the model had a simple structure that cannot adequately express the complexity of the Ryukyu Limestone aquifer. This lack of repeatability in the upstream sub-basins may not hinder long-term simulations in the reservoir area.

Prediction

The calibrated and verified model was applied to a simulation in the reservoir area for 100 years. The rainfall data were generated assuming that annual rainfall will decrease at a rate of 5.5% per 100 years. The simulated groundwater levels and NO_3-N concentrations are shown in **Figs. 36** and **37**. The minimum groundwater level for each year was calculated to change from −13.5 m for the third year to −15.8 m for the eighty-third year (**Fig. 36**). Lowering of the minimum groundwater level in the reservoir area could cause an increase in saltwater intrusion through the cut-off wall and the basement. The trends of NO_3-N concentrations in the reservoir area were estimated to rise by 0.79–1.46 mg L^{-1} (**Fig. 37**). This implies that it is important to continue to encourage environment-friendly agriculture.

The results of the present study were merely a trial application using rainfall data generated by a simple assumption. Nevertheless, a framework for evaluating the effects of future climate changes on groundwater stored behind subsurface dams was presented. In addition, the proposed model remains applicable to simulations even if the land uses and fertilization methods are changed.

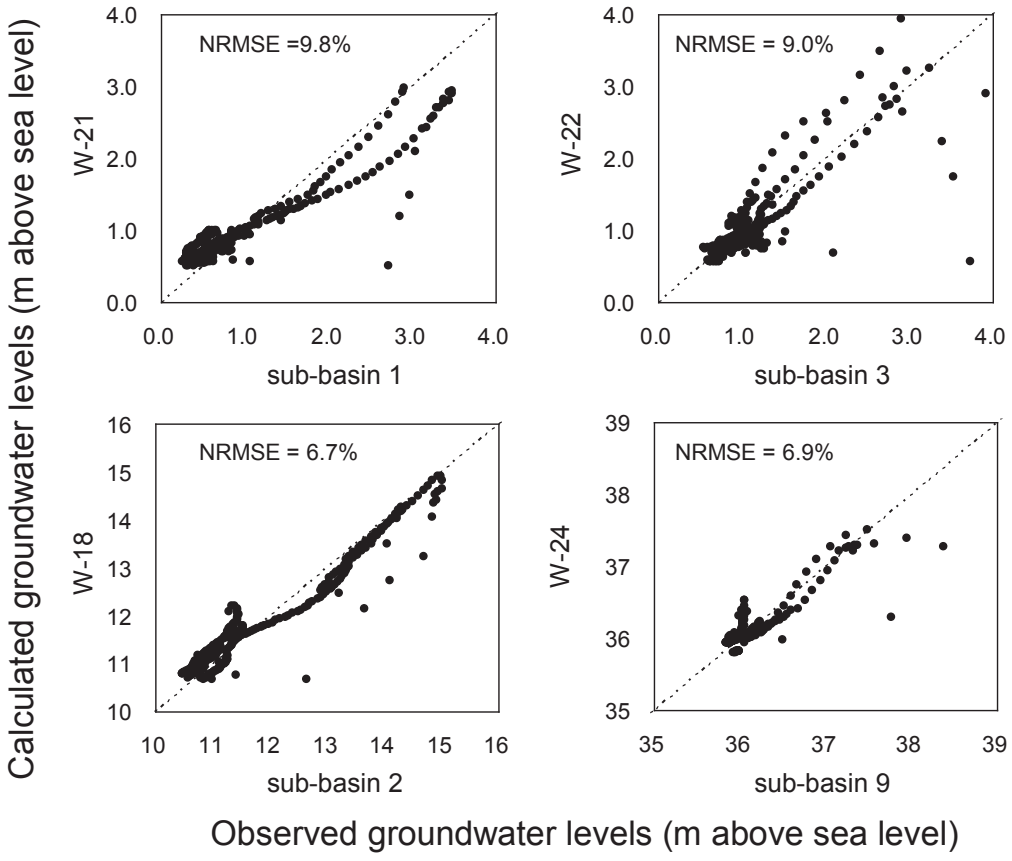

Fig. 35 Relationship between observed and calculated groundwater levels

4 Conclusions

A model using a series of tank models as the water balance submodel and the Kiho-Islam model as the nitrogen balance submodel was proposed to simulate groundwater nitrate in a reservoir area of a subsurface dam in the Ryukyu Limestone region.

The model was calibrated and verified by observed data before and after the dam construction. Calculations for long-term changes in NO_3-N in the reservoir area were adequately calibrated and verified, although the results for short-term fluctuations in upstream sub-basins did not closely match the observed concentrations. This may have been because the model structure agreed with the situation that groundwater is well mixed in the reservoir area. Therefore, the model appears to be applicable to long-term prediction of changes in NO_3-N in the reservoir area.

A trial simulation was executed using the proposed model under a simple assumption that annual rainfall will decrease at a rate of 5.5% per 100 years, and the results showed that the minimum groundwater level will decrease and NO_3-N will increase. Thus, the model can be used for simulations even if the climate, land uses and fertilization methods are changed in the basins of subsurface dams.

5 Appendix

Formulas and parameters in the model were summarized in **Tables 9** and **10**.

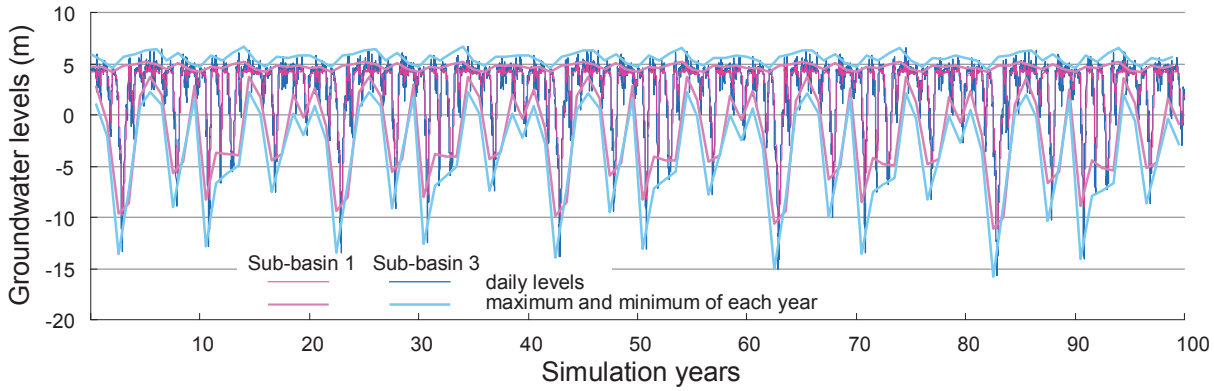

Fig. 36 Simulated groundwater levels for the 100 years

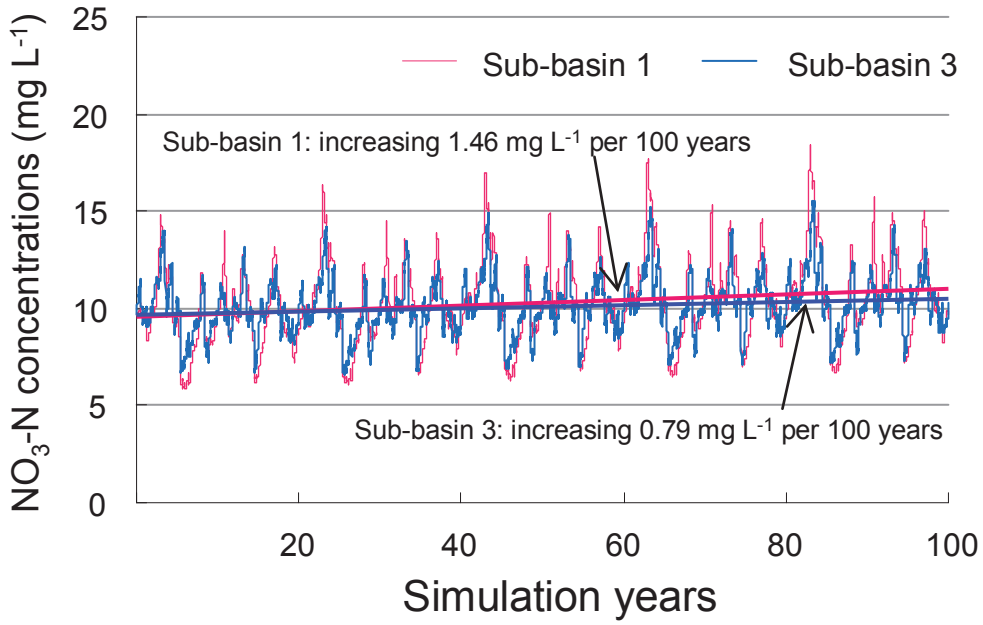

Fig. 37 Simulated NO3-N concentrations for the 100 years

Table 9 Formulas for changes in amounts of nitrogen in various forms

Items	Formulas or calculation procedures	Notations (units), values and descriptions
Nitrate nitrogen: A_N	$A_N(t+1) = A_N(t) + F_R(t) + N_N(t) - D_N(t) - \Delta Y_N(t) - H_N(t) + \Sigma I_N(t) + \Sigma X_N(t)$	F_R: nitrogen in rainfall (kg) N_N: nitrification (kg) D_N: denitrification (kg) ΔY_N: plant uptake of NO_3-N (kg) H_N: organization of nitrogen from NO_3-N (kg) ΣI_N: NO_3-N movements by irrigation and pumping-up (kg) ΣX_N: summation of leaching and lateral transports (kg)
Ammonia nitrogen: A_A	$A_A(t+1) = A_A(t) + M_C(t) + M_H(t) + Z_A(t) + F_E(t) + F_A(t) - N_N(t) - \Delta Y_A(t) - H_A(t)$	A_A: amount of NH_4-N in the uppermost tank (kg) M_C: mineralization of compost (kg) M_H: mineralization of humus (kg) Z_A: dissolution of chemical fertilizer (kg) F_E: NH_4-N loading in effluent from septic tanks (kg) F_A: NH_4-N loading in livestock manure (kg) ΔY_A: plant uptake of NH_4-N (kg) H_A: organization of nitrogen from NH_4-N (kg)
Chemical fertilizer: A_F	$A_F(t+1) = A_F(t) - Z_A(t) + F_F(t) \times G \times \varphi_G$	F_F: applied chemical fertilizer (kg m^{-2} day^{-1}) φ_G: ratio of planted area (m^3 m^{-3}) to 0.21, calculated from the acreages of sugarcane, vegetables and flowers in Itoman City in 2006–2007 (Okinawa Prefecture, 2009).
Compost: A_C	$A_C(t+1) = A_C(t) - H_C(t) - M_C(t) + F_C(t) \times G \times \varphi_G$	H_C: nitrogen generated in humus from compost (kg day^{-1}) M_C: ammonia nitrogen generated from compost (kg day^{-1}) F_C: nitrogen in applied compost (kg m^{-2} day^{-1}).
Plant residues: A_P	$A_P(t+1) = A_P(t) - H_P(t) + F_P(t)$	H_P: nitrogen in humus generated from plant residues (kg day^{-1}) F_P: nitrogen in plant residues left in the fields (kg day^{-1}).
Humus: A_H	$A_H(t+1) = A_H(t) - M_H(t) + H_C(t) + H_P(t) + H_O(t)$	M_H: mineralized nitrogen from humus (kg day^{-1}) H_O: organic nitrogen biochemically converted from NH_4-N and NO_3-N (kg day^{-1})
Domestic wastewater: F_E	$F_E = m_P \times f_E$	m_P: population in each sub-basin (person) f_E: emission factors for nitrogen in effluents from old-fashioned septic tanks (kg per person per day) set at 3.1×10^{-3}
Livestock manure: F_A	$F_A = m_A \times f_A - c_D$	m_P: livestock numbers f_A: emission factors for c_D: constant deduction for disposal by composting and the like determined to 50,000 kg $year^{-1}$ after trials.
Rainfall nitrogen: F_R	$F_R = r \times C_R$	C_R: average NO_3-N concentrations (mg L^{-1}) set at 0.5 (Tashiro and Takahira, 2001)
Leaching and lateral transports: X_N	$X_N = q_i \times C$ for $i = 2, 4, 5$, $X_N = q_i \times C_R$ for $i = 1, 3$	q_i: infiltration or percolation flow through each pipe or groundwater flow C: NO_3-N concentration in each tank
Capillary action	not considered	It is because downward flow is predominant in permeable and porous aquifers such as the Ryukyu Limestone
Irrigation and pump-ing-up: I_N	considered only after the dam consideration $I_N = p \times C_N - i \times C_{N(1,3)}$	C_N: NO_3-N concentration in the lowest tank $C_{N(1,3)}$: averaged NO_3-N concentration between sub-basins 1 and 3.

Table 10 Formulas for chemical and biochemical reactions of nitrogen

Items	Equations	Notations (values, units, literatures) and descriptions
Ground temperature function: τ	$\tau = \zeta^{\{(T-TS)/10\}}$	T: ground temperature (°C), same as air temperature in the uppermost tank, 21.0 °C (the annual mean air temperature) in the lowermost tank, the intermediate value in the middle tank. T_S: standard temperature (21.0 °C) ζ: temperature coefficient (2.2, dimensionless)
Soil moisture function: μ **Fertilizer dissolution function**: μ_F **Denitrification function**: μ_D	$\mu = \eta / \eta_{FC}$ $\mu_F = (\eta - \eta_{FC} \times 0.6) / (\eta_{SM} - \eta_{FC} \times 0.6)$ $\mu_D = (\eta - \eta_{FC} \times 0.9) / (\eta_{SM} - \eta_{FC} \times 0.9)$	η: soil moisture (m), η_{FC}: field capacity (m), η_{SM}: saturated moisture content (m) η, η_{FC} and η_{SM} are equal to h_1, z_2 and z_1 in the uppermost tank respectively, 1 in the lowermost tank, and the intermediate values in the middle tank.
Nitrification: N_N	$N_N = (A_A + M_C + M_H + Z_A) \times \alpha_N \times \tau \times \mu$,	α_N: nitrification coefficient (0.15 day^{-1})
Denitrification: D_N	$D_N = A_N \times \alpha_D \times \tau \times \mu$	α_D: denitrification coefficient (0.006 day^{-1})
Dissolution of chemical fertilizer: Z_A	$Z_A = A_F \times \alpha_F \times \tau \times \mu_F$	α_F: coefficient for fertilizer dissolution (0.206 day^{-1})
Humification of compost: H_C **Mineralization of compost**: M_C	$H_C = A_C \times \alpha_C \times \tau \times \mu \times \rho_C \times \chi_Z / \rho_H$ $M_C = A_C \times \alpha_C \times \tau \times \mu - H_C$	α_C: coefficient of compost decomposition (0.0188 day^{-1}; Goto and Eguchi, 1998) χ_Z: parameter of carbon residual (0.5, dimensionless) ρ_C: carbon/nitrogen ratios of compost (8.9 kg kg^{-1}; Goto and Eguchi, 1998) ρ_H: carbon/nitrogen ratios of humus (25 kg kg^{-1}; Robertson and Thorburn, 2007)
Humification of plant residues: H_P	$H_P = A_P \times \alpha_P \times \tau \times \mu$	α_P: coefficient of decomposition of plant residues (0.0045day^{-1}; Robertson and Thorburn, 2007)
Mineralization of humus: M_H	$M_H = (A_H + H_C + H_P) \times \xi_2 \times \alpha_H \times \tau \times \mu$	α_H: spped coefficient of humus mineralization (0.0045 day^{-1}; equal to α_P) ξ_2: possibility coefficient of humus mineralization (1, dimensionless; i.e. ignored)
Biochemical conversion to organic nitrogen: H_O Generated ammonia nitrogen: H_A Generated nitrate nitrogen: H_N	$H_O = H_P \times (\rho_P / \rho_H \times \chi_Z - 1)$ $H_A = H_O \times (A_A + M_C + M_H + Z_A + F_E - N_N) / (A_A + M_C + M_H + Z_A + A_N + F_E + F_R)$, $H_N = H_O - H_A$	ρ_P: carbon/nitrogen ratio of plant residues (93.5 kg kg^{-1}; Robertson and Thorburn, 2007)
Plant uptake: ΔY Up-taken ammonia nitrogen: ΔY_A Up-taken nitrate nitrogen: ΔY_N	$\Delta Y(t_C) = \{Y(t_C) - Y(t_C - 1)\} \times G \times \varphi_G$ $Y(t_C) = Y_L / [1 + \exp\{\gamma \times (t_C - t_L/2)\}]$ $\Delta Y_A = \Delta Y \times (A_A + M_C + M_H + Z_A + F_E - N_N) / (A_A + M_C + M_H + Z_A + A_N + F_E + F_R)$, $\Delta Y_N = \Delta Y - \Delta Y_A$.	t_C: day in the cultivation cycle (see **Table 7**) t_L: cultivation period (500 day; see **Table 7**) Y_L: eventual yield of nitrogen in whole sugarcane (6.59 kg m^{-2}; Okinawa Prefecture, 2009) γ: coefficient for the logistic curve ($-15.57 / t_L$; Kiho and Islam, 1995)

* The parameter values without descriptions of literatures were set after Kiho and Islam (1995).

VII Summation

1 Research Summary

This thesis presents the hydrogeological properties in the Ryukyu Limestone aquifer of the southern part of Okinawa Island. These properties were investigated through the analysis of groundwater levels and NO_3-N concentrations and geochemical and isotopic investigations such as ^{15}N and ^{222}Rn. In addition, a numerical model able to simulate changes in groundwater levels and NO_3-N in the reservoir area of a subsurface dam was developed and applied to the Komesu subsurface dam.

In Chapter 4, the hydrogeological properties of the Ryukyu Limestone aquifer in the Komesu basin were discussed through the categorization of groundwater level and NO_3-N fluctuations and the time-series analysis of groundwater hydrographs. The Ryukyu Limestone aquifer is considered to be a "mixed type", in which both matrix flow and fracture flow exist. Data on groundwater levels and NO_3-N concentrations were monitored for the subsurface dam project. The short-term fluctuation patterns of groundwater levels and NO_3-N concentrations were categorized into two types, and the long-term trend of NO_3-N was obtained by using a nonparametric regression analysis. In addition, a statistical model was applied to the rainfall and groundwater level data to clarify the differences between diffuse and conduit flow in the Ryukyu Limestone aquifer.

In Chapter 5, the properties of water and solute transport in the Ryukyu Limestone of southern Okinawa Island were discussed. Firstly, the trend in estimated amounts of nitrogen emission from chemical fertilizer, livestock manure and domestic wastewater was compared to the long-term changes in NO_3-N concentrations in groundwater, to discuss the predominant nitrogen source affecting the groundwater quality. Secondly, the content of major ions, rate of nitrogen isotopes in nitrate ($\delta^{15}N$), and radon (^{222}Rn) concentration were measured, to discuss the groundwater flow and the transport and potential source of groundwater nitrates.

In Chapter 6, a regional quantitative model developed to describe prolonged daily groundwater recharge and nitrogen dynamics in the catchment area of a subsurface dam was described. The model uses a series of tank models as a water balance submodel and the Kiho-Islam model as a nitrogen balance submodel. The model was calibrated using data observed prior to the dam construction, and was verified to reflect the effect of the dam construction, after which the parameters of the model were optimized. In addition, the model was used to forecast long-term changes in groundwater levels and nitrate concentrations in the reservoir area of a subsurface dam under decreasing precipitation conditions.

2 Conclusions

Through the hydrological investigations described in Chapter 4, the hydrogeological properties of the Ryukyu Limestone aquifer were discussed. The short-term fluctuations of NO_3-N concentrations in groundwater are classified into two types: large short-term fluctuations and small short-term fluctuations. The springs showing large NO_3-N fluctuations were near caves, where rainwater rapidly enters the groundwater and dilutes the NO_3-N concentration. Similarly, boreholes in which groundwater level rose rapidly after rainfall events are also located near caves. Furthermore, the groundwater hydrographs can be broken down into low- and high-frequency components, where the low-frequency response was interpreted to reflect slow diffuse groundwater flow in the rock matrix, and the high-frequency response to reflect rapid conduit flow in the caves and caverns. These results suggest that the Ryukyu Limestone aquifer is a "mixed flow" aquifer with the coexistence of slow diffuse flow in the matrices and rapid conduit flow in the caves and caverns. On the other hand, the long-term trend in NO^3-N concentration observed at all springs was the same: generally decreasing since the mid-1990s.

Through the geochemical and isotopic investigations described in Chapter 5, the groundwater flow and the transport and potential source of groundwater nitrates in the Ryukyu limestone were discussed. The distribution of relatively low concentrations of ^{222}Rn near caverns also suggests that the Ryukyu Limestone aquifer is a "mixed flow" aquifer. To elucidate the nitrate sources and movement, the sampling sites were categorized into upland field (UF) type, residential area (RA) type and cave and cavern (CC) type, according to the land-use and hydrogeological settings near two large caverns, even though CC should be categorized as the UF type from the viewpoint of land use. The average $\delta^{15}N$ value for CC was similar to that for RA. This was considered as evidence that CC groundwater nitrates were carried by groundwater flow through caves and caverns from the upstream residential areas. According to previous studies related to ^{15}N, animal and human waste is considered the predominant source of nitrogen for RA and CC, although the correspondence of the long-term trend in NO_3-N and the emitted load from chemical fertilizer seems to suggest that the application of chemical fertilizer predominantly affects groundwater quality. On the other hand, the $\delta^{15}N$ values for UF were higher than those reported in literature for groundwater nitrates beneath fertilized upland fields. Denitrification and multiple sources

are considered as explanations for this dissociation, but denitrification is unlikely to be the sole cause. Consequently, considering that the origin of UF groundwater nitrates is complex, multiple sources seem reasonable. This was also confirmed from the relatively high correlation between the calculated contribution ratio of chemical fertilizer and the rate of upland areas and residential areas upstream of the sites.

In Chapter 6, a numerical model to simulate the reservoir area of the Komesu subsurface dam was proposed. The model was calibrated and verified by observed data before and after the dam construction. Calculations for long-term changes in NO_3-N in the reservoir area were adequately calibrated and verified, although the results for short-term fluctuations in upstream sub-basins did not closely match the observed concentrations. This may have been because the model structure agreed with the fact that groundwater is well mixed in the reservoir area. Therefore, the model seemed applicable to long-term prediction of changes in NO_3-N in the reservoir area. A trial simulation was executed using the proposed model under decreasing precipitation conditions, and the results showed that the minimum groundwater level will decrease and NO_3-N will increase.

3 Future Work

Throughout the world, carbonate aquifers provide an important water resource, and thus are the subject of intensive research and conservation measures. However, the hydrogeology in carbonate terrains is still not well understood. In the case of the Ryukyu Limestone aquifer, studies are still in the early stage.

The double porosity of Ryukyu Limestone has been confirmed by the categorization of fluctuations in groundwater levels and NO_3-N concentrations and the time-series analysis of groundwater hydrographs, but quantification such as the rate of diffuse flow to conduit flow is yet to be achieved. Furthermore, heterogeneities such as the buffer effect of filling clay remain unexplained.

The source and transport of nitrates in the groundwater of the Ryukyu Limestone aquifer has been discussed though the application of geochemical and isotopic approaches such as ^{15}N and ^{222}Rn. The mechanism of nitrate movement was revealed in a specific area on Okinawa Island, but has not yet been generalized. It would be necessary to research other regions where Ryukyu Limestone is distributed, and to add other chemical, biological and isotopic components such as trace metals, bacteria and ^{13}C in carbonate to surveys and discussions on water and solute transport.

The proposed model using a series of tank models and the Kiho-Islam model could simulate long-term NO_3-N changes in the reservoir area of the Komesu subsurface dam. From the perspective of more accurate management of groundwater quality, distributed models such as finite-element models are more ideal. However, there are several difficulties related to heterogeneity in the Ryukyu Limestone aquifer, for instance, the rapid groundwater flow in caves is difficult to represent using distributed models. Developing a model that overcomes such difficulties is also a future task.

Lastly, the most important work is to apply the knowledge on hydrogeological and geochemical aspects gained through this study for management and conservation of the catchment and reservoir areas of subsurface dams. The results obtained could help explain the complex hydrogeological properties of the Ryukyu Limestone aquifers in Okinawa, and contribute to the protection of sustainable groundwater resources.

The author wishes to express his sincere gratitude to Dr. Toshihiko Kawachi, Professor of Water Resources Engineering, Division of Environmental Science and Technology, Graduate School of Agricultural Science, Kyoto University, and Chairperson of the Examination Committee, for his keen guidance, valuable suggestions and constructive criticisms in the completion of this research.

The author also wishes to extend his sincere appreciation to the members of his Examination Committee, Professor Dr. Akira Murakami and Professor Dr. Shigeto Kawashima, for their discussions and constructive suggestions in reviewing and improving this thesis.

The author is very grateful to Dr. Masayuki Imaizumi, Director of Renewable Resources Engineering Research Division, National Institute for Rural Engineering, for his technical assistance and valuable advice. The author wishes to thanks and Dr. Takao Masumoto and Dr. Satoshi Ishida, Chief and Senior Researchers of Renewable Resources Engineering Research Division, National Institute for Rural Engineering; Dr. Takeo Tsuchihara, Deputy Director of Secretariat of Agriculture, Forestry and Fisheries Research Council, for their assistances. Special thanks are due to Dr. Norio Nawa, Dr. Tadashi Yamashita, Mr. Tokue Taira and Mr. Jin Nakao, Ministry of Agriculture Forestry and Fisheries; Mr. Haruo Bajo and Mr. Mitsuhiko Miyazato, the Okinawa Hontoh Nanbu Land Improvement District, for their helpful assistance on this study.

The author acknowledges all the members of National Institute for Rural Engineering with special emphasis to Dr. Hiromasa Hamada, Mr. Takashi Baba, Mr. Keiji Watabe, Mr. Hiroki Minakawa, Dr. Ryoji Kudo, Ms. Fumiko Suzuki, Ms. Midori Iwashita,

Ms. Natsuko Kumagai, Mr. Masatoshi Ishizuka, Ms. Tomomi Yoshida, Mr. Moono Shin and Dr. Satoshi Kono for their sincere cooperation and assistance.

This report is based on the author's doctoral thesis defended at Kyoto University.

References

1) Agata, S., Satake, H., Tokuyama, A. (2001): Chemical characteristics and isotopic compositions of spring and river waters in Okinawa Island (in Japanese). *Geochemistry* (*Chikyukagaku*), **35**, 27–41.
2) Agricultural Structure Improvement Bureau (1993): *Third draft for the guideline of planning and design for subsurface dams*. 188
3) Abelin, H., Birgersson, L., Moreno, L., Widen, H., Agren, T., Neretnieks, I. (1991): A large-scale flow tracer experiment in granite 2: results and interpretation. *Water Resources Research*, **27**(12), 3119–3135.
4) Almasri, M.N., Kaluarachchi, J.J. (2007): Modeling nitrate contamination of groundwater in agricultural watersheds. *Journal of Hydrology*, **343**, 211–229.
5) Andrews, R.J., Lloyd, J.W., Lerner, D.N. (1997): Modelling of nitrate leaching from arable land into unsaturated soil and chalk. 2. Model confirmation and application to agricultural and sewage sludge management. *Journal of Hydrology*, **200**, 198–221.
6) Atetsu Research Group (1970): Notes on the cave geology 5: Limestone caves and river terraces in Atetsu plateau, western Japan (in Japanese). *Earth Science* (*Chikyu Kagaku*), **24**(6), 225–227.
7) Beven, K., Germinn, P. (1982): Macropores and water flow in soils. *Water Resources Research*, **18**, 1311–1325.
8) Birkinshaw, S.J., Ewen, J. (2000): Nitrogen transformation component for SHETRAN catchment nitrate transport modelling. *Journal of Hydrology*, **230**, 1–17.
9) Böhlke, J.K., Denver, J.M. (1995): Combined use of groundwater dating, chemical, and isotopic analyses to resolve the history and fate of nitrate contamination in two agricultural watersheds, atlantic coastal Plain, Maryland. *Water Resources Research*, **31**(9), 2319–2339.
10) Böhlke, J.K. (2002): Groundwater recharge and agricultural contamination. *Hydrogeology Journal*, **10**, 153–179.
11) Carey, M.A., Lloyd, J.W. (1985): Modelling non-point sources of nitrate pollution of groundwater in the Great Ouse Chalk, U.K. *Journal of Hydrology*, **78**, 83–106.
12) Chen, Z., Grasby, S.E., Osadetz, K.G. (2002): Predicting average annual groundwater levels from climatic variables: an empirical model. *Journal of Hydrology*, **260**, 102–117.
13) Chen, Z., Grasby, S.E., Osadetz, K.G. (2004): Relation between climate variability and groundwater levels in the upper carbonate aquifer, southern Manitoba, Canada. *Journal of Hydrology*, **290**, 43–62.
14) Domenico, P.A., Schwartz, F.W. (1998): Physical and chemical hydrogeology (2nd ed). 506
15) Dongarrà, G., Hauser, S., Censi, P., Brai, M. (1995): Water chemistry, $\delta^{13}C$ values and ^{222}Rn activity in groundwaters of western Sicily. *Nuclear Geophysics*, **9**(5), 461–470.
16) Drogue, C. (1980): Essai d'identification d'un type de structure de magasins carbonates, fissurés (in French), *Mémoire hors série de la Société Géologique de France*, **11**, 101–108.
17) Field, M.S. (1988): The vulnerability of karst aquifers to chemical contamination. *Hydrological Science and Technology*, **4**, 130–142.
18) Fogg, G.E., Rolston, D.E., Decker, D.L., Louie, D.T., Grismer, M.E. (1998): Spatial variation in nitrogen isotopic values beneath nitrate contamination sources. *Ground Water*, **36**(3), 418–426.
19) Furukawa, H., Shibasaki, T. Ohno, S. (1976): Groundwater resources for irrigation in Okinawa (in Japanese). *Geological Studies in Ryukyu Islands*, **1**, 75–78.
20) Goto, S., Eguchi, H. (1998): Decomposition kinetics of organic materials under field conditions in Dark Red Soil derived from Ryukyu Lime Stone (in Japanese). *Japanese Journal of Soil Science and Plant Nutrition*, **69**(2), 129–134.
21) Hamada, H., Komae, T. (1998): Analysis of recharge by paddy field irrigation using ^{222}Rn concentration in groundwater as an indicator. *Journal of Hydrology*, **205**, 92–100.
22) Hanshaw, B.B., Back, W. (1979): Major geochemical processes in the evolution of carbonate-aquifer systems. *Journal of Hydrology*, **43**, 287–312.

23) Harbargh, A.W., McDonald, M.G. (1996): User's documentation for MODFLOW-96, an update to the US Geology Survey modular finite-difference ground-water flow model. *US Grological Survey Open-File Report* 96-485, 56

24) Heaton, T.H.E. (1986): Isotopic studies of nitrogen pollution in the hydrosphere and atmosphere — a review. *Chemical Geology*, **59**(1), 87–102.

25) Hendriks, R.F.A., Oostindie, K., Hamminga, P. (1999): Simulation of bromide tracer and nitrogen transport in a cracked clay with the FLOCR/ANIMO model combination. *Journal of Hydrology*, **215**, 94–115.

26) Hübner, H. (1986): Isotope effects of nitrogen in the soil and biosphere. In: Fritz, P., Fontes, J.C. (eds.) *Handbook of Environmental Isotope Geochemistry, 2b, The Terrestrial Environment*, Elsevier, 361–425.

27) Ii, H., Yamano, K., Hirata, T., Tanaka, T., Nishikawa, M. (2003): Nitrogen contamination from fertilizer in tea plantation, Kiku River basin, Japan. In: Kono, I., Nishigaki, M., Komatsu, M. (eds.) *Groundwater Engineering —Recent Advances*, Springer, 335–341.

28) Imaizumi, M., Okushima, S., Shiono, T. (2002a): Characteristics of spatial distribution of caves in Ryukyu Limestone in southern part of Okinawa Island (in Japanese). *Transactions of the Japanese Society of Irrigation Drainage and Reclamation Engineering*, **217**, 89–100.

29) Imaizumi, M., Okushima, S., Shiono, T., Takeuchi, M., Komae, T. (2002b): Salt water intrusion into a Ryukyu Limestone aquifer in Komesu Underground Dam Basin, southern part of Okinawa Island (in Japanese). *Transactions of the Japanese Society of Irrigation Drainage and Reclamation Engineering*, **221**, 11–23.

30) Inoue, K., Kobayashi, A., Aoyama, S. (2003): Mass transport analysis with nitrogen species transformation model in soil (in Japanese). *Transactions of the Japanese Society of Irrigation Drainage and Reclamation Engineering*, **225**, 33–42.

31) Ishida, S., Mori, K., Tsuchihara, T., Imaizumi, M. (2005): Infiltration velocity of preferred flow of artificial recharged water through macropores in terrace sand and graval layer (in Japanese). *Journal of the Japanese Society of Engineering Geoligy*, **46**(4), 207–219.

32) Ishida, S., Tsuchihara, T., Yoshimoto, S., Imaizumi, M. (2011): Sustainable use of groundwater with underground dams, *JARQ*, **45**(1), 51–61.

33) Ishiguro, M. (1994): Solute transport in soils as affected by macropores (in Japanese). *Japanese Journal of Soil Science and Plant Nutrition*, **65**(3), 349–356.

34) Kamahori, H., Fujibe, F. (2009): Long-term changes in precipitation and a drought in summer 2008 in Japan (in Japanese). In symposium on the integrated study in artificial rainfall and snow for countermeasures to drought. 33

35) Kaneko, K., Ujiié, H. (2006): Geology of the Itoman and Kudaka Jima Districts (in Japanese). *Quadrangle Series, 1:150,000, Geological Survey of Japan, AIST*. 47

36) Kiho, N., Islam, T. (1995): Nitrogen leaching estimation model for shallow groundwater (in Japanese). *Report of the Research Project Team of Kyushu National Agricultural Experiment Station*, **2**, 49–63.

37) Kirshenbaum, I., Smith, J.S., Crowell, T., Graff, J., McKee, R. (1947): Separation of nitrogen isotopes by the exchange reactions between ammonia and solutions of ammonium nitrate. *Journal of Chemical Physics*, **15**, 440–446.

38) Kita-Bingo Plateau Research Group (1969): On the age of the formation of limestone caves: an example (in Japanese with English abstract). *Journal of the Geological Society of Japan*, **75**(5), 281–287.

39) Kondo, H., Tase, N., Hirata, T. (1997): Nitrogen isotope ratio of nitrate of groundwater in Miyako Island, Okinawa Prefecture (in Japanese). *Journal of Groundwater Hydrology*, **39**(1), 1–15.

40) Kono, M. (1972): Formation of calcareous caves in Akiyoshi-dai (in Japanese). *Professor Iwai Jun-ichi Memorial*, 319–331.

41) Kreitler, C.W., Jones, D.C. (1975): Natural soil nitrate: The ause of the nitrate contamination of ground water in Runnels County, Texas. *Ground Water*, **13**(1), 53–61.

42) Kreitler, C.W. (1979): Nitrogen-isotope studies of soils and groundwater nitrate from alluvial fan aquifers in Texas. *Journal of Hydrology*, **42**, 147–170.

43) Kundzewicz, Z.W., Döll, P. (2009): Will groundwater ease freshwater stress under climate change? *Hydrological Science Journal*, **54**(4), 665–675.

44) Kunikane, S. (1996): Health effect of nitrate and nitrite nitrogen (in Japanese). *Journal of Japanese Society on Water Environment*, **19**, 965–968.

45) Létolle, R. (1980): Nitrogen-15 in the natural environment. In: Fritz, P., Fontes, J. (eds.) *Handbook of Environmental Isotope Geochemistry, Vol. 1*, Elsevier, 407–433.

46) Malcolm, R., Soulsby, C. (2000): Modelling the potential impact of climate change on a shallow coastal aquifer in northern Scotland. *Geological Society Special Publications*, **182**, 191–204.

47) Mariotti, A., Landreau, A., Simon, B. (1988): N isotope biogeochemistry and natural denitrification process in groundwater—Application to the chalk aquifer of northern France. *Geochimica et Cosmochimica Acta*, **52**, 1869–1878.

48) McClelland, J.W., Valiela, I. (1998): Linking nitrogen in estuarine producers to land-derived sources, *Limnology and Oceanography*, **43**, 577–585.

49) Ministry of Agriculture, Forestry and Fishery (MAFF) (2003): *Principles of the environmental policy in agriculture, forestry and fisheries* (in Japanese). http://www.maff.go.jp/j/kanbo/kankyo/seisaku/pdf/zentai.pdf

50) Ministry of Education, Culture, Sports, Science and Technology (MEXT), Japan Meteorological Agency (JMA), Ministry of the Environment (MOE) (2009): *Synthesis report on observations, projections, and impact assessments of climate change: Climate change and its impacts in Japan*, 74 http://www.env.go.jp/en/earth/cc/report_impacts.pdf

51) Ministry of the Environment (2002): *Handbook for protection of nitrate pollution in groundwater* (in Japanese), 359

52) Ministry of the Environment (2009): *Survey results on general waste disposal in 2006* (in Japanese). http://www.env.go.jp/recycle/waste_tech/ippan/h18/index.html

53) Momii, K., Shoji, J., Nakagawa, K., Jinno, K. (2003): Seawater intrusion analysis by sharp interface approach with groundwater recharge: Study on conservation and development of groundwater resources in island (in Japanese). *Transactions of the Japanese Society of Irrigation Drainage and Reclamation Engineering*, **224**, 81–87.

54) Nagata, J. (1993): Present condition of groundwater quality and method of its conservation in Miyakojima, Okinawa prefecture (in Japanese). *Journal of the Japanese Society of Irrigation Drainage and Reclamation Engineering*, **61**(4), 331–335.

55) Nakanishi, Y., Yamamoto, Y., Park, K.L., Kato, K., Kumazawa, K. (1995): Estimation and verification of origins of groundwater nitrate by using $\delta^{15}N$ values (in Japanese). *Japanese Journal of Soil Science and Plant Nutrition*, **66**(5), 544–551.

56) Nakanishi, Y., Shimoji, M., Takahira, K. (2005): Groundwater concentration and $\delta^{15}N$ of nitrate-nitrogen in the south area of Okinawa Is. (in Japanese). *Tropical Agriculture and Development*, **49**(ext. 1), 29–30.

57) Nawa, N., Miyazaki, K. (2009): The analysis of saltwater intrusion through Komesu underground dam and water quality management for salinity. *Paddy and Water Environment*, **7**(2), 71–82.

58) Nishiguchi, T. (1986): Method of sewage disposal in rural areas (in Japanese) In: Tabuchi, T. (ed.). *Introduction to Water Quality for Rural Engineers*, Japanese Society of Irrigation, Drainage and Reclamation Engineering: 127–138.

59) Novakowski, K.S., Lapcevic, P.A. (1994): Field measurement of radial solute transport in a discrete rock fracture. *Water Resources Research*, **30**(1), 37–44.

60) Oelmann, Y., Kreutziger, Y., Bol, R., Wilcke, W. (2007): Nitrate leaching in soil: Tracing the NO_3^- sources with the help of stable N and O isotopes. *Soil Biology and Biochemistry*, **39**, 3024–3033.

61) Okimura, Y., Takayasu, K. (1976): Recent advances in Quaternary geology 8: Quaternary geology in limestone regions (in Japanese). *Tsuchi-to-Kiso*, **24**(1), 65–72.

62) Okinawa General Bureau (1983): *Report on grouting operation tests for the subsurface dam project (4)* (in Japanese), 112

63) Okinawa General Bureau (2006): *Project magazine of Okinawa Hontoh Nanbu National Irrigation Project* (in Japanese), 629

64) Okinawa Prefecture (2001): *Current land use map of Itoman* (in Japanese).

65) Okinawa Prefecture (2003a): *Cultivation manual for vegetables* (in Japanese), 28

66) Okinawa Prefecture (2003b): *Agricultural statistics in Okinawa* (in Japanese), 205

67) Okinawa Prefecture (2006a): *Cultivation guidelines for sugarcane* (in Japanese), 94

68) Okinawa Prefecture (2006b): *Cultivation manual for flowers* (in Japanese), 21

69) Okinawa Prefecture (2008): *Livestock industry in Okinawa* (in Japanese), 40

70) Okinawa Prefecture (2009): *Agricultural statistics in Okinawa* (in Japanese), 195

71) Oren, O., Yechieli, Y., Böhlke, J.K., Dody, A. (2004): Contamination of groundwater under cultivated fields in an arid environment, central Arava Valley, Israel. *Journal of Hydrology*, **290**, 312–328.

72) Owor, M., Taylor, R.G., Tindimugaya, C., Mwesigwa, D. (2009): Rainfall intensity and groundwater recharge: empirical evidence from the Upper Nile Basin. *Environmental Research Letters*, **4**, 035009 doi:10.1088/1748-9326/4/3/035009

73) Pane, M.B. (1995): Le radon: traceur des circulations fluides dans les aquiféres karstiques. *Comptes Rendus de l'Académie*

des Science Paris série II a, 713–719.

74) Peterson, E.W., Davis, R.K., Brahana, J.V., Orndorff, H.A. (2002): Movement of nitrate through regolith covered karst terrane, northwest Arkansas. *Journal of Hydrology*, **256**, 35–47.

75) Quinlan, J.F., Ewers, R.O. (1985): Ground water flow in limestone terranes: Strategy, rationale and procedure for reliable, efficient monitoring of ground water quality in karst areas. *Proceedings of 5th National Symposium and Exposition on Aquifer Restoration and Ground Water Monitoring*, 197–235.

76) Robertson, F.A., Thorburn, P.J. (2007): Decomposition of sugarcane harvest residue in different climatic zones. *Australian Journal of Soil Research*, **45**, 1–11.

77) Rural Development Bureau, MAFF (1997): *Standards on project planning and design for land improvement, irrigation planning to upland fields*.

78) Sakura, Y. (1989): Infiltration (in Japanese). *Meteorological Research Note*, **167**, 275–285.

79) Scanlon, B.R. (1990): Relationships between groundwater contamination and major-ion chemistry in a karst aquifer. *Journal of Hydrology*, **119**, 271–291.

80) Scibek, J., Allen, D.M., Cannon, A.J., Whitfield, P.H. (2007): Groundwater–surface water interaction under scenarios of climate change using a high-resolution transient groundwater model. *Journal of Hydrology*, **333**, 165–181.

81) Shoji, J., Momii, K., Fujino, K., Kunitake, M. (1999): Analysis of seawater intrusion into a Ryukyu Limestone coastal aquifer using an immiscible approach: Development and conservation of groundwater resources on small island (I) (in Japanese). *Transactions of the Japanese Society of Irrigation Drainage and Reclamation Engineering*, **201**, 59–66.

82) Simonoff, J.S. (1996): *Smoothing methods in statistics*. Springer-Verlag, 338

83) Skagius, K., Neretnieks, I. (1986): Porosities and diffusivities of. some nonsorbing species in crystalline rock. *Water Resources Research*, **22**(3), 389–398.

84) Somura, H., Goto, A., Mizutani, M. (2003): Modeling analysis of nitrate nitrogen pollution processes of groundwater in Nasunogahara Basin. *Transactions of the Japanese Society of Irrigation Drainage and Reclamation Engineering*, **226**, 1–10.

85) Spalding, R.F., Exner, M.E., Lindou, C.W., Eaton, D.W. (1982): Investigation of sources of groundwater nitrate contamination in the Burbank-Wallula area of Washington, U.S.A. *Journal of Hydrology*, **58**, 307–324.

86) Statistics Bureau (2006): *Population census* (in Japanese). http://www.stat.go.jp/data/kokusei/2005/

87) Takeuchi, J., Kawachi, T. (2007): Optimum fertilizer application for controlling rainfall/irrigation-induced nitrate leaching to groundwater. *Transactions of the Japanese Society of Irrigation Drainage and Reclamation Engineering*, **247**, 1–9.

88) Tase, N. (2003) Present situation and research on nitrate contamination in groundwater (in Japanese). *Journal of Japanese Society on Water Environment*, **26**, 2–5.

89) Tashiro, Y., Takahira, K. (2001): Long-term trend of nitrogen emission and nitrogen concentration of groundwater in Miyako Island, Okinawa (in Japanese). *Journal of Japanese Society on Water Environment*, **24**, 733–738.

90) Taylor, R.G., Howard, K.W.F. (1996): Groundwater recharge in the Victoria Nile basin of east Africa: support for the soil moisture balance approach using stable isotope tracers and flow modelling. *Journal of Hydrology*, **180**, 31–53.

91) Tokuyama, A., Yonaha, Y., Ohde, S. (1990): Nitrate concentration of rain, river and groundwaters in the Okinawa Islands 1 (in Japanese). *Industrial Water*, **379**, 15–25.

92) Townsend, A.R., Howarth, R.W., Bazzaz, F.A., Booth, M.S., Cleveland, C.C., Collinge, S.K., Dobson, A.P., Epstein, P.R., Holland, E.A., Keeney, D.R., Mallin, M.A., Rogers, C.A., Wayne, P., Wolfe, A.H. (2003): Human health effects of a changing global nitrogen cycle. *Frontiers in Ecology and the Environment*, **1**(5), 240–246.

93) Tsuiki, M., Harada, Y. (1994): Program for estimating the amount of nitrogen in livestock manure (in Japanese). *Animal Husbandry*, **48**, 773–776.

94) Urata, S., Kuraoka, T., Ninomiya, K., Kawata, K. (2007): Amount of nitrogen and phosphorus in effluent water from each type of small-scale wastewater treatment facilities (Johkasou) (in Japanese). *Journal of Water and Waste*, **49**(5), 77–80.

95) Wellings, S.R. (1984): Recharge of the Chalk aquifer at a site in Hampshire, England—2. Solute movement. *Journal of Hydrology*, **69**, 275–285.

96) Williams, P.W. (1983): The role of the subcutaneous zone in karst hydrology. *Journal of Hydrology*, **61**, 45–67.

97) World Health Organization (WHO) (1970): *European standards for drinking water, second edition*, 58

98) Yasuhara, M., Marui, A., Yasuike, S., Suzuki, Y. (1992): An experimental study on the behavior of infiltrating water in soils with a macropore (in Japanese). *Journal of Japanese Association of Hydrological Science*, **22**, 3–15.

99) Yasuike, S. (1996): Laboratory experiments and numerical analysis of rain infiltration considering the effect of macropores and pore air pressure in soils (in Japanese). *Geographical Review of Japan*, **69A**-10, 832–846.

100) Yi, M.J., Lee, K.K. (2004): Transfer function-noise modelling of irregularly observed groundwater heads using precipitation data. *Journal of Hydrology*, **288**, 272–287.

101) Yoneyama, T. (1987): Natural abundances of ^{13}C, ^{15}N, ^{18}O, D and ^{34}S in soils and plants: variations, implication and utilization (in Japanese). *Japanese Journal of Soil Science and Plant Nutrition*, **58**(2), 252–268.

102) York, J.P., Person, M., Gutowski, W.J., Winter, T.C. (2002): Putting aquifers into atmospheric simulation models: an example from the Mill Creek Watershed, northeastern Kansas. *Advances in Water Resources*, **25**, 221–238.

103) Yoshimoto, S., Tsuchihara, T., Ishida, S., Imaizumi, M. (2007): Nitrate dynamics in groundwater in Ryukyu Limestone region—case study in Komesu Groundwater basin, Okinawa, Japan (in Japanese). *Transactions of the Japanese Society of Irrigation Drainage and Reclamation Engineering*, **251**, 69–82.

104) Yoshimoto, S., Tsuchihara, T., Ishida, S., Imaizumi, M. (2008): Characteristics of groundwater flow in Ryukyu Limestone aquifer: Study on artificial recharge to groundwater at Miyako-jima, Okinawa, Japan (in Japanese). *Abstract of the 2011 Annual Meeting of the Japanese Society of Irrigation, Drainage and Rural Engineering*, **372**–373.

105) Yoshimoto, S., Tsuchihara, T., Ishida, S., Masumoto, T., Imaizumi, M. (2011): Groundwater flow and transport and potential sources of groundwater nitrates in the Ryukyu Limestone as a mixed flow aquifer in Okinawa Island, Japan. *Paddy and Water Environment*, **9**(4), 367–384.

106) Yoshimoto, S., Tsuchihara, T., Ishida, S., Imaizumi, M. (2012): Development of a numerical model for nitrates in groundwater in the reservoir area of the Komesu subsurface dam, Okinawa, Japan. *Environmental Earth Science*, doi:10.1007/s12665-011-1356-6

107) Young, C.P., Oakes, D.B., Wilkinson, W.B. (1976): Prediction of future nitrate concentrations in ground water. *Ground Water*, **14**(6), 426–439.

108) Zheng, C., Wang, P.P. (1999): MT3DMS, A modular three-dimensional multi-species transport model for simulation of advection, dispersion and chemical reactions of contaminants in groundwater systems; documentation and user's guide. *US Army Engineer Research and Development Center Contract Report SERDP-99-1*, 169

沖縄本島南部の石灰岩帯水層における地下水硝酸性窒素の挙動

吉本 周平

要 旨

南西諸島の琉球石灰岩が分布する地域では，農業用水資源の開発を目的として地下ダムが建設されている。一方で，南西諸島では，これまでに地下水硝酸性窒素の問題が顕在化しているとともに，気候変動に伴う降水パターンの変動や海面の上昇による水資源量および水質への影響も懸念されている。このように，地下ダムを持続的に利用するためには質・量両方の観点からの保全管理が重要である。南西諸島の地下ダムを対象とした保全対策の策定には，琉球石灰岩帯水層に特有の地下水流動および物質輸送の特性を理解した上で，将来の水資源量および水質を予測することが不可欠である。本論文は，世界最初の本格的塩水侵入阻止型地下ダムが建設された沖縄本島南部地区を対象として琉球石灰岩帯水層における水・溶質動態を解明するとともに，硝酸性窒素濃度の変動を予測する手法について検討したものであり，以下の7章から構成されている。

第1章は緒論であり，石灰岩分布地域の地下ダム建設による農業用水開発および地下水硝酸性窒素の問題の現状について先行研究を整理して地下ダムの持続的利用のために水資源量と水質の両面での保全が重要であることを示し，本論文の目的と意義を述べている。

第2章では，炭酸塩岩帯水層における空洞ネットワークの発達史と水・溶質動態について既往の研究に基づいて述べるとともに，主要イオンや窒素安定同位体，ラドンを用いた水・溶質動態の調査方法，並びに地下水の水質予測モデルに関する先行研究を渉猟，整理している。

第3章では，本研究の対象である沖縄本島南部地区について，地質，地下水および土地利用の面について，既往の文献や地質図，統計資料などから整理し，調査地区の第四紀琉球石灰岩がマトリックス流と亀裂流の両方を有する混合型の帯水層であること，並びに都市化が進展ている近郊型農業地域であることを示している。

第4章では，琉球石灰岩帯水層における地下水流動および溶質輸送の特性を把握するために，沖縄本島南部地区で地下ダム建設前に観測された地下水位と硝酸性窒素濃度の短期的な変動パターンを分類するとともに，これらの観測地点と洞窟の分布を比較している。また，地下水位変動には短期・長期両方の涵養成分が寄与していると考えて，観測されたハイドログラフを混合モデルに当てはめてパラメータを推定することによって短期成分と長期成分の寄与の割合を計算している。これらの結果から，洞窟の分布など琉球石灰岩帯水層の水理地質特性が地下水位や硝酸性窒素濃度の変動に与える影響を検討している。

第5章では，沖縄本島南部地区の琉球石灰岩帯水層における地下水硝酸性窒素の挙動をより仔細に把握するために，糸満市の農業統計から原単位法によって計算される窒素負荷排出量と地下ダム建設前の硝酸性窒素濃度の長期的変動を比較するとともに，現地調査によって採取した地下水試料の主要イオン濃度，窒素安定同位体比，ラドン濃度などの水文地球化学的指標を測定し，調査地区の水理地質や土地利用の分布とともに整理している。また，調査地区の主要な負荷源が化学肥料，家畜排泄物・生活排水，土壌窒素からなるとみなして，硝酸性窒素濃度と窒素安定同位体比の連立方程式からそれぞれの負荷源の寄与率を算定している。これらの調査の結果から，地下水硝酸性窒素に影響を与える潜在的な負荷源や，洞窟の存在が硝酸性窒素の輸送経路へ与える影響について検討している。

第6章では，地下ダム貯留域の将来的な硝酸性窒素濃度変動を予測するために，水収支サブモデルと窒素収支サブモデルからなる数値予測モデルを開発している。水収支サブモデルはタンクモデルによって構成され，最下段のタンクで飽和帯の地下水流動を表現し，不飽和帯水層を通過する亀裂流での希釈や地下ダム止水壁の建設の影響を考慮した構造である。窒素収支サブモデルでは，沖縄本島南部地区の土地利用を反映して，化学肥料や堆肥などによる窒素の複雑な形態の変化を定式化している。モデルは，地下ダム建設前のデータでキャリブレーションし，地下ダム建設後に観測されたデータで検証している。また，検証されたモデルを用いて，気候変動に伴う降水量の減少を仮定した上で，地下ダム貯留域の地下水位および硝酸性窒素濃度の変動をシミュレーションしている。

第7章は終章であり，以上によって得られた知見を要約・整理するとともに，今後の課題について述べている。

キーワード：地下水資源，水質保全，数値予測モデル，カルスト水文学，地球化学，水理地質学